TECHNISCHE UNIVERSITÄT WIEN

ESEA Institut für Energiesysteme und Elektrische Antriebe

Impact of transformer placement on the behaviour of low-voltage Grid-Links with high PV share and houses with modern equipment

Master Thesis

In partial fulfillment of the requirements for the degree

Diplom-Ingenieur (Dipl.-Ing.)

committed by

Univ.-Prof. Dr. ing. Wolfgang Gawlik
Ass.-Prof. Dr. techn. Albana Ilo

of the

Technische Universität Wien
Faculty of Electrical Engineering and Information Technology
Institute of Energy Systems and Electrical Drives

by
Andreas Potucek 0825358
Schönburgstr. 25
1040 Vienna
Austria

Vienna, November 2019

Department: Energy Systems
A-1040 Wien, Gusshausstr. 27, Internet: http://www.ea.tuwien.ac.at

Acknowledgments

This thesis completes my studies of electrical engineering at the TU Wien. To reach this goal several people supported me, in this part I want to thank them. I especially thank Dr. Albana Ilo for her help and support in writing my thesis. She also showed me different points of view onto the electrical power systems. I also want to thank Daniel-Leon Schultis who provided me with the data for my simulations and helped me to get a deeper understanding of the simulations. Prof. Wolfgang Gawlik enabled me to write about this topic, I want to thank him for this opportunity.
On my way to my final degree the "Fachschaft Elektrotechnik" supported me in my studies. I also thank the "Hochschüler- und Hochschülerinnenschaft an der Technischen Universität Wien" (HTU) to give me several opportunities to test and also develop my soft skills. In this time special thanks to Abd El Hamid Lashin, Anna Klampfer and Denise Schaffer, with whom I was in the chairteam of the HTU.
In my first days on university I got to know Christoph Peinsipp, Davor Frkat and Martin Mosbeck, with whom I got through diverse exams and prlonged learning periods. I am glad to now call them my friends and hope that this friendship will last.
My parents supported me through my whole education and always encouraged me in my desicions. I thank my whole family who have always encouraged me in my education.

Kurzfassung

Diese Arbeit untersucht Herausforderungen, die sich aus dem zunehmenden Anteil der dezentralen Erzeugung in Niederspannungsnetzen ergeben. Die Erhöhung der eingespeisten Wirkleistung durch das Netz erhöht die Spannung, wodurch die obere Spannungsgrenze verletzt werden kann. Es gibt verschiedene Möglichkeiten, mit diesen Spannungsverletzungen umzugehen. In dieser Arbeit werden die Auswirkungen des Längsreglers in Niederspannungsnetzen und des Verteilnetztransformators mit Laststufenschalter untersucht. Europäische Verteilungsnetze sind das Untersuchungsobjekt. Es werden zwei verschiedene Arten von Verteilungsnetzen simuliert: ein sehr großes städtisches und ein ländliches Netz. Kundenanlagen, die in diesen Netzen angeschlossen sind, weisen drei Besonderheiten auf: In jeder von ihnen ist eine Dachanlage installiert; sie gelten als $Q - Autark$ (Blindleistung autark); und um über moderne elektronische Geräte wie LED usw. zu verfügen, setzt die $Q - Autarkie$ Regelung der Kundenanlagen den Austausch von Blindleistung zwischen den Kunden und dem Niederspannungsnetz auf Null. Während die Elektronik das Lastverhalten von induktiv auf kapazitiv ändert. Somit verbrauchen oder speisen die Kundenanlagen Wirkleistung aus oder in das Netz ein. Mit SINCAL werden Leistungsflusssimulationen durchgeführt. Letztere werden für drei verschiedene Zeitpunkte des Lastprofils durchgeführt: Mittag, 12:00 - maximale PV-Einspeisung ins Netz; Nachmittag, 17:00 Uhr - Last mit maximalem induktivem Verhalten; keine PV-Einspeisung ins Netz; abends 22:00 - laden mit maximal kapazitivem verhalten. Drei verschiedene Spannungen auf der Primärseite des Verteilernetztransformators werden berücksichtigt: 0,96, 1,01 und 1,06 p.u. Die Ergebnisse zeigen, dass Spannungsverletzungen nahe am Abzweig beginnen. Infolgedessen werden die LVRs in der Nähe der Niederspannungssammelschiene des DTR installiert. Unter diesen Bedingungen wird die Auswirkung eines mit OLTC aktualisierten DTR untersucht. Die Ergebnisse zeigen, dass in beiden Fällen (Verwendung von LVRs oder OLTC-DTR) die Belastung des DTR im ländlichen und großen städtischen Netz leicht zunimmt. Dieser Anstieg ist beim OLTC-DTR etwas größer als beim LVR. In allen Fällen ist der Blindleistungsaustausch und -verlust bei Verwendung des OLTC-DTR höher. Der Einsatz von $Q - Autarkie$ zeigt im Vergleich zu keiner $Q - Autarkie$ etwas höhere Spannungen, aber deutliche Vorteile gegenüber dem Blindleistungsaustausch mit dem überlagerten Netz (Mittelspannungsnetz), Verlusten und der Belastung des Verteilnetztransformators. Der induktive Leistungsaustausch mit dem überlagerten Netz ist mindestens halbiert, während das kapazitive Verhalten der Last am Abend verschwindet.

Abstract

This thesis investigates challenges emerging from the increasing share of distributed generation in low voltage grids. The increase of the injected active power through the grid boosts the voltage, which may violate the upper voltage limit. There are several ways to handle those voltage violations. In this thesis the impact of the line voltage regulator and the distribution grid transformer equipped with on-load-tap-changer are investigated. European distribution grids are the study object. Two different types of distribution grids are simulated: a real large urban and a rural grid. Customer plants connected in these grids have three special features: In each of them a rooftop facility is installed; they are considered to be $Q - Autarkic$ (reactive power self sufficient); and to have modern electronic equipment like LED, etc. the $Q - Autarky$ feature of customer plants sets the exchange of reactive power between the customers and the low voltage grid to zero. While the electronic equipment change the load behaviour from inductive to capacitive. SINCAL is used to perform power flow simulations. Thus the customer plants consume or inject active power from or into the grid. Simulations are performed for three different time points of the load profile: Midday, 12:00 - maximum PV injection into the grid; afternoon, 17:00 - load with the maximum inductive behaviour; no PV injection into the grid; evening, 22:00 - load with the maximum capacitive behaviour. Three different voltage on the primary side of distrubtion grid transformer are considered: 0.96, 1.01 and 1.06 p.u. Results show that voltage violations appear close to the feeder begin. As a result, the LVRs are installed close to the low voltage bus bar of the DTR. In these conditions the effect of a DTR upgraded with OLTC is investigated. Results show that in both cases (use of LVRs or OLTC-DTR) the loading of the DTR in the rural and large urban grid slightly increases. This increase is a bit larger for OLTC-DTR than for LVR. In all cases the reactive power exchange and loss results higher when using the OLTC-DTR. The use of $Q - Autarky$ shows slightly higher voltages compared to the case of no $Q - Autarky$ but shows significant advantages over the reactive power exchange with the overlaid grid (medium voltage grid), losses and the loading of the distribution grid transformer. The inductive power exchange with the overlaid grid is at least halved, while the capacitive behaviour of the load in the evening disappears.

Abbreviations

CPG	Customer Plant Grid
DG	Distribution Generator
DSO	Distribution System Operator
DTR	Distribution Transformer
LVL	Low Voltage Level
LVR	Line Voltage Regulator
MV	Medium Voltage
MVL	Medium Voltage Level
OLTC	On Load Tap Changer
OLTC-DTR	On Load Tap Changer equipped Distribution Transformer
pu	per unit
PV	Photovoltaic
Q_{Aut}	$Q - Autarky$
$\neg Q_{Aut}$	without $Q - Autarky$
TSO	Transmission System Operator
VHV	Very High Voltage
VHVL	Very High Voltage Level

Contents

1 Introduction

1.1 Background

The anthropogenic climate change is one of the biggest challenges of this century. The climate on earth is getting warmer on earth and as the expulsion of CO_2 is not stopped by fossil energy, it will be getting hotter. If the temperature is rising furthermore, the sea level will be rising and even some islands will cease to exist. Not only islands are affected, there will be more heat periods during the summer months which will be causing crop failure. In the past few decades politics have done, to turn the tide on climate change, some even do not believe that there is an anthropogenic climate change. The demographic group who will be mainly affected are young people, because of this every friday they are protesting for their future. In consideration of those facts, many countries want to get independent of fossil energy and turn their energy mix to renewable energy sources like wind, sun and water. In Europe there is a big exchange of different energy sources, due to the European Union and big networks like for electricity or natural Gas. European Union needs to define goals on their way to a sustainable energy supply. The European Union, defined as the longterm goal, to reduce of greenhouse gas emmission in the year 2050 by 80% to the levels of 1990. In Table 1.1 the goals for diverse energy sectors are shown. Electricity will be the central role of these milestones as it is more efficient and can nearly eliminate CO_2 emissions and substitute most fossil use in transport and heating [1].

GHG reductions compared to 1990	**2005**	**2030**	**2050**
Total	-7%	-40 to -44%	-79 to -82%
Sectors			
Power (CO_2)	-7%	-54 to -68%	-93 to -99%
Industry (CO_2)	-20%	-34 to -40%	-83 to -87%
Transport (incl. CO_2 aviation, excl. maritime)	+30%	+20 to -9%	-54 to -67%
Residential and services (CO_2)	-12%	-37 to -53%	-88 to -91%
Agriculture (non-CO_2)	-20%	-36 to -37%	-42 to -49%
Other non-CO_2 emmissions	-30%	-72 to -73%	-70 to -78%

Table 1.1: Sectoral reductions of greenhouse emissions [1].

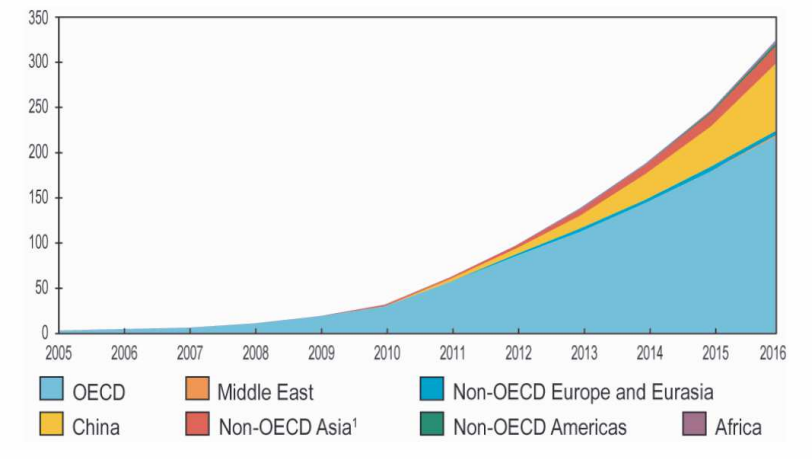

(a) Solar PV

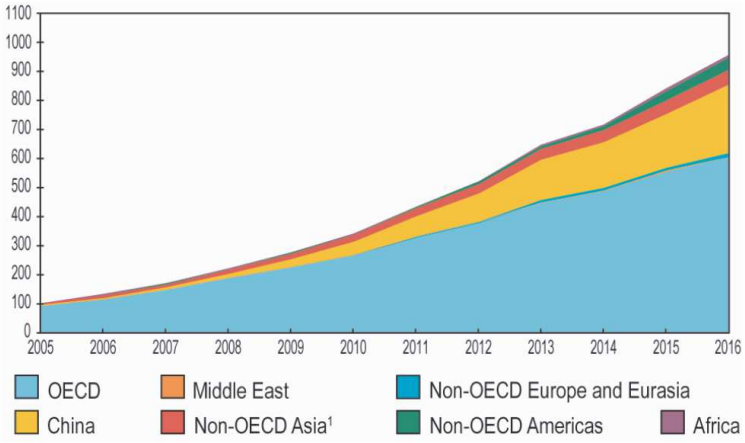

(b) Wind

Figure 1.1: World electricity production of solar PV and wind from 2005 to 2016 by region (TWh) [2].

The high increase of PV (Photo-Voltaics) generation is obvious as the potential of PV actually is on a very and has very high potential to make up an even larger part of the energy mix. As an example in Austria the installed PV power in 2017 is 1.2 GW and the potential for PV on buildings is estimated 31 GW [3, 4]. Especially the high proliferation of distributed generation of utility scale solar photovoltaics create challenges for the existing distribution grids. Figure 1.1 shows that the share of Distributed Generation (DG) like wind or PV from 2005 to 2016 is rapidly rising. The worldwide increase of net installed capacity of wind electricity power was 53.4 GW in comparision to the increase of PV electricity power was 79.9 GW [2, 5].

The changes for a distribution grid, especially considering large scale PV-penetration inculde:

- changes in feeder voltage profiles, violations of the upper voltage limit, because of voltage rise
- changes in feeder loading, including potential overcurrents caused by too much energy injection
- there can be more frequent operation of voltage-control and regulation devices, such as load tap changers, Line Voltage Regulators (LVR)
- possible increase of reactive-power flow fluctuations due to the higher numbers of reactive devices controlled locally
- changes in the power quality, distributed photovoltaics intermittency may lead to voltage fluctuation issues
- changes in overcurrent and voltage limit violation protection, including misoperation of overcurrent protection equipment and temporary voltage limit violation

The severity of the impact of those challenges varies with the penetration level, the location of photovoltaics and the type of the distribution grid [6].

1.2 Motivation

As discussed above, the DG penetration challenges the grid operation. The main duty of Distribution System Operator (DSO) is to provide electricity to the consumers with a certain quality, which is defined by European and national laws as well as by standard specifications. For example the voltage range is from 0.9 to 1.1 of the nominal voltage [7]. The voltage of the grid has a substantial role to keep these values in their respective limits. If they cannot stay inside the voltage limits, cost intensive measures have to be taken, like reconstructing the grid. In the low voltage level of the distribution grid, the DGs are mainly the PV of the residential customers. The average production of PV worldwide in 2016 was about 1093 hours, that is about an eighth of the whole year [2]. The fact that photovoltaics reach their full power only for few hours on a daily basis makes it obvious, that a big investment in the grid, due to photovoltaics, is not economical. It is essential to install PVs on every house, to use as much of the solar potential. If we consider to install PVs not only on buildings, we are in conflict with agriculture or forestry, as those are the other places where PVs could be installed. If the woods are cleared for PV generation, the climate change would be getting more severe, as a tree is gathering CO_2 from the athmosphere. If we used the fields used for agriculture, there is a conflict with the food production, which is no option too. To handle the challenge to stay within the voltage limits, smart solutions are needed: like LVRs with autonomous tap changers in the feeder branches of the low voltage grid

or On-Load-Tap-Changers equipped Distribution Transformers (OLTC-DTR). Another smart solution is to use the inverters or use reactive devices as it is done in [8]. As the same grids are investigated as in [8], it is possible to compare the results. Besides of the technically possible solutions, there are other criterias like data privacy of the residentials, which also has to be taken in account. The challenge is to not only find the best technical solution, but the solution which combines the best technical and social solution.

1.3 Objectives

This thesis shall provide solutions for the voltage violations by a high PV-share in future low voltage grids. Considering the PVs are to be installed at the residential customers. Those photovoltaics are expected to violate the voltage limits. To mitigate these violations, LVRs and an OLTC-DTR are used. The thesis examines their capability to control the voltage band and to keep it within the limits, which is an essential part. The change and the exchange of reactive and active power shall be analyzed, especially by using different voltage control strategies. The interaction of voltage regulators with inverters of the utility scale photovoltaics is also given attention to, especially with a $Q-Autarkic$ behaviour of the customers. The behaviour of the LVRs in diffferent types of grids is investigated, in a rural or a large urban grid. Also the different impact of the LVR on cable and overhead line feeders, is part of the thesis.

1.4 Scope

The scope of this thesis is the PV-penetration in a low voltage grid of European style. The customers are modelled, as black boxes with a load and generation model, Simultaneity factor is used, so all customers can be assumed to have the same load and the same generation. In the main part of the thesis the focus is on the low voltage grid, the medium voltage grid is only present by the distribution transformer. The exchange of active and reactive power is also examined, especially if this exchange vary with the use of different voltage control strategies installed in low voltage feeders. The medium voltage grid and the overlaid grid defines the voltage setpoint. The thesis investigates into the impact of series transformers to control the line voltage limits in the feeders of the low voltage grid.

1.5 Thesis Structure

In Chapter 2 the theoretical background needed to understand the simulation, like voltage and power control is established. The voltage and power supply norms is also covered. Furthermore the new paradigm, which the Grid-LINK model shall provide, is presented. In Chapter 2 the optimal sizing and positioning of the LVRs are shown. Chapter 3 describes the models which are used in the simulations, like the grid, the

transformer, the load and the voltage control. In Chapter 3 the different voltage control strategies are presented and also the load profiles in presence of modern equipment are shown. Chapter 4 defines the scenarios which are used in the simulations. In Chapter 5 the results of the simulations, the impact of the voltage control and the impact of the new load model is presented. In Chapter 6 the results of Chapter 5 are discussed and a conclusion is drawn.

2 Theoretical background

Section 2.1 describes the structure and operation of the European power grid. Section 2.2 introduces the Link-Solution as a new paradigm for the organisation, management and controlling of power sectors. Furthermore section 2.3 describes the behaviour of distribution grids, voltage profiles, the loading of the electrical equipment, the load-voltage dependency and various voltage control strategies. Section 2.4 describes the load model and the load-voltage dependency of different loads. Section 2.5 investigates into the sizing and positioning of LVRs, as well as autotransformer as LVR.

2.1 Overview of the European power grid

There are different types of structures for power grids, the European grid type or the North American grid type. In the thesis the focus lies on the European grid type, which is also explained in the following sections. Nevertheless, there are some comparisons to the North American grid type [9].

2.1.1 Structure of the European power grid

The European electrical power grid is managed by ENTSO-E, which contains 36 countries and 43 Transmission System Operators (TSO), ENTSO-E supplies more than 500 million people with electricity [10]. Due to this large network the security of supply in Europe is very high, it varies between 99,990% and 99,995% [11]. ENTSO-E is also responsible to adjust and develop the different codes, which are grouped in three different families, the Market codes, the Operation codes and the Connection codes. They define the rules within the ENTSO-E network for the different sections [10]. In this structure the TSO is responsible for operating the Very High Voltage Level (VHV or VHVL) and also parts of the High Voltage Level (HV or HVL), the Distribution System Operators (DSO), is responsible for their parts of the HVL, the Medium Voltage Level (MVL or MV) and the Low Voltage Level (LV or LVL) [9]. In Europe the VHVL, the HVL and the MVL are meshed grids, except for two point connections, also the grid is built with n-1 security level. This means if one utility is failing the grid can be operated further without any outage. The LVL is a radial grid type and has like, all the other voltage levels, all three phases in every connection point. It is compared to the other levels not n-1 secure, if an utility of the grid like an overhead line fails, there will be an outage, but only few consumers will be disconnected. Compared to a failure in the higher voltage levels, no customers are disconnected due to the n-1 security. Figure 2.1 presents a representative model of the European grid structure. To operate the grid it is essential

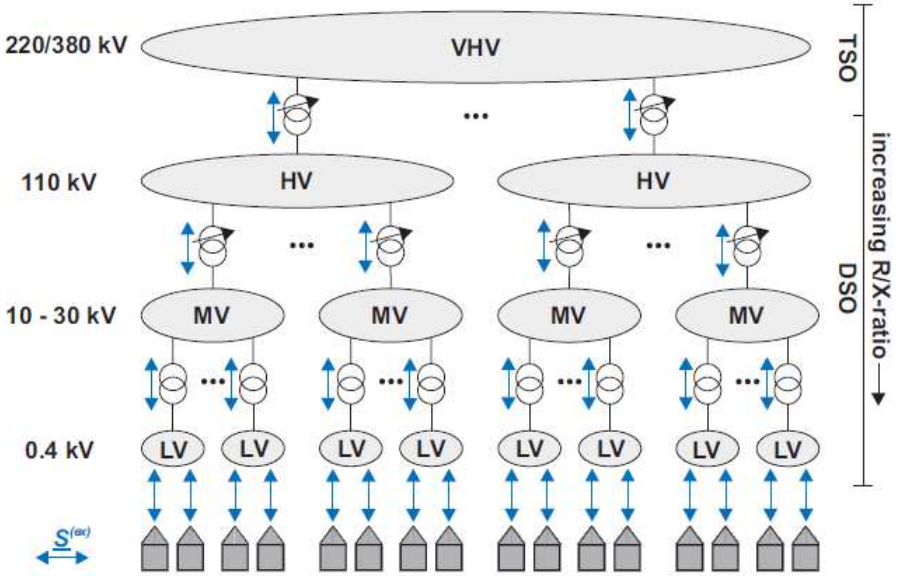

Figure 2.1: European power grid structure [14].

to control the power flows through the grid, this is done by the TSOs. The power flows cannot be controlled, they are monitored by the voltage, the frequency and the phase angles [12]. As all phases in every connection point exist it can be assumed that the grids are symmetric, which enables us to use a single phase equivalent of the grids [13].

2.2 Grid Architecture

This section focuses on the architecture of a Smart Grid Architecture in a holistic way. The Link-Paradigm is such a smart grid architecture to model the entire power System, from the customers to the TSOs. The model is based from the grid point of view, but it can also be used for the economical point of view onto the power system. The model is based on the model of "The Energy Supply Chain Net", which also uses "Links" or "Chains" between the power grids, the coupling is only between neighbours. The Link-Paradigm is defined as a compound of electrical equipment, a related control scheme and a Link-Interface to communicate with other parts of the grid, Figure 2.3 (a) illustrates the Link-Paradigm. There are three main components in the energy supply chain, the "Grid-Link", the "Producer-Link" and the "Storage-Link", shown in Figure 2.3 (b). The Grid-Links size is variable and defined by the area, where the secondary control is active, it may represent a microgrid or even a large transmission grid, it is independent from the voltage level. The Producer-Link is defined as a composition of an electricity production device, like a generator, photovoltaics, etc. The Storage-Link is defined as an electrical device, which can store energy like the generator of a pump power plant, batteries, etc. The Customers are also Links on their own, but in this case the owner is also the operater of the Link. They are called Customer Plants, like the prosumers, they have loads and

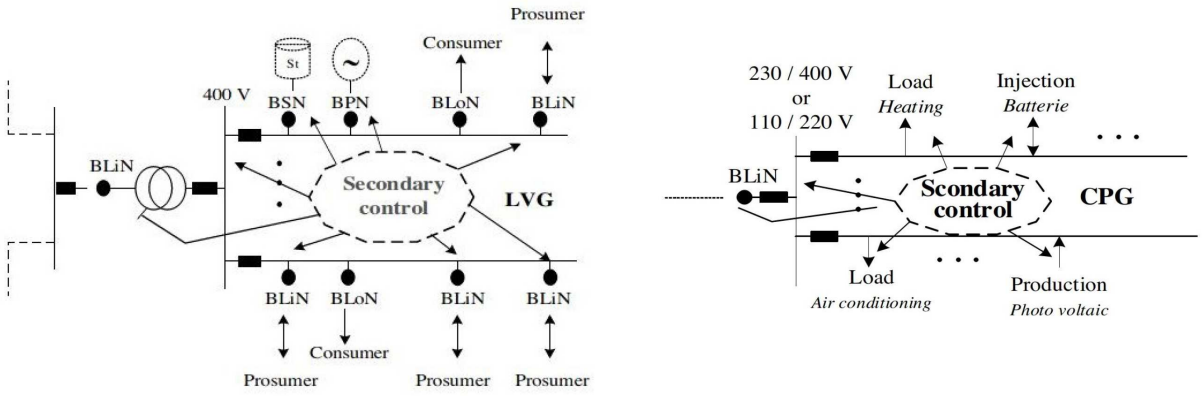

Figure 2.2: Model of a (a) low voltage grid link (LVG) and (b) customer plant grid (CPG) [9].

also production units. The Link-paradigm foresees that the inhabitants of the house may want to control the devices in the house via the internet, but strictly seperates the communication with the overlaid grid from the internet by a house management unit. This unit is responsible for the communication with the grid, it will only communicate via safe ways the summarized need of power of the house and gets the set points for active and reactive power from the grid operator in return.

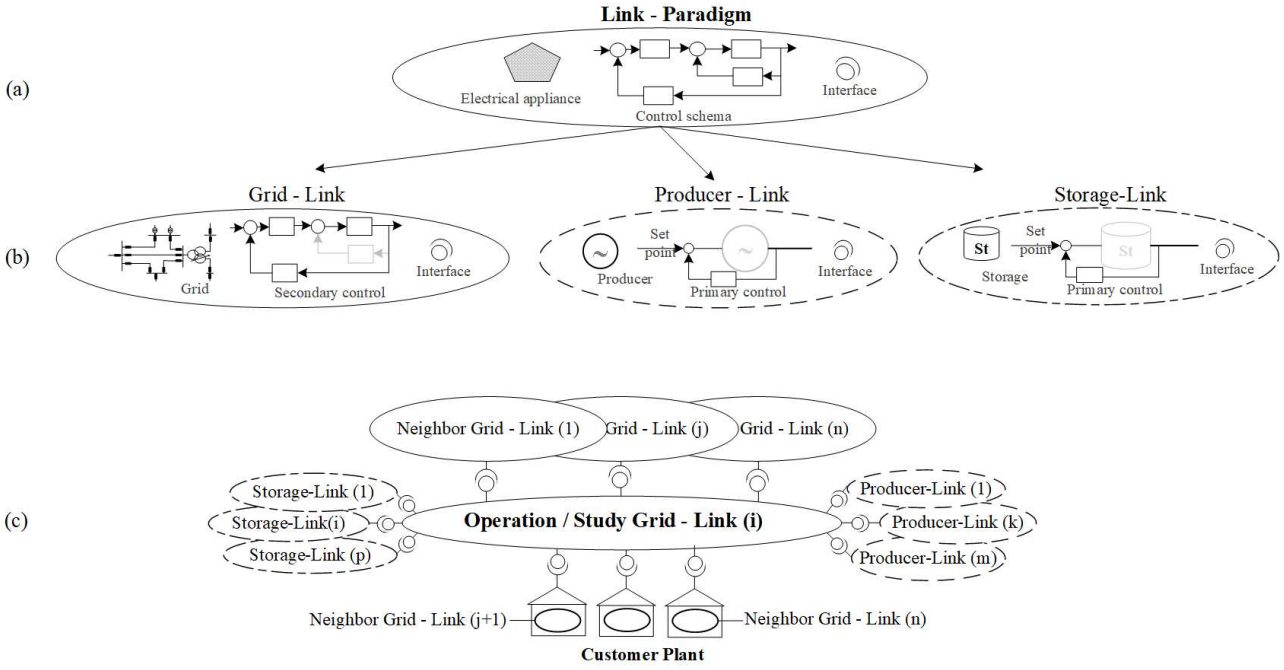

Figure 2.3: Overview of (a) the Link-Paradigm, (b) the deduced architecture components and (c) the resulting link based architecture [9].

As this thesis is focusing on the low voltage level and the customers, Figure 2.2 shows a model of a low voltage link and a model of a customer plant. The interfaces are connected

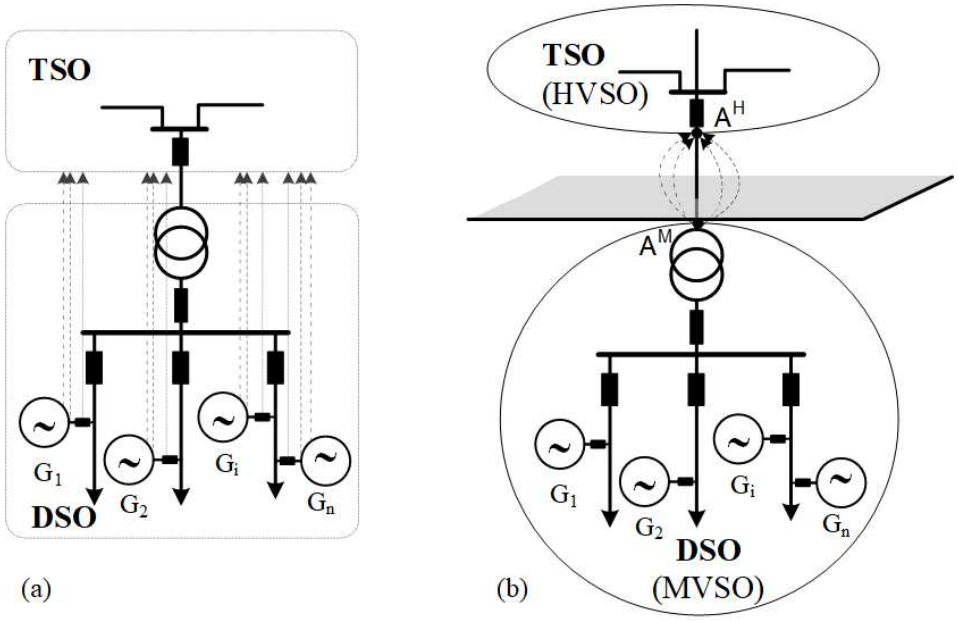

Figure 2.4: Scheduled data exchange on two different architectures: (a) centralized and (b) decentralized [9].

via "Boundary Link Nodes" like the BPN in Figure 2.2 which is a so called "Boundary Production Node" or the BSN which is called "Boundary Storage Node" [9]. A main part of the architecture is that every Grid-Link has its own "volt/var secondary control loop" and is calculating optimal set points for the control variables like an OLTC. Those control variables are optimised under the premise of the static constraints of the own grid and the dynamic constraints of adjacent Links. The situation is recalculated with the dynamic constraints in realtime to get to a resilient set point for the Grid-Link. As already mentioned the exchanges of reactive power can be limited, this makes the exchange to a control variable and also a constraint. It is depending on the current situation in the grid, which nature the exchange of reactive power will be. The recalculation of the constraints can lead to a new proposal of the requested Q-exchange with another Grid-Link. In Figure 2.5 the model of the "volt/var secondary control loop" is illustrated from the transmission grid down to the Customer Plant Grid (CPG) [15]. Another main goal of the architecture is to reduce the data-exchange, this is done by the Link-Interfaces which only shall communicate with the other connected Link. In figure 2.4 the difference between a centralized and a decentralized architecture is shown, for scheduled data-exchange, like dayahead data [9].

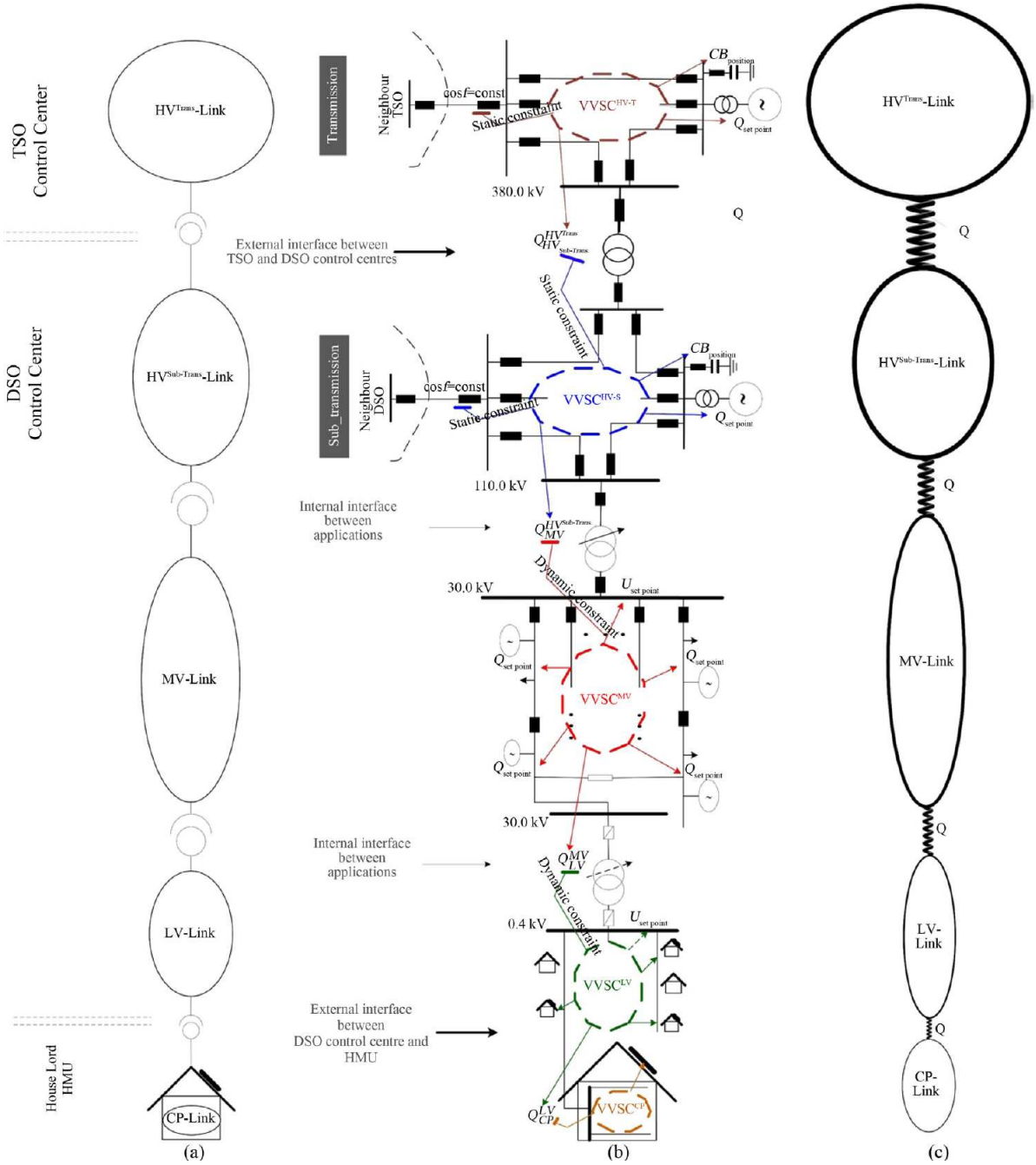

Figure 2.5: Model of the volt/var secondary control chain (a) Link-structure, (b) volt/var control loops, (c) resilient connection over the reactive power [15].

2.3 Volt/var behaviour of distribution grids

In this section distribution grids are discussed. Distribution grids can be split into two voltage levels, the MVL and the LVL, where the CPGs are connected to. Figure 2.6 shows the different connection points of the Grid-Links. The MVL is partly meshed and partly a radial grid. It depends whether the grid is in an urban or in a rural area. If there are many consumers on a feeder the redundance is higher than if there are only few consumers. Most of the feeders have a redundancy to achieve a high percentage of security of supply, as this is one of the main goals of a DSO. Nevertheless the LV_Grid-Link is a radial grid and the thesis focuses on the LVL, as there are the main problems with voltage limit violations. In a distribution grid there can be found following electrical equipment power transformers, cables or overhead lines, reactive devices, different types of generation and of course the consumers, who are supplied by the grid. The equipment of the grid is performing ideal, if there are no power flows, which are loading the equipment. The electrical euquipment has active and reactive power losses, they can be reduced, if the voltage is set to the limit of the allowed band or the impedances of the devices are reduced. To understand those interactions a simplified network element is introduced, as shown in figure 2.7, the impedance $\underline{Z}^{(emt)}$ can be a power transformer, a reactive power device or a line segment. The power flows on both sides can be calculated with the equations 2.1 and 2.2 [14].

$$\underline{S}_1 = \underline{I}^* \cdot \underline{U}_1 \tag{2.1}$$

$$\underline{S}_2 = \underline{I}^* \cdot \underline{U}_2 \tag{2.2}$$

If many of those network elements are combined in a radial construct, the result is a radial distribution grid, as shown in figure 2.8. In this modell, $\underline{Z}^{(tr)}$ is representing the power transformer and $\underline{Z}^{(sgm)}_{f,n}$ are representing the line segments as overhead lines or cables. This general structure represents F feeders with N_f nodes, each node has a lumped load represented by its consumption of $\underline{S}_{f,n}$. This general structure is most likely representing a LV_Grid-Link, whereas the lumped load can be several types of connected grid costumers, like a consumer, a prosumer, a storage, a producer or a whole branch of the LV_Grid-Link itself. The power flow in a LV_Grid-Link was from the feeding transformer to the feeders and the lumped loads, nowadays the power flow can also be reversed, due to the rising numbers of distributed generation. Nevertheless the equations 2.4 and 2.3 to calculate the power flows within the radial grid are not affected by this change. Equation 2.4 can calculate the power flow at the power transformer and with this the interaction with the overlaid grid, with equation 2.3 the power flow on the feeder can be calculated [14].

$$\underline{S}^{sgm}_{f,n} \approx -\underline{U}_{f,n} \cdot \sum_{j=n}^{N_f} \frac{\underline{S}^{(lpd)}_{f,j}}{U_{f,j}} \tag{2.3}$$

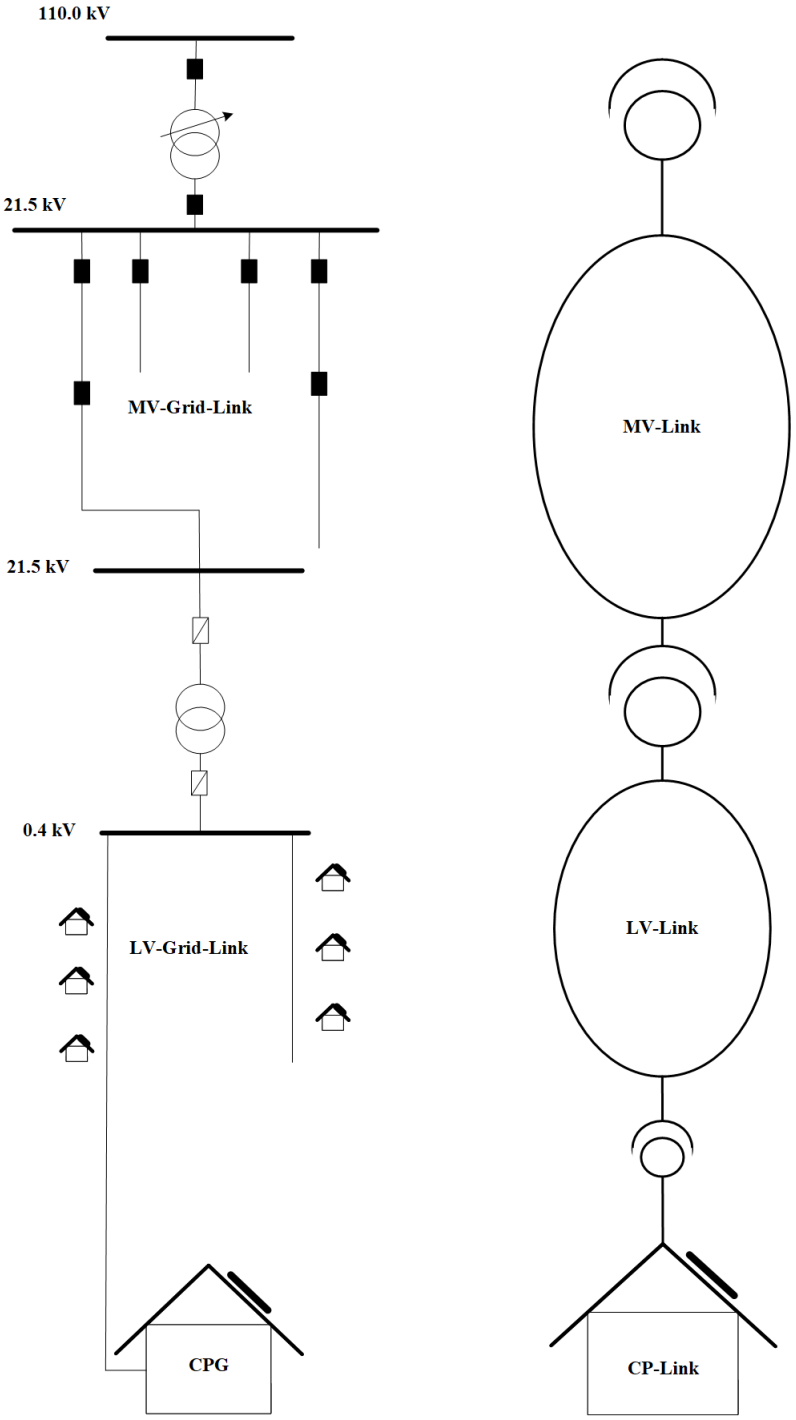

Figure 2.6: Simplified distribution grid with Link-Link to HVL.

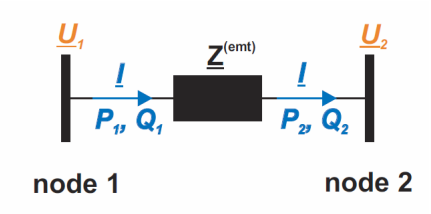

Figure 2.7: Simplified single phase network element [14].

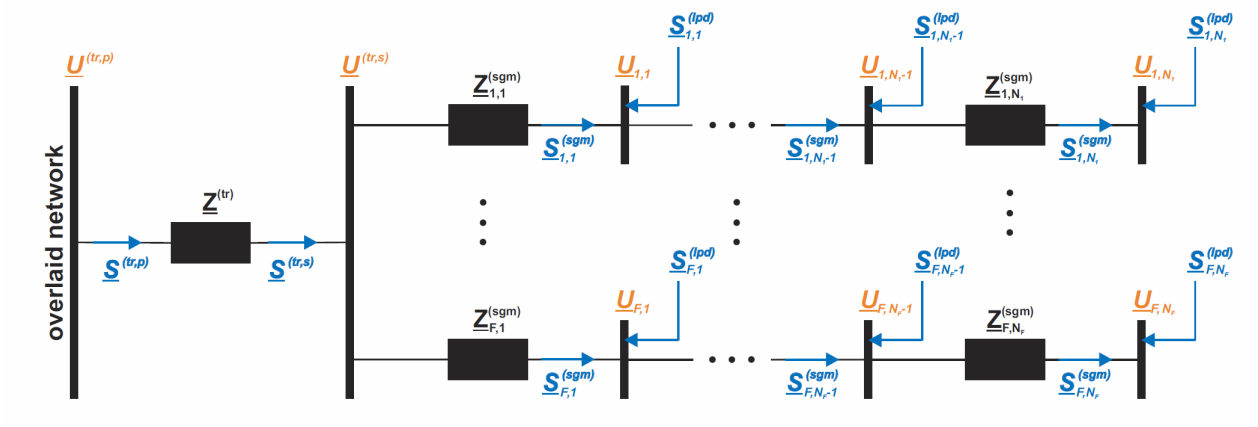

Figure 2.8: Radial multifeeder distribution grid [14].

$$\underline{S}^{tr,p} \approx -\underline{U}^{(tr,p)} \cdot \sum_{i=1}^{F} \sum_{j=1}^{N_i} \frac{\underline{S}_{i,j}^{(lpd)}}{U_{i,j}} \tag{2.4}$$

In Figure 2.9 a structure of a prosumer is given, it is a combination of a consumer and a producer, each part can be connected without the other. The model is required because of the rising number of DGs. In this thesis a producer is a PV array as the investigated Grid-Links only have PV as DG. The power flow of the prosumer can be calculated with the following equations:

$$\underline{S}_{f,n}^{(pro)} = (P_{f,n}^{(inv)} - P_{f,n}^{(load)}) + j(Q_{f,n}^{(inv)} - Q_{f,n}^{(load)}) \tag{2.5}$$

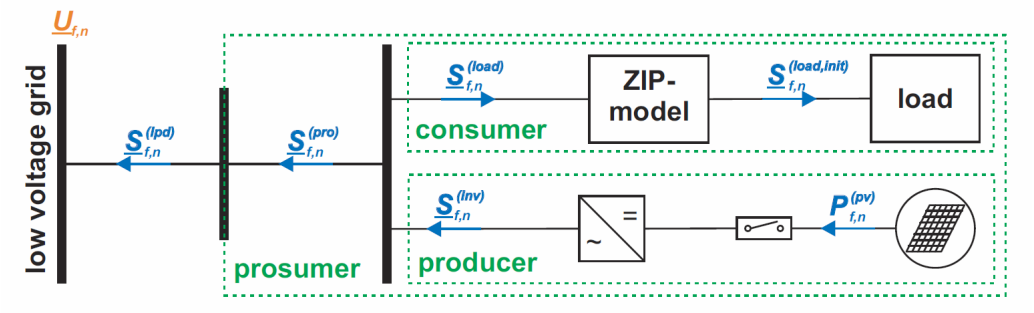

Figure 2.9: Structure of a prosumer [14].

$$\underline{S}^{(pro)} = \sum_{i=1}^{F} \sum_{j=1}^{N_i} \underline{S}_{i,j}^{(pro)} \tag{2.6}$$

2.3.1 Voltage profile

As already mentioned is the power flow interacting with the voltage of the electrical equipment and further on with the voltage profile of a distribution grid. The voltage profile is a diagram over the feeders length. The EN 50160 defines the voltage levels and their band, as in the LVL this band is ±10% of 400 V between two phases, this european norm is implemented as national law by the members of the ENTSO-E grid. The HV/MV power transformer is usually implemented with an OLTC which is regulated automatically, to a predefined voltage level [13]. Depending on the lumped loads connected to the medium voltage feeder the voltage level is affected and can lead to overvoltage or undervoltage limit violations, this happens usually in critical situations. Based on the Figure 2.7 and the equations 2.1 and 2.2 the following equations can be formulated to get an impression of how the power flow is affecting the voltage profile along a network element. Figure 2.10 presents exemplary voltage profiles of a LV_Grid-Link with different voltage levels of the DTR's primary side, different times and a high PV share.

$$\Delta U = U_2 - U_1 = U^{(emt)} \tag{2.7}$$

$$U^{(emt)} \approx -\frac{P_1 \cdot R^{(emt)} + Q_1 \cdot X^{(emt)}}{U_1} \approx -\frac{P_2 \cdot R^{(emt)} + Q_2 \cdot X^{(emt)}}{U_2} \tag{2.8}$$

The impact of the active and reactive power flow on the voltage is dependent on the associated impedance, as it can be seen in equation 2.8. Especially the R/X ratio describes which kind of power flow has more impact on to the voltage. To be able to compare the different voltage levels, the voltage will further on be normalised, nominal variables will be in small letters and named per unit (pu).

$$u = \frac{U}{U_N} \qquad s = \frac{S}{S_N} \qquad z = \frac{Z}{Z_N} \tag{2.9}$$

As mentioned before every electrical equipment which is part of the power flow is causing a voltage variation, like line segments or the transformer itself. The transformer has additionally the option of the tap changer, most likely the tap changer of the medium to low voltage level transformer is not an OLTC, the transformer needs to be at zero-potential to be able to change the position. The employees of the DSO are checking the voltage measurements of the transformer from time to time, and if necessary are changing the position of the tap changer [12]. So the ratio between the MV Grid-Link and the LV Grid-Link is fixed and the ratio of the tap position can also be seen as fixed for a long term view. The two voltage variations can be calculated with the normalised voltage levels of the secondary open circuit (soc), the transformers primary voltage (tr,p)

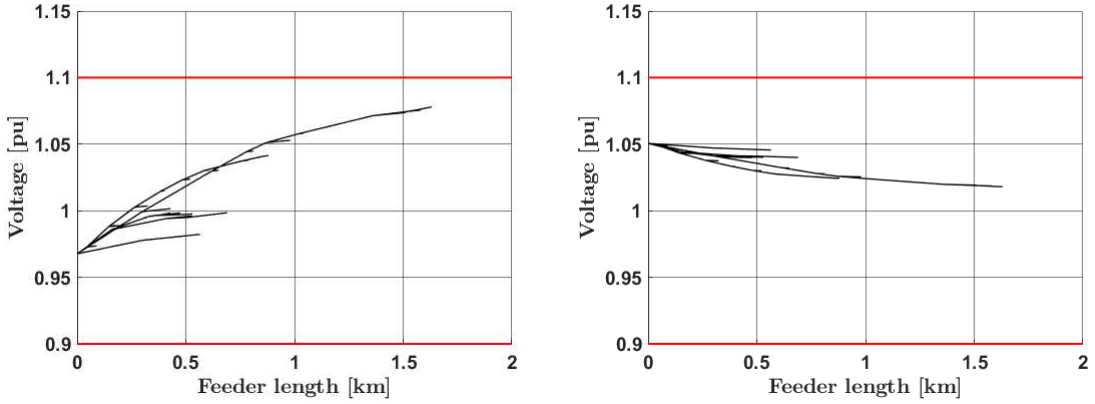

(a) (b)

Figure 2.10: Voltage profiles of a LV_Grid-Link (a) $v = 0.96$ at 12:00, (b) $v = 1.06$ at 20:00.

and the transformers secondary voltage (tr,s) [14].

$$t^{(tr)} = \frac{U^{(r,tr,p)}}{U^{(r,tr,s)}} \qquad t^{(grid)} = \frac{U^{(tr,mv)}}{U^{(tr,lv)}} \tag{2.10}$$

$$\Delta u^{(tr,tap)} = u^{(tr,soc)} - u^{(tr,p)} = \left(\frac{t^{(grid)}}{t^{(tr)}} - 1\right) \cdot u^{(tr,p)} \tag{2.11}$$

$$\Delta u^{(tr,pf)} = u^{(tr,s)} - u^{(tr,soc)} = -\frac{r^{(tr)} \cdot p^{(tr,p)} + x^{(tr)} \cdot q^{(tr,p)}}{u^{(tr,p)}} \tag{2.12}$$

$$\Delta u^{(tr)} = (\frac{t^{(grid)}}{t^{(tr)}} - 1) \cdot u^{(tr,p)} - \frac{r^{(tr)} \cdot p^{(tr,p)} + x^{(tr)} \cdot q^{(tr,p)}}{u^{(tr,p)}} \tag{2.13}$$

Equations 2.10 are the ratios of the transformer voltages, one for the grid and one for the tap changer. The voltage variations are seperated by the following equations, 2.11 is for the tap changer and 2.12 describes the voltage variation of the whole transformer by using equation 2.8. By using equation 2.8 the voltage variation of a line segment can also be determined:

$$\Delta u_{f,n}^{(sgm)} = u_{(f,n)} - u_{(f,n-1)} = -\frac{r_{f,n}^{(sgm)} \cdot p_{f,n}^{(sgm)} + x_{f,n}^{(sgm)} \cdot q_{f,n}^{(sgm)}}{u_{f,n}} \tag{2.14}$$

The voltage variation along a feeder to any position in a grid can now be calculated. The tap changer is affecting the whole underlaid grids voltage, but not always is it possible to change the position of the tap changer, to get rid of a voltage violation. In some cases one feeder has a voltage violation of the upper limit and another feeder connected to the same transformer has a voltage violation of the lower limit. In this case the transformer tap can not be changed, because the vice versa feeder is always affected in a negative way, independent of the change of the transformers tap position. The reason for this can

be the different lines used to supply the customers, i.e. one feeder is built with overhead lines and the other one is built with cable. This effect can be described by the different $\frac{R}{X}$ ratio and is dependent on the length of the line in a grid as seen in the following equation 2.15:

$$\frac{R}{X}(l) = \frac{R^{(tr)} + R^{(sgm)'} \cdot l}{X^{(tr)} + X^{(sgm)'} \cdot l} \tag{2.15}$$

By using the following overhead line parameters $\frac{R'}{X'} = 0,92$ made of aluminium core with a cross section of $95[mm^2]$ and a cable with $\frac{R'}{X'} = 2,58$ and $150[mm^2]$,the difference of the impedances over the length of a feeder line is visualized in Figure 2.11.

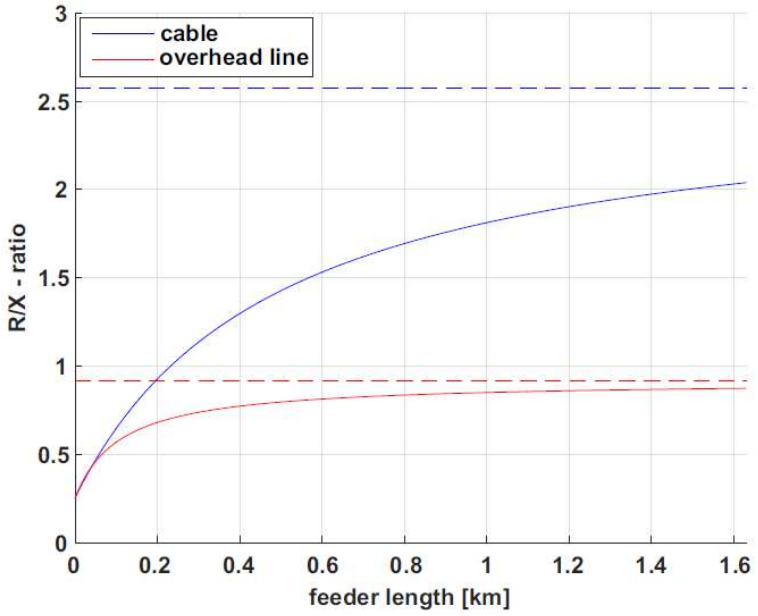

Figure 2.11: Comparision of the R to X ratio of a cable and an overhead line [14].

2.3.2 Losses of different electrical equipment

Electrical equipment usually consumes active power and in several cases also reactive power. As this consumption is often not requested or useable these consumptions are losses by the grid and should be kept low, as they are also responsible for the aging of the equipment in long terms due to heating by the current. The consumed power of a typical network element like the one in Figure 2.7 can be calculated by equation 2.16. It can also be seen as a result of the voltage variation.

$$\underline{S}^{(loss,emt)} = \underline{I^*} \cdot (\underline{U}_1 - \underline{U}_2) = I^2 \cdot \underline{Z} \tag{2.16}$$

The result, by spliting the equation 2.16 into real and imaginary part, is the active and reactive power consumption.

$$P^{(loss,emt)} \approx R^{(emt)} \cdot \frac{P_1^2 + Q_1^2}{U_1^2} \approx R^{(emt)} \cdot \frac{P_1^2 + Q_1^2}{U_2^2} \tag{2.17}$$

$$Q^{(loss,emt)} \approx X^{(emt)} \cdot \frac{P_1^2 + Q_1^2}{U_1^2} \approx X^{(emt)} \cdot \frac{P_1^2 + Q_1^2}{U_2^2} \tag{2.18}$$

By comparing equations 2.17 and 2.18 the different influece of the two parts by the electrical equipment itself and its $\frac{R}{X}$ ratio can be determined. Nevertheless both parts are losses by the grid and should be kept low, as they lead to a higher loading and heating of the equipment, to higher voltage variations and to quicker aging of the equipment. To calculate the power consumption of a Grid-Link the infeeding power cannot just be taken, because this way the consumed power of the customers is also added to the grid losses. So it is needed to sum all the Grid-Link element losses, transformers, lines and reactive power devices, except the customer consumption, by using the equations 2.17 and 2.18.

$$P^{(loss)} = P^{(loss,tr)} + \sum_{i=1}^{F} \sum_{j=1}^{N_i} \left(P_{i,j}^{(loss,sgm)} + P_{i,j}^{(loss,rct)} \right) \tag{2.19}$$

$$Q^{(loss)} = Q^{(loss,tr)} + \sum_{i=1}^{F} \sum_{j=1}^{N_i} \left(Q_{i,j}^{(loss,sgm)} + Q_{i,j}^{(loss,rct)} \right) \tag{2.20}$$

As discussed the reactive power is also causing additional losses of the equipment. So to minimise the losses by the reactive power, the reactive power flows through all elements are set to to zero.

$$Q^{(tr,p)} = Q_{f,n}^{(sgm)} = Q_{f,n}^{(lvr)} = 0 \qquad \forall f, n \tag{2.21}$$

To influence the voltage variation alongside the transformers there are two ways, one via the tap changer and also by influencing the reactive power flow through the transformers impedance. So the reactive power flow can be minimised by setting the tap position to an appropriate level [14].

$$\left(\frac{t^{(grid)}}{t^{(tr)}} - 1 \right) = \frac{R^{(tr)} \cdot P^{(tr,p)} + X^{(tr)} \cdot Q^{(tr,p)}}{U^{(tr,p)}} \tag{2.22}$$

If no OLTC is available, as it is common for most of the distribution Grid-Link transformers connecting the LVL to the MVL, the reactive power flow can be used to compensate the voltage variations by the active power flow [14].

$$Q^{(tr,p)} = -P^{(tr,p)} \cdot \frac{R^{(tr)}}{X^{(tr)}} \tag{2.23}$$

The goal is to minimise the active and reactive power consumption of the transformer, the line segments and the line voltage regulators. This is done by setting their reactive

power flows to zero. In this case all the connected consumers need to have a reactive power source to cover their own reactive power demand. The optimal reactive power exchange depends on the strategy of the Grind-Link operator, the DSO can choose between the posibilities, which are presented in the previous section. For an optimal performance the overall balance should be set to zero, so that everyone has to cover his own reactive power need, but it is also possible to target specific values if those strategy is useful for the overlaid grid. Both strategies are covered by the following equations [14].

$$Q^{(tr,p)} = 0 \qquad Q^{(tr,p)} = Q_0^{(tr,p)} \tag{2.24}$$

As the section shows there is a conflict between loss minimisation and voltage profile optimisation, as voltage profile optimisation causes more losses by the reactive power by the increasing load of the electrical equipment. If the losses caused by the reactive power flow are optimised, the capabilities of optimisation of the voltage profile are limited. As the strategies which define discrete reactive power flow values at the connection point also limits the capabilities to optimise the voltage profile. To have a greater dynamic scope for the voltage profile optimisation and the loss minimisation, the most promising strategy is the one of Figure 2.12.

2.3.3 Reactive power exchange with the overlaid grids

As the number of DG is rising, the exchange of reactive power between the Grid-Links is getting more and more relevant for the TSO and the DSO. The distributed generation is the cause for the shut down of several conventional power plants, which had also been responsible for some services like to provide reactive power for the transport of power [16]. The transmission of power at the transmission limit with voltage support needs injection of reactive power to be able to transmit the active power. The injected reactive power at the beginning needs to be equivalent to the transmitted active power and negative equivalent at the end of the line [17]. The outage of such a reactive power injection means that the whole system can get instable. It is crucial to define the exchange between the DSO and the TSO [16, 17]. There are several strategies for this exchange at the coupling points, there can be no limits, use-case dependent target values and a limitation of Q-exchange by active power, shown in Figure 2.12. The DSO is responsible to hold the permitted voltage profile, to do so the DSO can conclude contracts with the connected customers of his grid for reactive power injection or install utilities to compensate the reactive power on his own [18]. The different possible control strategies are discussed in the next section. As the DSO is responsible for his reactive power flows he needs to optimise the need of reactive power as more needed utilities also means the operation of the Grid-Link itself is getting more expensive. The rising number of DG is also responsible for the need of more reactive power as the transmission of the active power needs reactive power to stabilize the voltage [14, 16]. The conflict between the DSO and the TSO caused by the reactive power exchange at the connection points is getting intense by installing more and more DGs [16].

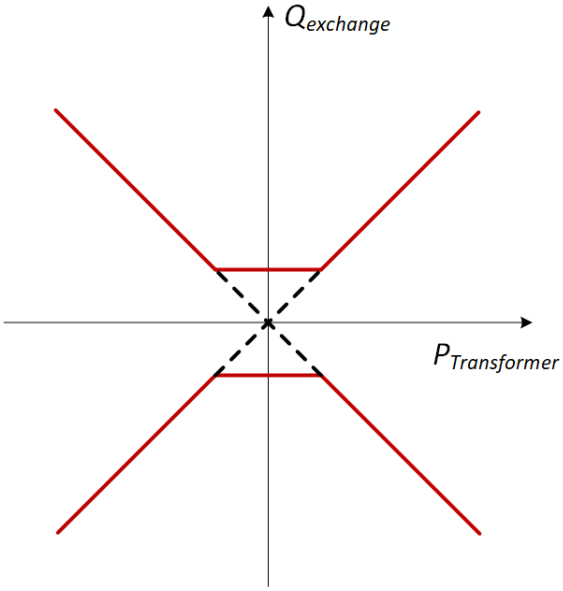

Figure 2.12: Limitation of Q-exchange by active power [16].

2.3.4 Volt/var control strategies

The previous section discussed the exchange of reactive power and how this leads to a rising conflict between the DSO and the TSO. This section is investigating in how this conflict can be solved by different control strategies for the voltage and the reactive power. Also the DSO is responsible to provide a certain voltage band for the customers in his part of the Grid-Link. This task is not always easy as the DG can jeopardise this goal. To stay within the voltage band at all times the DSO can limit the installed power of DG, this action is mostly applied to photovoltaics. If the amount of photovoltaics shall be increased it is needed to take other actions to secure the voltage band. As there is a voltage spreading caused by the DGs over the whole day the solutions have to include an automated control, the following control strategies are all automated options [14].

$\cos \varphi(P)$

This control strategy uses a characteristic of the power factor in correspondence of the active power generation. The power factor stays the same until a certain point of active power output where it is slowly decreasing to the advantage of a reactive power consumption. The presumption of this strategy is that the highest voltage level comes always along with the highest power generation. There are scenarios like high generation and also high consumption of power, in this case this strategy can cause problems for the voltage stability, as the strategy does not take the voltage situation into account, by its control [19].

$P(U)$

This control strategy is similar to the control strategy of $\cos\varphi(P)$ but does not use a reactive power consumption to get rid of high voltage levels. In this case the inverter reduces the injected power if the voltage level is too high, to prevent the over voltage protection from getting active and cutting the whole inverter from the grid. The assumption is also that the voltage is too high because of the distributed generation [19].

$Q(U)$

The control strategy is like the $P(U)$ control strategy but as the name makes it obvious this time the reactive power is used to reduce a possible over voltage to prevent the inverters over voltage protection of getting active. The inverter consumes reactive power to reduce the voltage level and is not reducing the generated power [19].

$Q(U)$ combined with $P(U)$

This control strategy combines the control strategies of $Q(U)$ and $P(U)$. First the $Q(U)$ strategy gets active to reduce the overvoltage and if the overvoltage is still at a very high level the inverter reduces additionally the generated active power. As [19] has been investigating further into this strategy in their set up the $P(U)$ control is only active one third of the time and leads to generation losses by about 2,5% [19].

$L(U)$

This control strategy proposes a inductance along the feeder which absorbs reactive power at a high voltage level to stop the voltage from rising further. This inductance is most likely a coil which can be controlled continuously to hold the voltage at a predefined set point. As this device is part of the grid no customer has a reduction of its distributed generation hence this strategy is free of discrimination [14].

Q-Autarkic customers

The control strategy $Q - Autarky$ proposes that every customer has to provide its own reactive power and the grid has not the function of providing reactive power or consuming reactive power anymore. At the Link-Link of the LVL and the CPG the exchange of reactive power shall be zero and only active power shall be exchanged. The advantage of this strategy is that the grid operator of the overlaid distribution grid only have to manage their own reactive power balance [14].

2.3.5 Legal framework

In the previous sections it was already mentioned, that there is a legal framework which has to be considered before applying conditions for the consumers, if they want to connect to the grid and get prosumers. In Austria the grid code differs between DGs

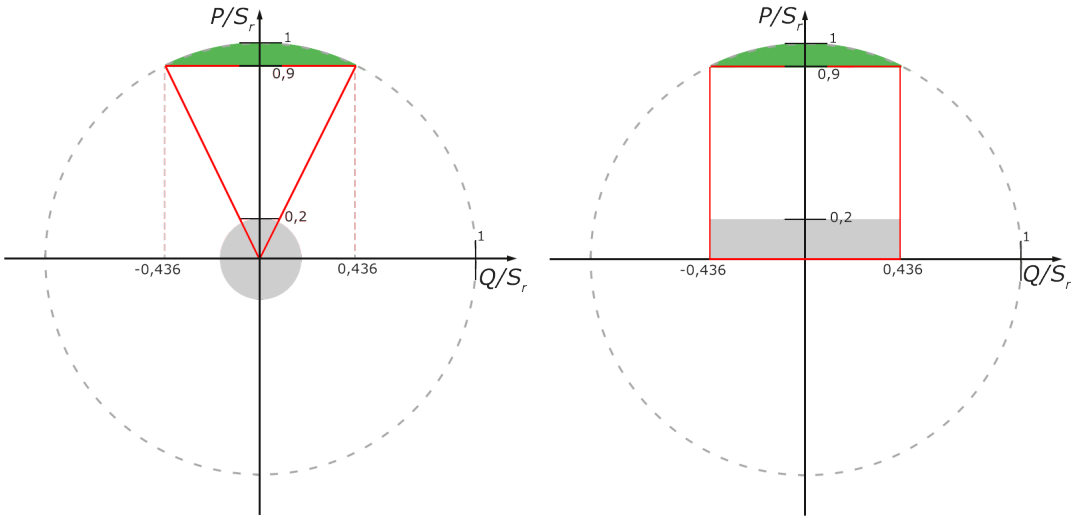

Figure 2.13: Legal framework for different inverter power (a) $S_r <= 3,68kVA$ (b) $S_r > 3,68kVA$ [20].

by the installed electrical power of the inverter and also whether the connection point is in the MVG or LVG. As this thesis investigates on the voltage control in the LVG only the terms for the LVG is explained. If the inverter power is equal or lower than S_r=3,68 kVA the terms for the conncetion are simpler. Below an active power infeed of $0,2 \cdot S_r$ the inverter does not need to follow any rules, the grey area in Figure 2.13 (a). From $P = 0,2 \cdot S_r$ to $P = 0,9 \cdot S_r$ the inverter has to be able to follow a certain reactive power target, from $\cos(\varphi) = 0,90$ underexcited to $\cos(\varphi) = 0,90$ overexcited, specified by the DSO, illustrated by the red triangle in Figure 2.13 (a). If the active power infeed exceeds $0,9 \cdot S_r$ the inverter has to be freely adjustable to the requirements of the DSO. If the inverter power is higher than S_r = 3,68 kVA the terms that the inverter has to fulfill are more sophisticated. Again in the scope below $P = 0,2 \cdot S_r$ the inverter does not need to follow exactly the ruling of the DSO, grey area in the Figure 2.13. In the range of $P = 0,2 \cdot S_r \ldots 0,9 \cdot S_r$ the inverter has to be able to support the DSO with $\cos(\varphi) = 0,9$ both over- and underexcited, in the Figure 2.13 (b) the red framed area. If the inverter power exceeds the active power infeed of $P = 0,9 \cdot S_r$ the inverter has to be able to reach any targeted value specified by the DSO, in the figure 2.13 (b) it is illustrated by the green area [20]. There are several strategies for the DSO to control the static voltage in the Grid-Link with the support of the DGs with an inverter power $S_r > 3,68kVA$, like reactive power control or active power curtailment. These strategies require the inverter to be able to operate with a fixed power factor $\cos(\varphi)$, with a fixed reactive power operating point Q, with an active power output depending on the power factor $\cos(\varphi)(P)$ and with a voltage dependent reactive power operating point $Q(U)$. As long as there is no specific ruling of the DSO within the scope of the legal framework illustrated in Figure 2.13 the default value is $\cos(\varphi) = 1$. The DSO is permitted to give

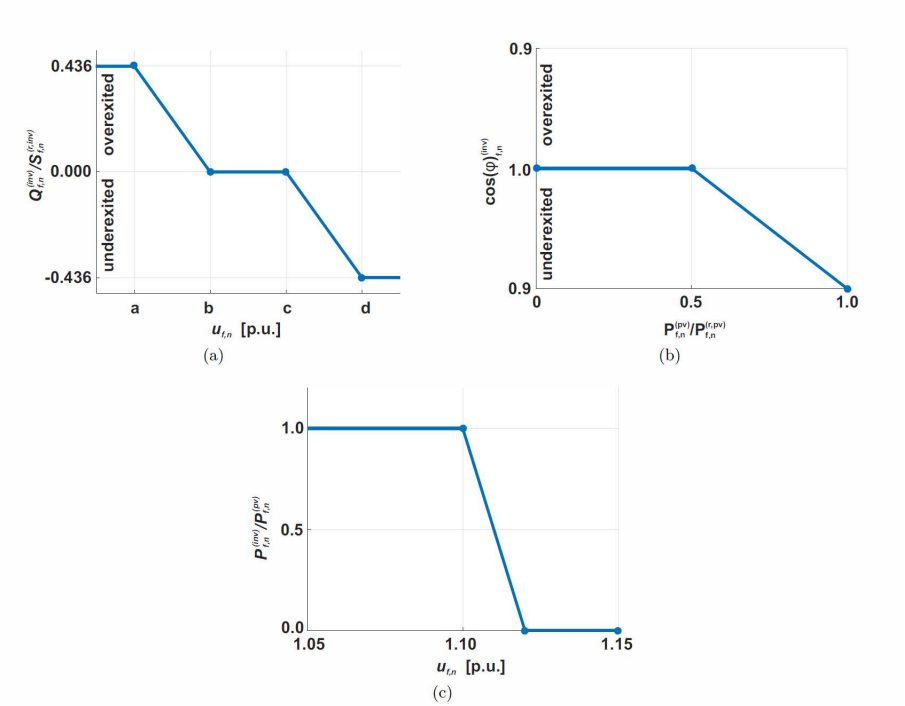

Figure 2.14: Standard characteristics for inverters with $S_r > 3,86kVA$ defined in [20] (a) $Q(U)$ strategy, (b) $\cos(\varphi)(P)$ strategy, (c) $P(U)$ strategy [14].

different inverters different rulings, since the voltage is a local value and no global value like the frequency. In Figure 2.14(a) the standard $Q(U)$ control stragy is illustrated, there has to be minimal four points defined for the reactive power control. All points have to be in the legal framework, as long as not every phase is controlled the phase with the highest voltage has to be considered for the control strategy. Figure 2.14(b) presents the standard characteristic for a $\cos(\varphi)(P)$ control strategy and in Figure 2.14(c) the $P(U)$ control strategy is shown. All characteristics can be adapted by the DSO to the local inverters and grid requirements as long as they are still in the legal framework. The control strategies may not cause any dynamic problems, as they only shall help with static problems in the grid [20]. As already told overvoltages can be controlled by active power curtailment, so a strategy could be to lower the infeed of a DG to prevent their overvoltage protection device to cut the whole generator from the grid, by this the generation is more stable and less volatile in critical grid situations with initial high voltages given by the overlaid grid. The inverters which are connected to the MVG and those who are controllable and connected to the LVG, have to fulfill also the following frequency dependent behaviour. They are only allowed to operate between a grid frequency from 47,5 to 51,5 Hz, if the frequency is out of these bounds the inverter has to shut down. These boundaries can be useful i.e. for repowering the grid after a black out, if the DGs are too volatile for a secure grid operation. There is also a ruling in the frequency scope in which the inverter is allowed to be active, this ruling shall prevent a shut down of all DGs from full infeed at 51,5 Hz, the inverters have to curtail

their active power output, from 50,2 Hz on the active power infeed has to be reduced by 40%/Hz of the actual power infeed of the inverter at the moment of the over-frequency.

2.4 Load model

There are different ways to describe the static loads in a grid i.e. the load can be modelled via constant impedance load model, constant power load model, constant current load model, exponential load model or via a polynomial load model. The polynomial model is the simplified exponential model. In this thesis the ZIP model is used, which describes the static loads via a polynomial characteristic. The model seperates the load into active and reactive power and combines each of them with a mix of three loads with different characteristics shown in Figure 2.15. There is also a frequency dependent part $(1 + k_{pf} \cdot \Delta f)$, which is a result of a Taylor approximation of the term $\left(\frac{f}{f_n}\right)^{k_{pf}}$, f_n is the nominal frequency, f is the frequency at the bus bar, the exponents k_{pf} and k_{qf} are sensitivity factors. It is getting obvious by equation 2.27, that the frequency dependent part can be discarded if there is no significant change in the frequency [21].

$$P = P_n \cdot \left[Z_p \cdot \left(\frac{U}{U_n} \right)^2 + I_p \cdot \left(\frac{U}{U_n} \right) + P_p \right] \cdot \left(1 + k_{pf} \Delta f \right) \tag{2.25}$$

$$Q = Q_n \cdot \left[Z_q \cdot \left(\frac{U}{U_n} \right)^2 + I_q \cdot \left(\frac{U}{U_n} \right) + P_q \right] \cdot \left(1 + k_{qf} \Delta f \right) \tag{2.26}$$

$$\Delta f = \frac{f - f_n}{f_n} \tag{2.27}$$

Further on in this thesis only the voltage dependent part of the load model is used shown in equations 2.28 and 2.29, as the frequency is not changed significantly. The coefficients of the model $Z_p, I_p, P_p, Z_q, I_q, P_q$ are the parameters which define the percentages of constant impedance, constant current and constant power load [21].

$$P = P_n \cdot \left[Z_p \cdot \left(\frac{U}{U_n} \right)^2 + I_p \cdot \left(\frac{U}{U_n} \right)^2 + P_p \right] \tag{2.28}$$

$$Q = Q_n \cdot \left[Z_q \cdot \left(\frac{U}{U_n} \right)^2 + I_q \cdot \left(\frac{U}{U_n} \right)^2 + P_q \right] \tag{2.29}$$

The loads of a houshold have a vast variety of different types. There are resistive loads like heating utilities, which can be characterized as a constant impedance load. Lightning by light-emitting diod, which behave as constant power loads. Electronic devices can be seperated into consumer electronics and in information communication technology loads, depending on the rated power of the device they need to be able to correct their power factor. The characterisitic of the electronic loads can be seen as a constant

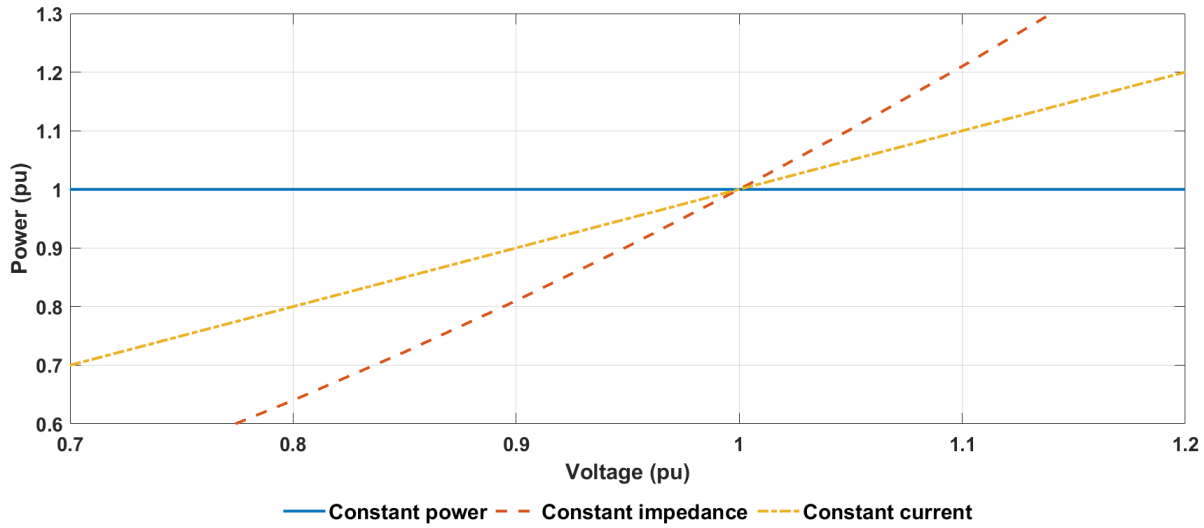

Figure 2.15: Load characteristics for constant impedance constant current and constant power loads.

power load. There are also single phase connected induction motors, which are powering dishwashers, refrigerators or washing machines and so forth. Their load characterisitc is depending on their mechanical behaviour therefor they need to be divided in the following types: constant torque, linear torque, quadratic torque or constant mechanical power. Additionally depending on the starting torque and speed requirements, they can be further classified into: "resistive start - inductive run", "capacitive start - inductive run" and "capacitive start - capacitive run" [21]. In table 2.1 there are examples for

Customer class	Z_P	I_P	P_P	Z_Q	I_Q	P_Q
Residential type A	1.31	-1.94	1.63	9.2	-15.27	7.07
Residential type B	0.96	-1.17	1.21	6.28	-10.16	4.88
Residential type C	1.18	-1.64	1.47	8.29	-13.67	6.38
Industrial	1.21	-1.61	1.41	4.35	-7.08	3.72

Table 2.1: ZIP coefficients of different load classes during summer period [14].

ZIP coefficients for three types of residential loads and an industrial load. Those ZIP coefficients can be used to describe different types of grids like the loads of a rural grid or an urban grid. The voltage dependency of the load model with the ZIP coefficients from the residential type B is shown in Figure 2.16.

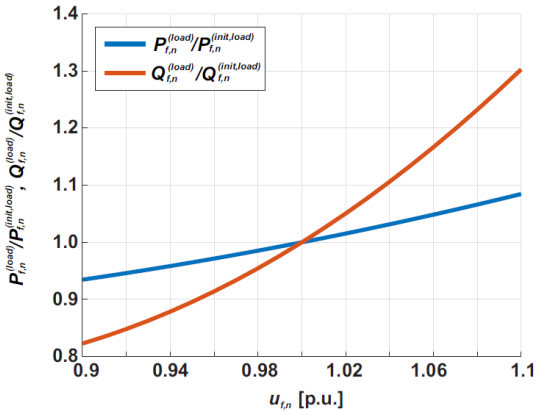

Figure 2.16: Voltage dependency of a residential customer (ZIP coefficients residential type B from table 2.1) [14].

2.5 Size and position of LVRs

The previous sections already discussed that, the DSO is responsible to provide a certain voltage band for the connected customers. The DSO has some measures that can be taken to ensure the voltage band, like reinforcing the grid to reduce the line impedances or control the active and reactive power flow within the grid, another measure is to install LVRs for the voltage control. In a smart grid all the actions shall be possible by measuring local variables like the frequency or the voltage, for optimising the power flows of P and Q. So there is no need to exchange data between customers and grid operator, for the local control of the grid. The customers need to be able to provide themselves with reactive power to be able to have a local control. This potential to increase the photovoltaics in the grid by a local control via the inverters was investigated in the project "morePV2grid" and the conclusion was that it is a very cost-efficient way to increase the amount of PV power in the grid [22]. Another possible way to control the voltage in the grid could be to use LVRs to set the voltage back into the limits in combination with the inverters, which is providing the reactive power for the prosumer. As already discussed the DSO can control the voltage in the grid via OLTCs if necessary and can also manually change the tap changers of the DTR from MVL to LVL, which is seldom done. In this case it is only possible to control the voltage in the whole MVG section and not in the individual LVG parts, where the voltage violations are. To be able to control the voltage in the LVG and to be sure to stay within the voltage band it is possible to install a LVR, which is basically a transformer with series regulation by an OLTC, due to cost-efficiency an autotransformer is chosen. The Figure 2.17 shows how the LVR is raising and reducing the voltage of a feeder. The LVR is considered to be a good option because it is possible to get rid of voltage violations by over-voltage and by under-voltage. The over-voltage and the under-voltage violations are the two cases, which need to be solved, because when the sun is high the grid is likely to have an over-voltage violation and in the evening it is possible to have an under-voltage violation. The voltage spreading over the day is because of the big gap between maximum feed in

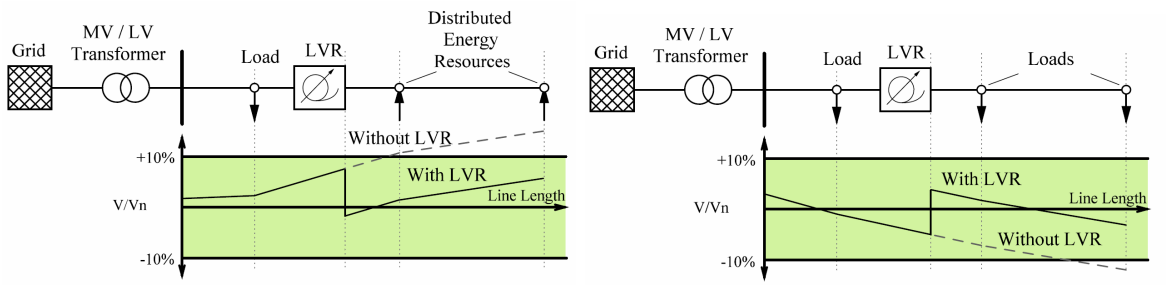

(a) (b)

Figure 2.17: Impact of a LVR to the voltage (a) Raising the voltage (b)Reducing the voltage [23].

and maximum demand by the customers.

2.5.1 Sizing and Positioning

The optimal placement of the LVR depends on the structure of the grid and of the first voltage violation of the feeder, the placement also defines the sizing of the LVR. The needed range of the autotransformers ratio n_t also has an impact to the sizing of the autotransformer S_{LVR} compared to a conventional size S_{conv} of an autotransformer with two windings. In equation 2.30 it is getting obvious that if the needed range is rising also the needed size is rising and so are the costs of the LVR. The equations 2.31 to 2.34 show how the LVR is affecting the voltage in the equations 2.31 and 2.32 the LVR is positioned further to the end of the feeder, in this position it is affecting the voltage less than in the equations 2.33 and 2.34, in which the position of the LVR is farer away from the end of the feeder. Only the terms which are multiplied with the autotransformer ratio n_t are affected by the autotransformers ratio. If the autotransformer is put further to the end of a line the losses by it are less, because $|I_{sgm(n-1)}| > |I_{sgm(n)}|$ but the needed ratio is higher and by this the sizing of the autotransformer is getting higher, as equation 2.30 illustrates. So the optimal placement is next to the first voltage violation either if

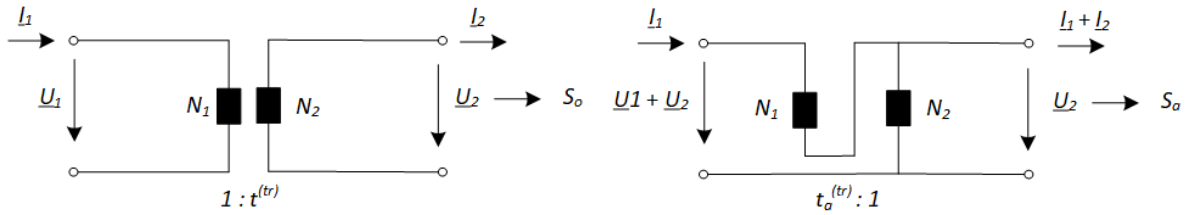

(a) (b)

Figure 2.18: Differences between an autotransformer and an normal transformer (a) Simplified normal transformer (b) Simplified autotransformer.

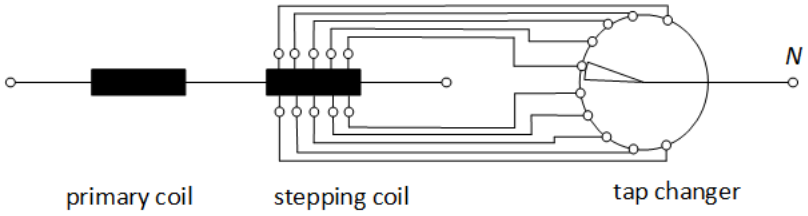

Figure 2.19: Simplified schematic of an OLTC.

it is an under or an over-voltage [24].

$$S_{LVR} = \frac{1 \pm n_t}{n_t} \cdot S_{conv} \tag{2.30}$$

$$\Delta \underline{U}_{(n-3)} = \underline{Z}_{(n-2)} \cdot \underline{I}_{sgm(n-2)} + \underline{Z}_{(n-1)} \cdot \underline{I}_{sgm(n-1)} + n_{t_{high}} \cdot \underline{Z}_n \cdot \underline{I}_{sgm(n)} \tag{2.31}$$

$$\Delta \underline{U}_{(n-2)} = \underline{Z}_{(n-1)} \cdot \underline{I}_{sgm(n-1)} + n_{t_{low}} \cdot \underline{Z}_n \cdot \underline{I}_{sgm(n)} \tag{2.32}$$

$$\Delta \underline{U}_{(n-3)} = n_{t_{high}} (\underline{Z}_{(n-2)} \cdot \underline{I}_{sgm(n-2)} + \underline{Z}_{(n-1)} \cdot \underline{I}_{sgm(n-1)} + \underline{Z}_n \cdot \underline{I}_{sgm(n)}) \tag{2.33}$$

$$\Delta \underline{U}_{(n-2)} = n_{t_{low}} (\underline{Z}_{(n-1)} \cdot \underline{I}_{sgm(n-1)} + \underline{Z}_n \cdot \underline{I}_{sgm(n)}) \tag{2.34}$$

2.5.2 Autotransformer

An autotransformer is a transformer which has only one coil for the primary and secondary side of the transformer. Each transformer with two coils can also be operated as an autotransformer by adding the secondary coil to the primary coil, as Figure 2.18 presents. The transformation ratio of the autotransformer changes in relation to a normal transformer, which is displayed in equation 2.35.

$$t_a^{(tr)} = \frac{N_1 + N_2}{N_2} = 1 + \frac{N_1}{N_2} = 1 + \frac{1}{t^{(tr)}} \tag{2.35}$$

The autotransformer is more cost efficient compared to the normal transformer, especially if the voltage ratio is very low from primary to secondary side. This efficiency is getting visible as the apparent power (S_a) is compared to the output power (S_o) of an autotransformer. As a normal transformer has the same apparent power as the output power (equation 2.36) the autotransformer has a higher output power than the apparent power. The output power is by the factor $(1 + t^{(tr)})$ bigger than the apparent power, as equation 2.37 makes obvious. The equations 2.36 and 2.37 can be deduced from Figure 2.18.

$$S_a = S_o = U_2 \cdot I_2 = U_1 \cdot I_1 \tag{2.36}$$

$$S_a = U_2 \cdot (I_1 + I_2) = (U_1 + U_2) \cdot I_1 = (1 + t^{(tr)}) \cdot S_o \tag{2.37}$$

This advantage is getting bigger as the transmission ratio of the full transformer is increasing or the transmission ratio of the autotransformer is decreasing. This gets apparent by equation 2.35, by this autotransformer are primarily used for the coupling of two different Grid-Links. One main disadvantage of the autotransformer is the missing galvanic seperation, which entails the full transfer of voltages relative to earth due to unsymmetrical errors. An autotransformer is only used, if both sides have their own grounding. Another disadvantage of the autotransformer is a higher short circuit current compared to a normal transformer, because of this the stray reactance needs to be designed bigger as usual. The OLTC of an autotransformer is similar to the normal transformer in star position, to only have the need of one tap changer, the difference is that the OLTC is not between primary side and star point, but between secondary coil and star point. Figure 2.19 shows the principal structure of an OLTC of an autotransformer [13].

3 Model Description

This chapter describes the modelling of the used grids, the transformer model, the line model, the load model, the Generation model and the used voltage control model. These models are used in the simulations. In section 3.1 the low voltage grid links are described from the topology over the customer structure to the electrical equipment of the grid link. In section 3.2 the model of the power transformer connecting the low voltage grid link with the medium voltage grid link. Section 3.3 describes the LVR model which is used in the Grid-Links and also the parameters of the used LVRs, the used voltage control strategy of the LVR is also presented. In section 3.4 the line model is shown and the used parameters for the overhead lines and the cable lines. Section 3.5 specifies the model of the native lumped loads, e.g. the used ZIP factors for the assumed voltage dependency. In section 3.6 the generation model for the PV is presented as well as the different strategies for an active or reactive power management.

3.1 Low Voltage Grid-Link

To get a broad insight into the effects of a LVR, two different low voltage grids European style are observed. The Grid-Links have certain specific characteristics and are differing in size, customer structure, cable to overhead line ratio, photovoltaic penetration or power transformer rating. As already mentioned the Grid-Links can be simulated with a single-phase model. The topology and technical data which are required for the simulation are provided by the "Institute of Energy Systems and Electrical Drives" of the "Technische Universität Wien". For each network the total annual energy consumption E_{sec}^{2016} and the peak active power $P_{sec}^{(2016)}$ was measured throughout the year 2016 at the transformers secondary sides. The different customers can be specified into classes, which are residential, commercial and industrial. Tables 3.1 and 3.2 are summarizing the properties of the different Grid-Links. The measured energy consumption includes PV-production, the customer's consumption and the grid losses during the whole year. To approximate the average energy consumption of a single residential customer in the residential Grid-Links, equation 3.1 can be used. The result of equation 3.1 is used to

Link-Grid	$N^{(res)}$ [1]	$N^{(com)}$ [1]	$N^{(ind)}$ [1]	$P^{(r,pv)}$ [kW]	$E_{sec}^{(2016)}$ [kWh]	$P_{sec}^{(2016)}$ [kW]
Large Urban	175	0	0	168	1127040	349
Rural	61	0	0	20	320165	85

Table 3.1: Overview of the customer structure in the used Grid-Link [14].

Grid-Link	F [1]	cable share [% of km]	total line length [km]	max feeder length [km]	$S^{(r,tr)}$ [kVA]
Large Urban	9	96.14	12.815	1.270	630
Rural	4	58.64	6.335	1.630	160

Table 3.2: Overview of the Grid-Link's size [14].

get the ZIP coefficients for the residents in the different Grid-Links, the assignment of the ZIP coefficients from table 2.1 are shown in table 3.7.

$$E_{res} = \frac{E_{sec}^{(2016)}}{N^{(res)}} \tag{3.1}$$

3.1.1 Rural Grid-Link

Figure 3.1 shows the simplified Grid-Link with only the main branches of the feeders visible in this figure. In the appendix Figure A.1 contains more details of the Grid-Link. The cable share is about 59%, the Grid-Link has 4 feeders, which are supplying 61 residential customers, which consume 5.25 MWh in average per year and resident. The slack in the simulations is located at the primary side of the DTR, which has no OLTC.

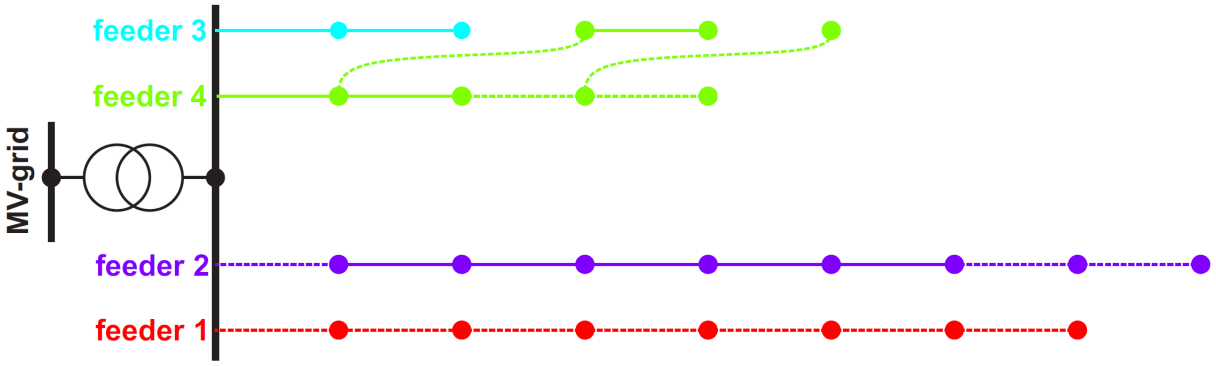

Figure 3.1: Rural Grid-Link (simplified) [14].

3.1.2 Large Urban Grid-Link

Figure 3.2 shows the simplified Grid-Link with only the main branches of the feeders are shown in this figure. In the appendix Figure A.3 contains more details of the Grid-Link. The cable share of this Grid-Link is about 96% and supplies only urban residents. The Grid-Link contains many new build single-family houses, which are larger than average residents. This gets obvious by a higher energy consumption of about 6.64 MWh per resident. The slack in the simulations is located at the primary side of the DTR, which

has no OLTC. The Grid-Link also contains nine feeders, as shown in Figure 3.2 and supplies 175 residential customers.

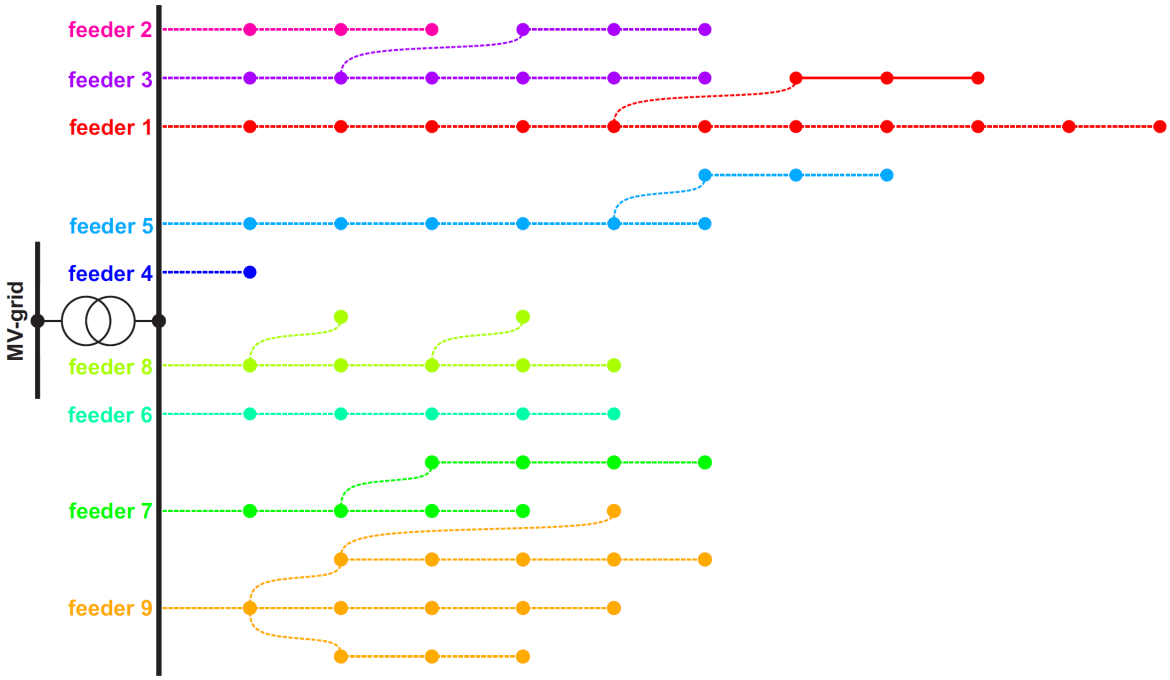

Figure 3.2: Large Urban Grid-Link (simplified) [14].

3.2 Transformer model

The transformers are modelled with the equivalent circuit diagram shown in Figure 3.3. The losses of the transformers core are neglected, by this $Y^{(tr)} = 0$ and is not further used. In combination with table 3.3 and equations 3.2 and 3.3, the model impedances can be calculated.

$$R^{(tr)} = u_r \cdot \frac{(U^{(r,tr,p)})^2}{S^{(r,tr)}} \tag{3.2}$$

$$X^{(tr)} = \sqrt{u_k^2 - u_r^2} \cdot \frac{(U^{(r,tr,p)})^2}{S^{(r,tr)}} \tag{3.3}$$

Grid-Link	$S^{(r,tr)}$ [kVA]	$U^{(r,tr,p)}$ [kV]	$U^{(r,tr,s)}$ [kV]	u_k [%]	u_r [%]	Vector group
Large Urban	630	20.00	0.40	4.00	1.00	Dyn5
Rural	160	20.00	0.40	4.04	1.00	Yzn5

Table 3.3: Data of the distribution transformers within the network models [14].

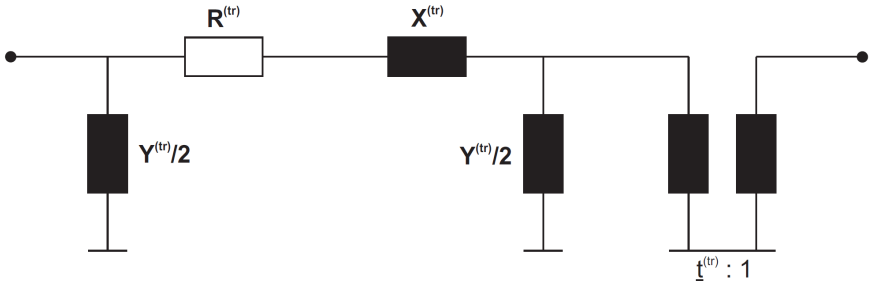

Figure 3.3: Equivalent circuit model of a transformer [14].

3.3 LVR model

The LVR is an autotransformer, which has, although the setup is different, the same equivalent circuit diagram as the normal transformer, shown in Figure 3.3, but with different parameters. The characteristic transformation ratio is determined in equation 3.4.

$$t^{(tr)} = 1.0 + \frac{(t_{max}^{(tr)} - (t_{min}^{(tr)})}{2} \tag{3.4}$$

The impedances of the autotransformer changes with the transformation ratio. It is calculated from the characheristic impedance, the characteristic transformation ratio and the present transformation ratio. In equation 3.6 it is getting apparent, that the impedance is changing quadratically with the transformation ratio. Table 3.4 shows the autotransformer data which are used in the thesis.

$S_r^{(tr)}$ [kVA]	$U^{(r,tr,p)}$ [kV]	$U^{(r,tr,s)}$ [kV]	$Z_k^{(tr)}$ Ω	$u_{k,n}$ [%]	$u_{k,min}$ [%]	$u_{k,max}$ [%]	Vector group
34	0.165- 0.295	0.23	0.0527	1.02	1.99	0.62	Y0
69	0.165- 0.295	0.23	0.0213	2.07	4.03	1.26	Y0
92	0.165- 0.295	0.23	0.0159	2.77	5.37	1.68	Y0
150	0.165- 0.295	0.23	0.0095	4.51	8.76	2.74	Y0

Table 3.4: Data of the autotransformers within the network models.

$$Z^{(tr)} = \sqrt{R^{(tr)^2} + X^{(tr)^2}} \tag{3.5}$$

$$Z_{act}^{(tr)} = Z^{(tr)} \cdot \frac{(1.0 - t_{act}^{(tr)})^2}{(1.0 - t^{(tr)})^2} \tag{3.6}$$

As with the DTR the losses of the transformers core are neglected again by $Y^{(tr)} = 0$. The rated short circuit voltage is calculated via equation 3.7. Table 3.4 shows the calculated autotransformer data which is used in the Link-Grids, the base data is used

from [25], the voltages are phase voltages. The OLTC has 13 steps to control the voltage.

$$u_k^{(tr)} = \frac{Z_k^{(tr)} \cdot S_r^{(tr)}}{U_{r(pr)}^{(tr)^2}} \tag{3.7}$$

3.4 Line model

Overhead lines as well as cables are modelled with the equivalent circuit diagram shown in Figure 3.4. The impedances of the model $R^{(sgm)}, X^{(sgm)} and B^{(sgm)}$ can be calculated with equations 3.8, 3.9 and 3.10, with the parameters from table 3.5. Table 3.5 shows different line data of cables and overhead lines which are used by the DSO, who owns the investigated Grid-Links. The variables not defined in table 3.5 are l, which is the length of the line and f the system frequency of 50 Hz.

Grid-Link	**A** $[mm^2]$	I_{th} [A]	**R'** $[\frac{\Omega}{km}]$	X'_L $[\frac{\Omega}{km}]$	**C'** $[\frac{\mu F}{km}]$	$\frac{R'}{X'_L}$
C-AL	25	100	1.2000	0.0890	0.550	13.48
	50	145	0.6410	0.0850	0.720	7.54
	95	215	0.3200	0.0820	0.950	3.90
	150	275	0.2060	0.0800	1.040	2.58
	240	360	0.1250	0.0800	1.200	1.56
C-CU	16	100	1.1500	0.0890	0.500	12.92
	25	130	0.7270	0.0880	0.550	8.26
	35	155	0.5240	0.0850	0.630	6.16
OL-AL	50	210	0.6152	0.3764	0.000	1.63
	95	320	0.3264	0.3557	0.000	0.92

Table 3.5: Data of the cables and overhead lines within the network models [14].

$$R^{(sgm)} = R' \cdot l \tag{3.8}$$

$$X^{(sgm)} = X'_L \cdot l \tag{3.9}$$

$$B^{(sgm)} = 2\pi f \cdot C' \cdot l \tag{3.10}$$

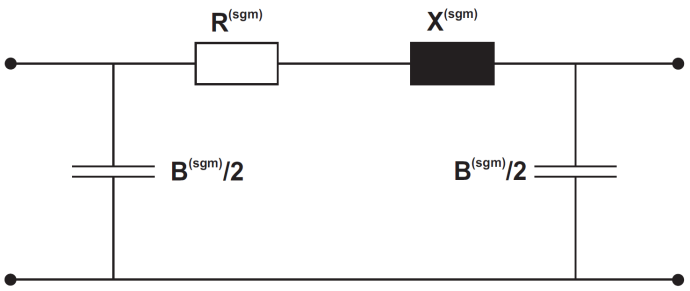

Figure 3.4: Equivalent circuit model of a line [14].

3.5 Load model of houses

The relevant information for the load flow simulation of the customers connected to each Grid-Link is the consumption of active and reactive power, by which they can be characterised. The initial values for the active and reactive power consumption are on one side defined by the scenario itself and on the other side by the assumed power factors, given by table 3.6.

	residential	commercial	industrial
$\cos(\varphi)^{(load,init)}$	0,95	0,90	0,90

Table 3.6: Power factors of different load classes and generators [14].

The load model which is used to model the customers is the ZIP model. The ZIP model defines loads as *PQ*-loads. The paper [26] tested different loads to evaluate their specific ZIP coefficients and suggests different sub classes for residential customers depending on their annual energy consumption. As for each Grid-Link only the summarised annual energy consumption is known, therefor all customers have the same annual energy consumption and the same sub class in one Grid-Link by this also the same ZIP-coefficients. The sub classes are categorized by their energy consumption from type A, which has the lowest annual energy consumption to type F, with the highest annual energy consumption, the assignment of the Grid-Links is listed in table 3.7, for this thesis only type A to type C is relevant. [26] also investigates into different commercial customers differing them by their business fields, the paper also proposes to use different subclasses.

3.5.1 Common load profile

The common load model is based upon [26]. The ZIP Coefficients are constant over the whole day. The coefficients used for the loads of the Residential Grid-Link and the Large Urban Grid-Link are summarised in table 2.1 they are coordinated with [14] and refer to [26]. Figure 3.5 shows the load profile of the active and the reactive power combined with the injection power of the installed PVs. The injection power of the installed DGs is considered later in this chapter.

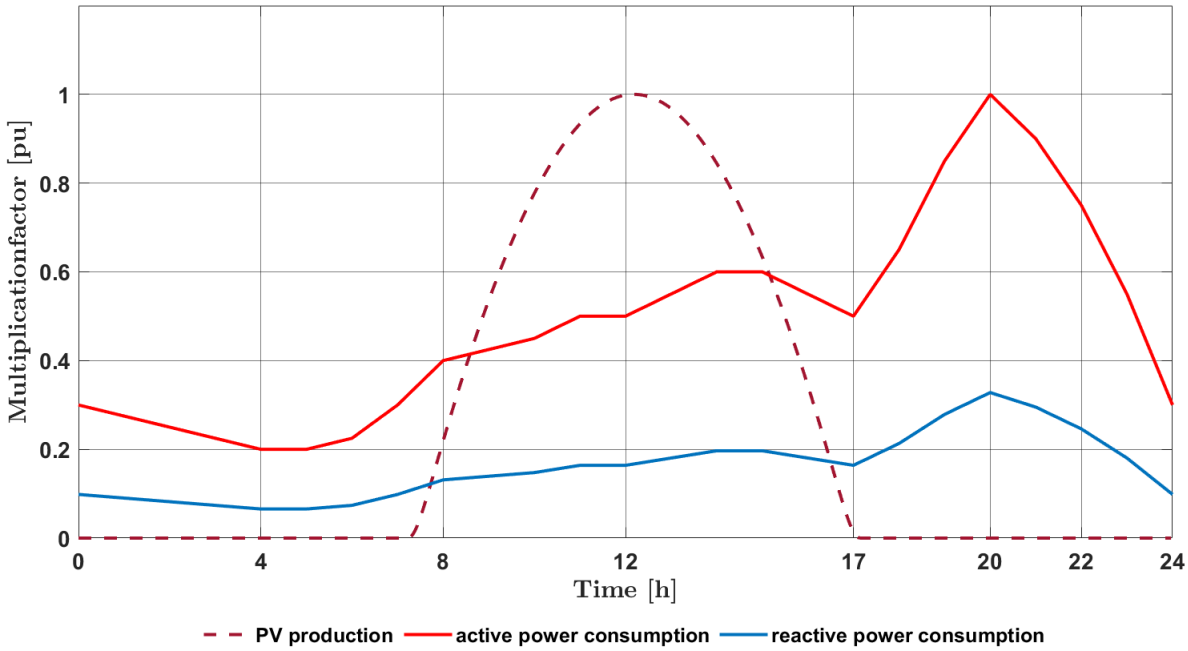

Figure 3.5: PV injection and load profile used for both Grid-Links

Grid-Link	Sub class	Z_P	I_P	P_P	Z_Q	I_Q	P_Q
Large Urban	type B	0.96	-1.17	1.21	6.28	-10.16	7.07
Rural	type B	0.96	-1.17	1.21	6.28	-10.16	7.07

Table 3.7: Assignment of ZIP coefficients to the different Grid-Links [26].

3.5.2 Load profile in presence of modern equipment

The thesis also investigates into a new model of ZIP coefficients and new load profile, which is considered a modern load characteristics of residentials by using only LED as lighting or a heat pump as an example. The model is presented by [27].

Time	Z_P	I_P	P_P	Z_Q	I_Q	P_Q	$P_{peak} \cdot f_P$	$P_{peak} \cdot f_Q$
12:00 PV$_{max}$	0.55	-0.08	0.53	1.14	-0.6	0.47	0.54	0.12
17:00 Q_{max}	0.58	-0.06	0.48	1.08	-0.48	0.4	0.95	0.18
22:00 Q_{min}	0.38	0.06	0.56	3.9	-3.26	0.36	0.55	-0.04

Table 3.8: Varied ZIP coefficients of different times [28].

The ZIP coefficients are changing over the day as the mix of electrical equipment used by the residential is. [27] also suggests a specific load profile which is varying the $\cos\varphi$ of the residentials, the base of the variation is the maximal active power. This thesis investigates into three characteristic times. The times are 12:00, when the PV injection

is at its maximum, 17:00 in this point the reactive power consumption is maximal and 22:00 when the reactive power consumption is minimal and is even getting negative. In table 3.8 the ZIP coefficients and the power multiplication factors are presented. In Figure 3.6 the new load profile is presented and the special times are marked [27].

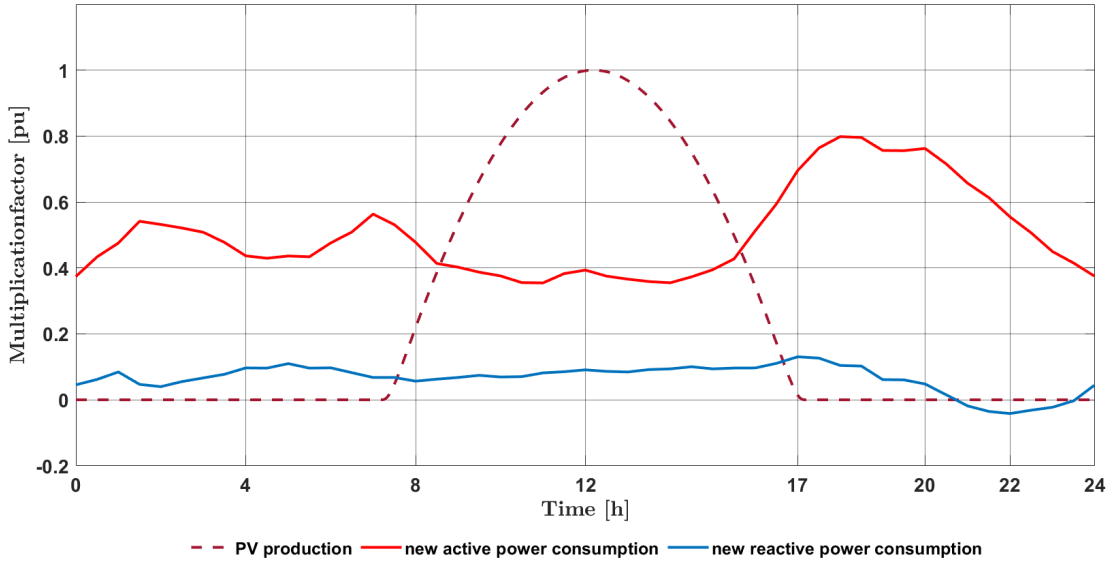

Figure 3.6: New load profile with new ZIP coefficients [27].

3.6 Various PV penetration levels

The PV penetration needs to be considered, as the voltage violation of the upper limit is dependent of the PV penetration level. The national states are promoting PV arrays differing by size, in Austria a PV with an active power output up to $P = 5$ kWp is treated different as the PVs above this threshold [29]. In this thesis it is assumed that every residential has a PV array of an active power injection of $P = 5$ kWp. This is also the threshold when voltage violations of the upper limits are occuring on the feeders. Figure 3.5 shows both the load profile and the PV profile and makes it obvious that the maxima and minima are at different locations during the day.

3.7 Control strategies

The DGs are photovoltaic systems, which contains a PV-Array, an inverter and an overvoltage protection. Before the active power is exchanged with the grid it has to pass the inverters control characteristic and the overvoltage protection. The inverters are assumed to be slightly over dimensioned, according to equation 3.11.

$$S_{f,n}^{(r,inv)} = \frac{1}{0,9} \cdot P_{f,n}^{(r,pv)} \tag{3.11}$$

The inverters are assumed to have an efficiency of 100%, their control characteristics are explained in the following sections. The overvoltage protection disconnects the inverter and so on the PV-array if the local voltage exceeds 1,1 p.u. of the nominal voltage. Figure 3.7 shows the characteristic of the overvoltage protection.

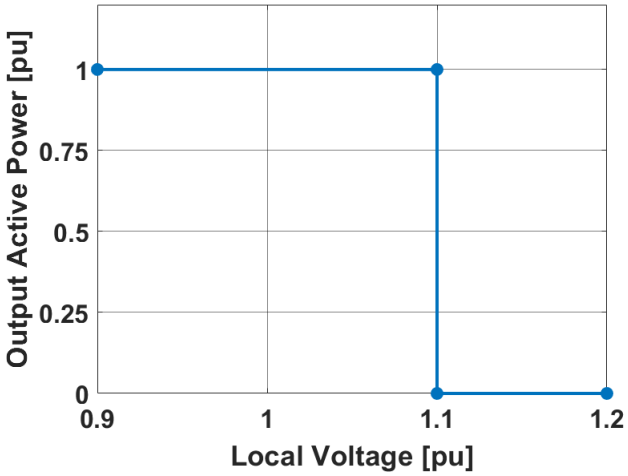

Figure 3.7: Overvoltage protection characteristic.

3.7.1 Inverter based control strategies

Uncontrolled inverter

To simulate CP-Producer-Links with uncontrolled inverters, the inverters are modelled as PQ-producer with an active power injection at $\cos(\varphi) = 1$.

$P(U)$

The PV-inverters are again modelled as PQ-producers which are injecting active power at $\cos(\varphi) = 1$. This time the inverters have additionally a $P(U)$-control. Figure 3.8 shows the characteristic of the $P(U)$ control strategy.

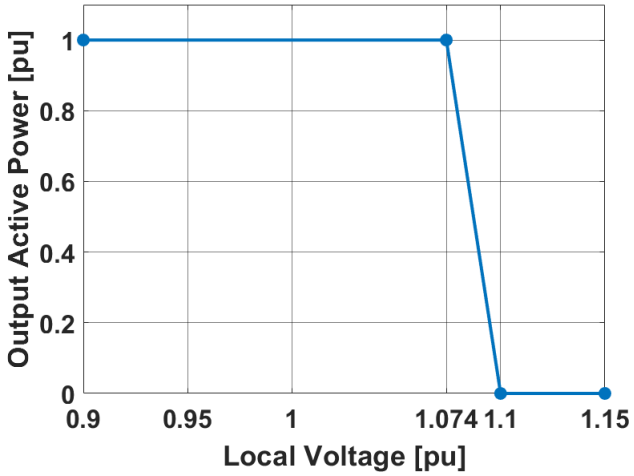

Figure 3.8: $P(U)$ characteristic.

$Q(U)$

The PV-inverters are modelled as a $Q = f(U)$-producer. In this case the active power is not influenced by the control strategy but the reactive power is. The reactive power injection or absorption is a function of the local voltage.Figure 3.9 shows the characteristic of the $P(U)$ control strategy.

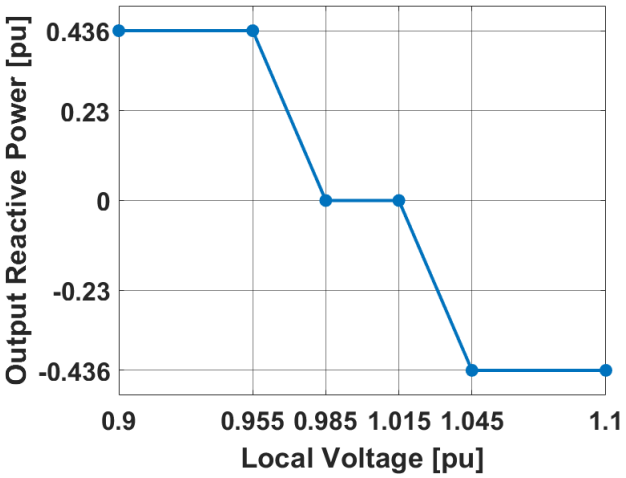

Figure 3.9: $Q(U)$ characteristic.

$\cos\varphi(P)$

This time the PV-inverters are modelled as a $\cos(\varphi) = f(P) - producer$. The active power is not influenced by the inverters control strategy, while the reactive power absorbtion or injection is manipulated. The reactive power is a function of the corresponding

PV-array's output power. Figure 3.10 shows the characteristic of the $P(U)$ control strategy.

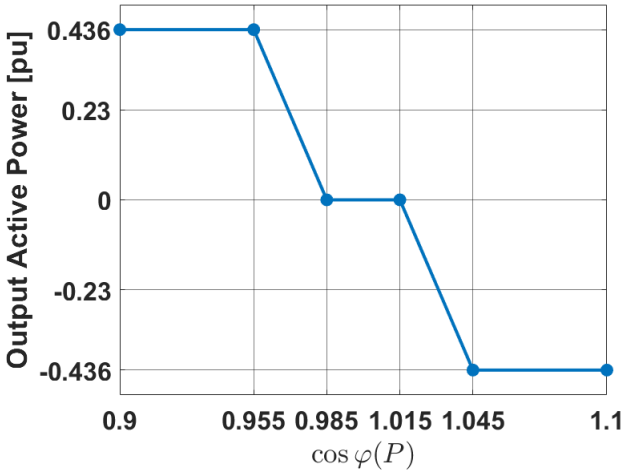

Figure 3.10: $\cos\varphi(P)$characteristic.

3.7.2 Q-Autarkic customers

To simulate $Q - Autarkic$ customers the CPG-Links will inject and consume power at $\cos(\varphi) = 1$. The PV-arrays are modelled as PQ-producers. The customers without a DG are assumed to consume power at $\cos(\varphi) = 1$.

4 Scenario Definition

In this chapter the investigated scenarios are defined, the base cases are presented, as well as the different posibilities of load values and PV penetrations in the Grid-Links. Different load profiles and production profiles are considered, as the profiles are essential for the different voltage violations. The primary voltage of the DTR is also to be considered, because it is essential for the voltage levels in the underlying Link-Grids. If the voltage level of the underlying Grid-Link is already at a high level, the violation of the voltage is getting more likely. The base cases are used to compare the different actions, which need to be taken to get rid of the voltage limit violations.

4.1 Primary voltages of the DTR

The primary voltage of the DTR is dependent on the OLTC position of the power transformer connecting the MVG to the overlaid Grid-Links. The DSO which gave the data for the investigation is controlling omatically the OLTC to hold the voltage in the following voltage levels, the upper limit of the regulation is 1.06 pu of the nominal voltage, the lower limit is 0.96 pu of the nominal voltage. The worst case scenario for the simulated LVG is the high voltage limit 1.06 pu which is causing high voltage levels in the whole LVG as the DTR has a fixed tap position. This is very likely to happen as the voltage along the MV feeder varies and can be high on one side and low on the other side, depending on the situation and on the structure of all the connected LVGs to the MVG feeder. Figure 4.1 illustrates the situation of different voltage levels along a MV feeder.

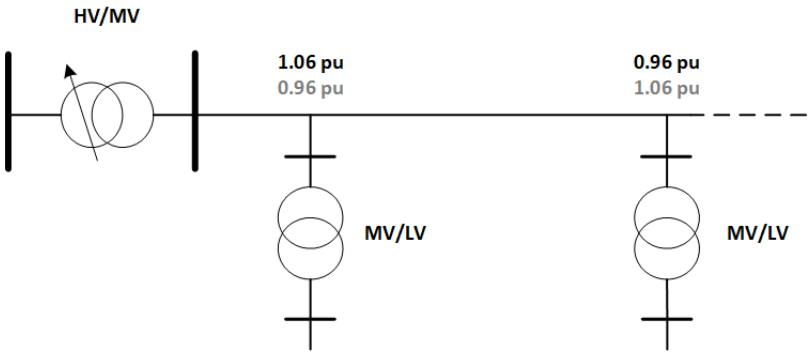

Figure 4.1: Voltage along a MV feeder with Links to HVG and LVGs.

4.2 Scenarios

In this section the different scenarios are defined and further investigated. Table 4.1 shows the different cases which are introduced for the Rural Grid-Link and the Large Urban Grid-Link

Scenarios	load profile	voltage level
base case	common	0.96
		1.01
		1.06
	new	0.96
		1.01
		1.06
LVR	new	0.96
		1.01
		1.06
OLTC-DTR	new	0.96
		1.01
		1.06

Table 4.1: Defined scenarios for Rural Grid-Link and Large Urban Grid-Link.

4.2.1 Base Cases

Each Grid-Link is based on the measured maximal active power flow of 2016 on the Rural DTRs secondary side. It is estimated that every customer of the Grid-Links has the same maximal active power which is calculated by dividing the measured maximal power flow by the number of the residentials in the Rural Grid-Link. The measured active power peak was $P_{peak} = 83,448$ kW and reactive power peak was $Q_{peak} = 27,428$ kVAr, which was measured on the secondary side of the Rural DTR. This result is also used for the Large Urban Grid-Link although it has more residentials and the residentials are mostly new buildings, which can be assumed to have a higher maximal electrical active power consumption. If the maximal active power load of the residentials is higher the voltage violations are slightly less. The voltage violations occur, if the DGs are at their maximal generation and the loads at a low level so a slight higher maximum active power consumption is not a big influence. The maximal reactive power of the customers is depending on the maximal active power of the customers as it is assumed that the residentials have a $\cos(\varphi) = 0,95$ in both Grid-Links. In the following table 4.2 the base parameters of the loads and their quantity in the Grid-Links are shown. The load profile is also relevant for the voltage violations. If the PV injection is at its maximum and there is a minimum of load a voltage violation is imminent, but if the load is also at a maximum there is a chance that there is no voltage violation at all. Figure 3.5 shows the implemented load profile for the residentials in both Grid-Links.

Grid-Link	$N^{(res)}$ [1]	$P^{load,init}$ [kW]	$Q^{load,init}$ [kVAr]
Large Urban	175	1.368	0.4496
Rural	61	1.368	0.4496

Table 4.2: Overview of the customer structure in the used Grid-Link [14].

4.2.2 New load profile cases

The base cases are altered by their load characteristics. The comparision of the base cases with the common load profile to the ones with the new load behaviour is done in the following chapter. Table 4.3 shows the base parameters of the cases with new load profile.

Grid-Link	$N^{(res)}$ [1]	time [h]	$P^{load,init}$ [kW]	$Q^{load,init}$ [kVAr]
Large Urban	175	12:00	0.54	0.12
		17:00	0.95	0.18
		22:00	0.55	-0.04
Rural	61	12:00	0.55	0.12
		17:00	0.95	0.18
		22:00	0.55	-0.04

Table 4.3: Overview of the new customer structure in the used Grid-Link.

4.2.3 LVR cases

As table 4.1 shows the LVR are only investigated with new load profiles. The voltage violations only occur if the PV share is very high which is assumed to be in the future. This leads to the point that the common load profile is not very likely to be active anymore. The LVR case is compared with the new load profile case and also compared with the OLTC-DTR case in the next chapter.

4.2.4 OLTC-DTR cases

In this case the DTR is equipped with an OLTC to handle the voltage violations. As already discussed in the LVR cases the loads are also having the new load characteristics as it is assumed that the Grid-Link is in a modern situation. The OLTC-DTR case is compared with the new load profile case. The differences in the voltage control between the LVR and the OLTC-DTR are also discussed in the upcoming chapter.

5 Impact of transformer placement on the behaviour of low-voltage Grid-Links

In this chapter the results of the base cases are presented. Further on the LVRs are placed and sized for the voltage control in the Grid-Links. The control strategy $Q - Autarky$ is combined with the control of the LVR and an OLTC-DTR. The ZIP coefficients and the load profile is also varied to get results for modern residentials. As an example in the modern load profile residentials are having only LED lights as electric lighting. The full presentation of all figures at all investigated times and all voltage levels is in the appendix.

5.1 Base Cases

In this section the base cases of the simulated Grid-Links are presented. The voltage profiles and voltage violations of different times are shown and analysed. The exchange with the overlaid grid is also presented and analysed. There are three different voltage levels which are investigated, 0.96 pu, 1.01 pu and 1.06 pu of the nominal voltage. Those voltages are presented in different grid situations, at maximum PV injection and minimum load, as well as zero PV injection and maximum load. These two situations occure at 12:00 and at 20:00, as it is shown in Figure 3.5. The grid losses and the loading of the DTR are as well presented and analysed. The voltage profiles of both Grid-Links suggest to set the voltage at the HV/MV power transformer to the low limit at 12:00 and to the high limit at 20:00, but as Figure 4.1 shows it is possible to have the low and high limit on the same MV feeder. This possibility shows, that it is useful to compare the worst cases at different times with different voltage levels of the DTRs primary voltage. The lower limit is also nearly reached in both Grid-Links, which is nearly as bad as a violation, because if the load is rising by more electrical equipment used by the residentials there is a violation.

5.1.1 Rural Grid-Link

In the following Figure 5.1, it can be seen that there are voltage violations of the upper limit. The maximal voltage violation is v=1.17 pu at the worst case scenario. It is also obvious if the primary voltage of the DTR is lower than the lower limit of the DSO's voltage control strategy, voltage violations of the lower limit are imminent. Another

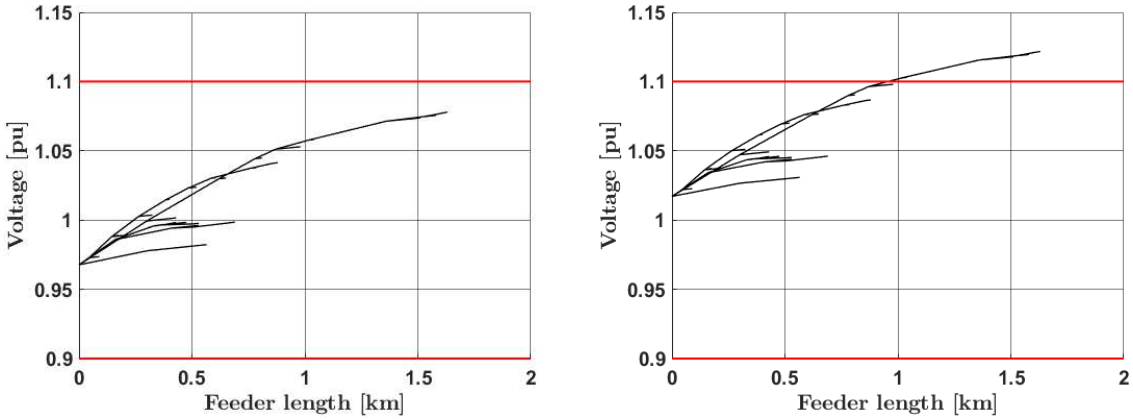

Figure 5.1: Different voltage profiles of the base case in the Rural Grid-Link at 12:00 (a) v=0.96pu (b) v = 1.06 pu.

posibility is that some customers are raising their electrical energy consumption, this way there are voltage violations of the lower limit. So the different voltage profiles show, that the Rural Link-Grid is in a bad situation. This possibility shows, that it is useful to compare the worst cases at the different times with different voltage levels of the DTR's primary voltage. Figure 5.1 (a) and (b) shows that there are voltage violations of the upper limit and also nearly of the low limit at worst Grid-Link conditions. The exchange of active and reactive power over the full day at different voltage levels is shown in the following Figure 5.2. The exchange of power does not differ very much by the different voltage levels.

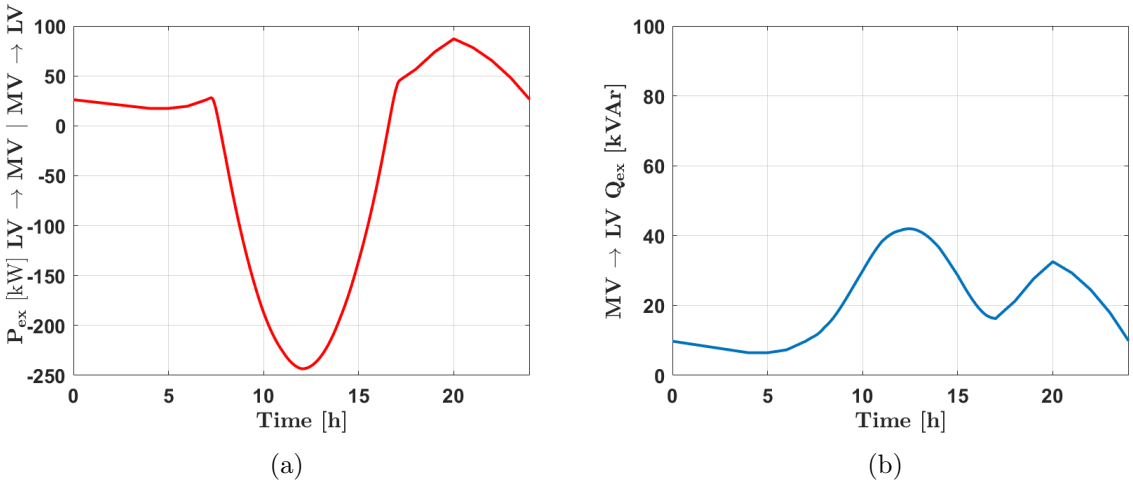

Figure 5.2: Power exchange of the Rural Grid-Link base case for v = 1.06 pu (a) Active power exchange (b) Reactive power exchange.

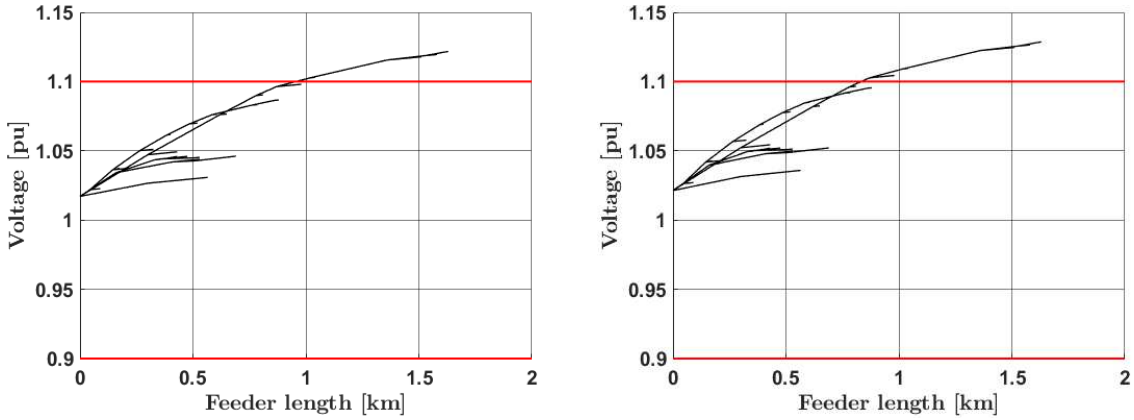

Figure 5.3: Voltage profile of the Rural Grid-Link base case (a) $v = 1.01$ pu at 12:00 $\neg Q_{Aut}$, (b) $v = 1.01$ pu at 12:00 with Q_{Aut}.

The difference of the maximum active power to the minimum active power is $P = 325$ kW and Figure 5.2 also shows that the high PV penetration level leads to a reversal of the power flow. Figure 5.5 (a) shows the exchange of reactive power at the primarly investigated times with the maximum primary DTR voltage of $v = 1.06$ pu. the comparision with the activated $Q - Autarky$ in Figure 5.5 (a) shows that the control strategy can nearly eliminate the reactive power flows, especially in the evening and at night. The Q_{ex} at $v = 1.06$ pu and 12:00 is 41.48 kVAr withouth $Q - Autarky$ and with $Q - Autarky$ it can be reduced to 20.61 kVAr. At 22:00 with $v = 1.06$ pu the activated $Q - Autarky$ can reduce the Q_{ex} from 24.44 kVAr to 1.34 kVAr.

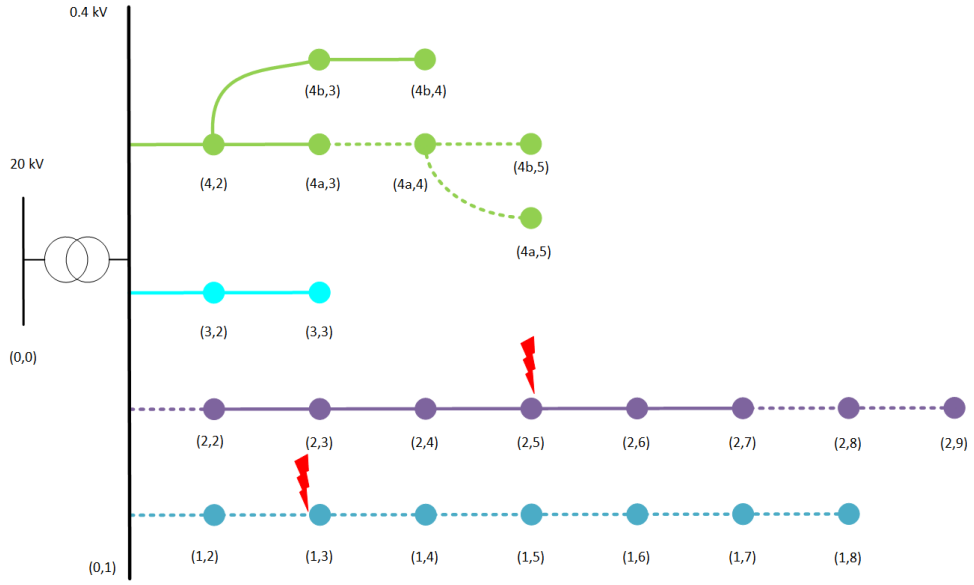

Figure 5.4: Position of voltage violations of the Rural Grid-Link at 12:00.

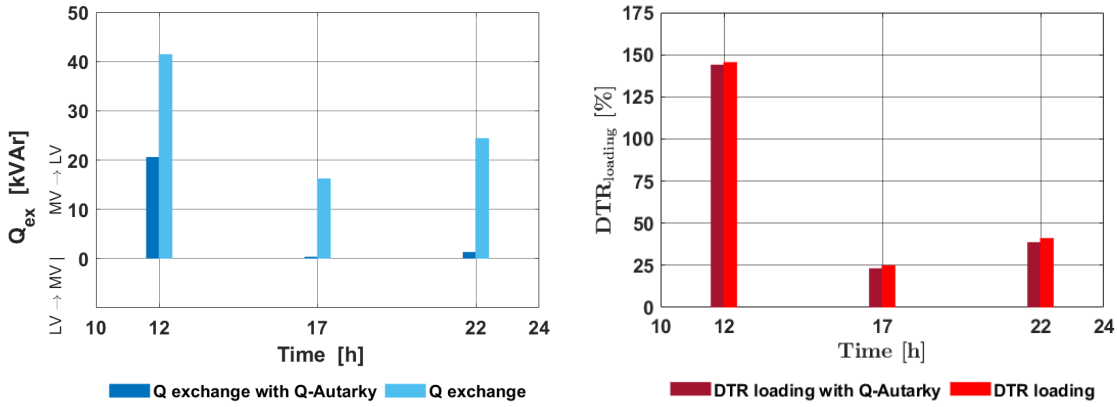

(a) (b)

Figure 5.5: Significant indicators of the Rural Grid-Link base case at primary DTR voltage of $v = 1.06$ pu (a) reactive power exchange (b) loading of the DTR.

It also shows that the need for reactive power is rising with the PV injection. The situation in the Rural Grid-Link gets even worse if the $Q - Autarky$ control is used for the residentials. In this case the voltage violations are earlier at 1.01 pu of the DTRs primary voltage. Figure 5.4 shows the place when the voltage violations appear for the first time marked with a red lightning. Figure 5.3 shows the described voltage violations, in comparision to Figure 5.1 (b) it can be seen, that the situation is getting worse at midday. The maximal voltage violation is without $Q-Autarky$ at $v = 1.122$ pu and with $Q-Autarky$ at $v = 1.129$ pu, so the $Q-Autarky$ is raising the voltage violation by $v = 0.007$ pu. The loading of the DTR is shown in Figure 5.5 (b) with the maximum voltage level of the primary side of the DTR of $v = 1.06$ pu. The DTR is clearly overloaded with the PV- injection and needs to be changed to a DTR with more apparent power, if the assumed PV penetration is reached.

Voltage [pu]	**Time**	$P_{PV\,sum}$ [kW]	
		$\neg Q_{Aut}$	Q_{Aut}
0.96	12:00	-304.51	-304.51
	17:00	-4.29	-4.29
	22:00	-0.00	-0.00
1.01	12:00	-304.51	-304.51
	17:00	-4.29	-4.29
	22:00	-0.00	-0.00
1.06	12:00	-304.51	-304.51
	17:00	-4.29	-4.29
	22:00	-0.00	-0.00

Table 5.1: PV power injection in the Rural Grid-Link.

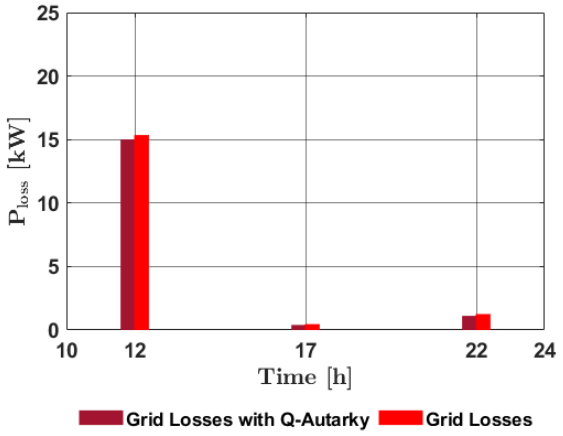

Figure 5.6: Losses of the Grid-Link at primary DTR voltage of $v = 1.06$ pu.

The loading of the DTR differes with the voltage levels, at $v = 0.96$ the loading of the DTR is at 160.7% and at $v = 1.06$ it is at 145.6% at midday. In Figure 5.5 (b) it can also be seen that the $Q - Autarky$ is not changing very much to the loading of the DTR, which means the DTR is primarily loaded with active power. The loading is reduced at $v = 0.96$ to 159.4% and at $v = 1.06$ to 144.1%. The maximum and minimum loading at $v = 1.06$ is at 12:00 145.6 % and at 17:00 it is 25.04 %. The losses of the Rural Grid-Link are presented in Figure 5.6 at $v = 1.06$ pu of the DTR's primary side. The losses are maximal at 12:00 with 15.35 kW and minimal at 17:00 with 0.47 kW. The losses of the Grid-Link correlate with the loading of the DTR as a high loading concludes in higher currents and the current is the main cause of losses in the Grid-Link. The results of the loading, the exchange of reactive power and the losses of the Grid-Link are summarized in table 5.2. This correlation can be easily seen in table 5.2. In table 5.1 the injection of the active power in the whole Rural Grid-Link is shown. The table 5.1 also shows that the injection is not changing with the voltage and not changing with activated $Q - Autarky$.

Voltage [pu]	**Time**	DTR_{load}[%]		Q_{ex} [kVAr]		P_{loss} [kW]		$P_{sumLoad}$ [kW]	
		$\neg Q_{Aut}$	Q_{Aut}	$\neg Q_{Aut}$	Q_{Aut}	$\neg Q_{Aut}$	Q_{Aut}	$\neg Q_{Aut}$	Q_{Aut}
0.96	12:00	160.70	159.40	40.55	25.31	18.62	18.31	42.42	42.61
	17:00	25.05	23.80	12.19	0.42	0.47	0.42	40.31	40.42
	22:00	41.83	40.10	18.78	1.48	1.30	1.20	60.14	60.37
1.01	12:00	152.90	151.50	40.60	22.82	16.89	16.56	43.96	44.21
	17:00	24.88	23.4	13.92	0.39	0.46	0.41	41.55	41.70
	22:00	41.23	39.23	21.15	1.40	1.27	1.15	61.92	62.23
1.06	12:00	145.60	144.10	41.48	20.61	15.35	15.01	45.75	46.05
	17:00	25.04	23.21	16.26	0.36	0.47	0.40	43.05	43.25
	22:00	41.13	38.70	24.44	1.34	1.26	1.12	64.08	64.51

Table 5.2: Data from the base case of the Rural Grid-Link.

5.1.2 Large Urban Grid-Link

In the following Figure 5.7, it can be seen that there are voltage violations of the upper limit. The different voltage profiles show, that the Large Urban Grid-Link is also in

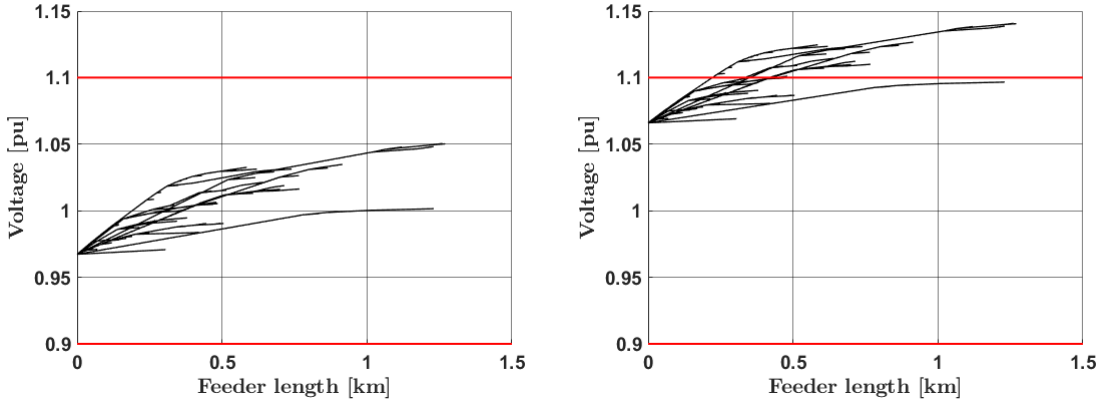

(a) (b)

Figure 5.7: Different voltage profiles in the Large Urban Grid-Link base case at 12:00 (a) $v = 0.96$ pu (b) $v = 1.06$ pu.

a bad situation. Figure 5.7 (b) shows that there are voltage violations of the upper limit. Figure 5.12 shows the places where the voltage violations appear for the first time marked with a red lightning. The maximal voltage violation is at $v = 1.14$ pu. The exchange of active and reactive power over the full day at different voltage levels is shown in the following Figure 5.8. The exchange of power does not differ very much by the different voltage levels.

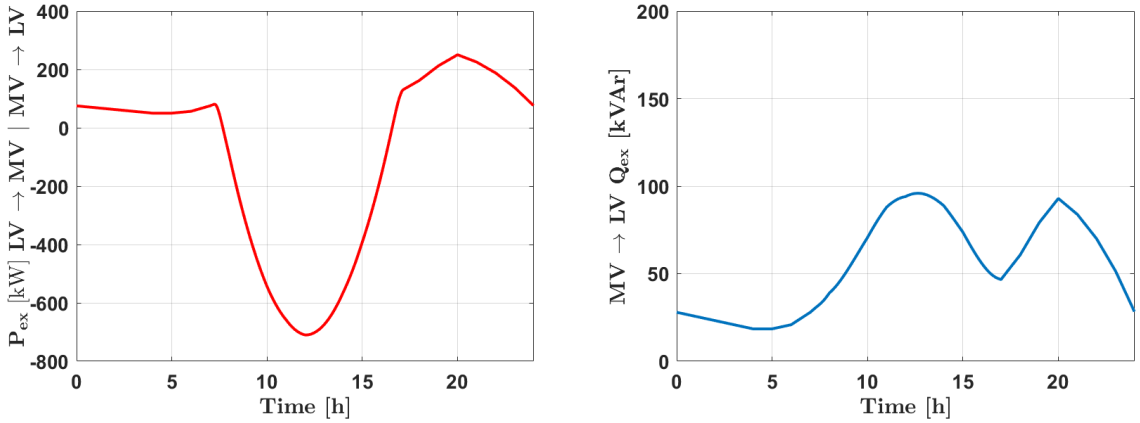

(a) (b)

Figure 5.8: Power exchange of the Large Urban Grid-Link base case for $v = 1.06$ pu (a) Active power exchange (b) Reactive power exchange.

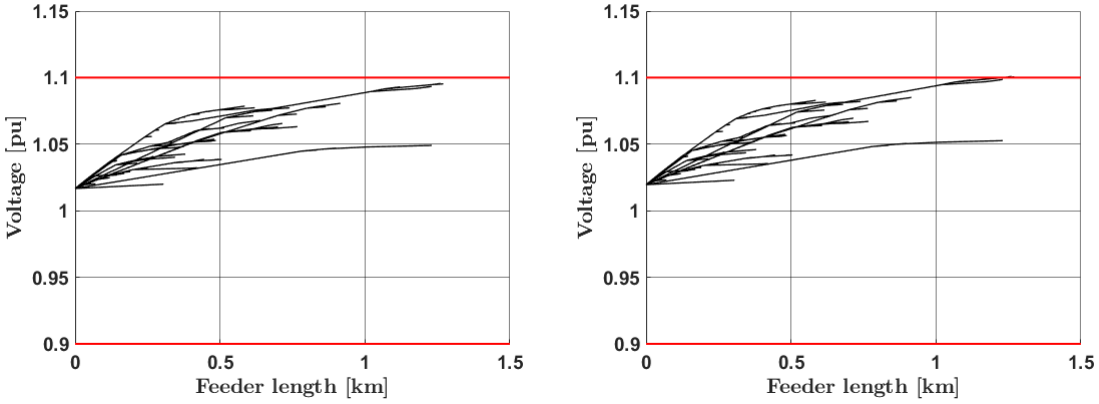

(a) (b)

Figure 5.9: Voltage profile of the Large Urban Grid-Link base case at 12:00 (a) $v = 1.01$ pu $\neg Q_{Aut}$ (b) $v = 1.01$ pu with Q_{Aut}.

The difference of the maximum active power to the minimum active power is $P = 960$ kW and Figure 5.8 also shows that the high PV penetration level leads to a reversal of the power flow. It also shows that the need for reactive power is rising with the PV injection. Figure 5.10 (a) shows the reactive power exchange at different times with the maximum voltage of $v = 1.06$ pu on the DTR's primaries side. The Figure 5.10 (a) also compares the exchange of reactive power with the overlaid Grid-Link with activated $Q - Autarky$. It can be seen that the exchange can be reduced significantly to the needs of the equipment of the Grid-Link itself. The Q_{ex} of the Large Urban Grid-Link at 22:00 and $v = 1.06$ pu can be reduced from 69.98 kVAr to 2.07 kVAr. The situation in the Large-Urban Grid-Link gets even worse for the voltage levels if the $Q - Autarky$ control is used for the residentials. In this case the voltage violations are already at 1.01 pu of the DTRs primary voltage.

Voltage [pu]	**Time**	$\boldsymbol{DTR_{load}}$[%]		$\boldsymbol{Q_{ex}}$ [kVAr]		$\boldsymbol{P_{loss}}$ [kW]		$\boldsymbol{P_{sumLoad}}$ [kW]	
		$\boldsymbol{\neg Q_{Aut}}$	$\boldsymbol{Q_{Aut}}$	$\boldsymbol{\neg Q_{Aut}}$	$\boldsymbol{Q_{Aut}}$	$\boldsymbol{\neg Q_{Aut}}$	$\boldsymbol{Q_{Aut}}$	$\boldsymbol{\neg Q_{Aut}}$	$\boldsymbol{Q_{Aut}}$
0.96	12:00	118.00	118.60	87.22	46.01	41.11	40.66	120.57	120.87
	17:00	18.22	17.32	34.61	0.51	0.99	0.89	115.94	116.14
	22:00	30.37	29.13	52.71	2.37	2.75	2.53	173.23	173.66
1.01	12:00	112.70	112.00	89.56	41.39	37.18	36.58	124.89	125.40
	17:00	18.12	17.04	39.74	0.42	1.03	0.92	119.59	117.41
	22:00	30.00	28.53	59.99	2.20	2.68	2.42	178.54	179.12
1.06	12:00	107.20	106.50	94.05	37.28	33.70	33.19	129.92	130.41
	17:00	18.26	16.91	46.66	0.35	0.99	0.85	124.00	124.36
	22:00	29.99	28.17	69.98	2.07	2.67	2.36	184.98	185.76

Table 5.3: Data from the base case of the Large Urban Grid-Link.

Voltage [pu]	Time	$P_{PV\,sum}$ [kW]	
		$\neg Q_{Aut}$	Q_{Aut}
0.96	12:00	-873.59	-873.59
	17:00	-12.30	-12.30
	22:00	-0.00	-0.00
1.01	12:00	-873.59	-873.59
	17:00	-12.30	-12.30
	22:00	-0.00	-0.00
1.06	12:00	-873.59	-873.59
	17:00	-12.30	-12.30
	22:00	-0.00	-0.00

Table 5.4: PV power injection of the Large Urban Grid-Link.

Figure 5.9 (b) shows the described voltage violations, in comparision with Figure 5.9 (a) it can be seen that there are now voltage violations. The voltage violation is at $v = 1.101$ the voltage was raised by the $Q - Autarky$ by $v = 0.006$ pu. The loading of the DTR is presented in Figure 5.10 (b) and compares to the the results with the activated $Q - Autarky$. The $Q - Autarky$ is not affecting the loading very much, as the loading is mainly by the active power flow. The difference at the maximum loading at 12:00 with $v = 0.96$ pu is from 118% to 118.6%. It can be seen that the DTR is overloaded and needs to be changed with a DTR with more apparent power. The losses of the Grid-Link are presented in Figure 5.11 and also compared with the losses with activated $Q - Autarky$. The $Q - Autarky$ is also not changing very much to the losses of the Grid-Link but it can be seen that it correlates with the loading of the Grid-Link. The loading is reduced by the higher voltage levels at $v = 1.06$ the loading is 107.2 % without $Q - Autarky$ compared to 118 % at $v = 0.96$ pu.

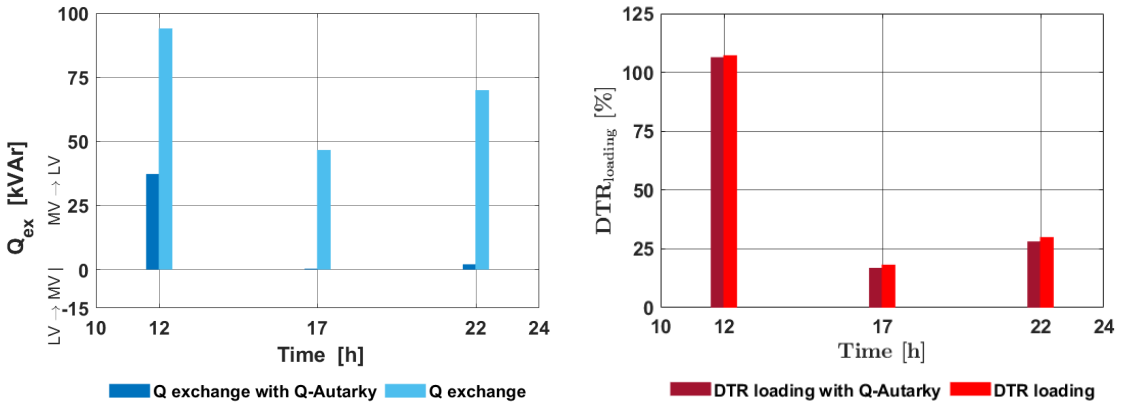

(a) (b)

Figure 5.10: Significant indicators of the Large Urban Grid-Link base case at primary DTR voltage of $v = 1.06$ pu (a) reactive power exchange (b) loading of the DTR.

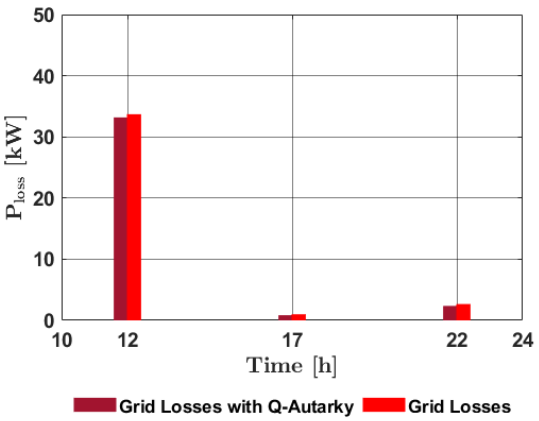

Figure 5.11: Losses of the Large Urban Grid-Link at 12:00 and primary DTR voltage of $v = 1.06$ pu.

The losses at 12:00 with $v = 0.96$ pu are 41.11 kW and with activated $Q - Autarky$ the losses are 40.66 kW. The results of the loading, the exchange of reactive power and the losses of the Grid-Link are summarized in table 5.3. In table 5.4 the injection of the active power in the whole Large Urban Grid-Link is shown. The table 5.4 also shows that the injection is not changing with the voltage and not changing with activated $Q - Autarky$.

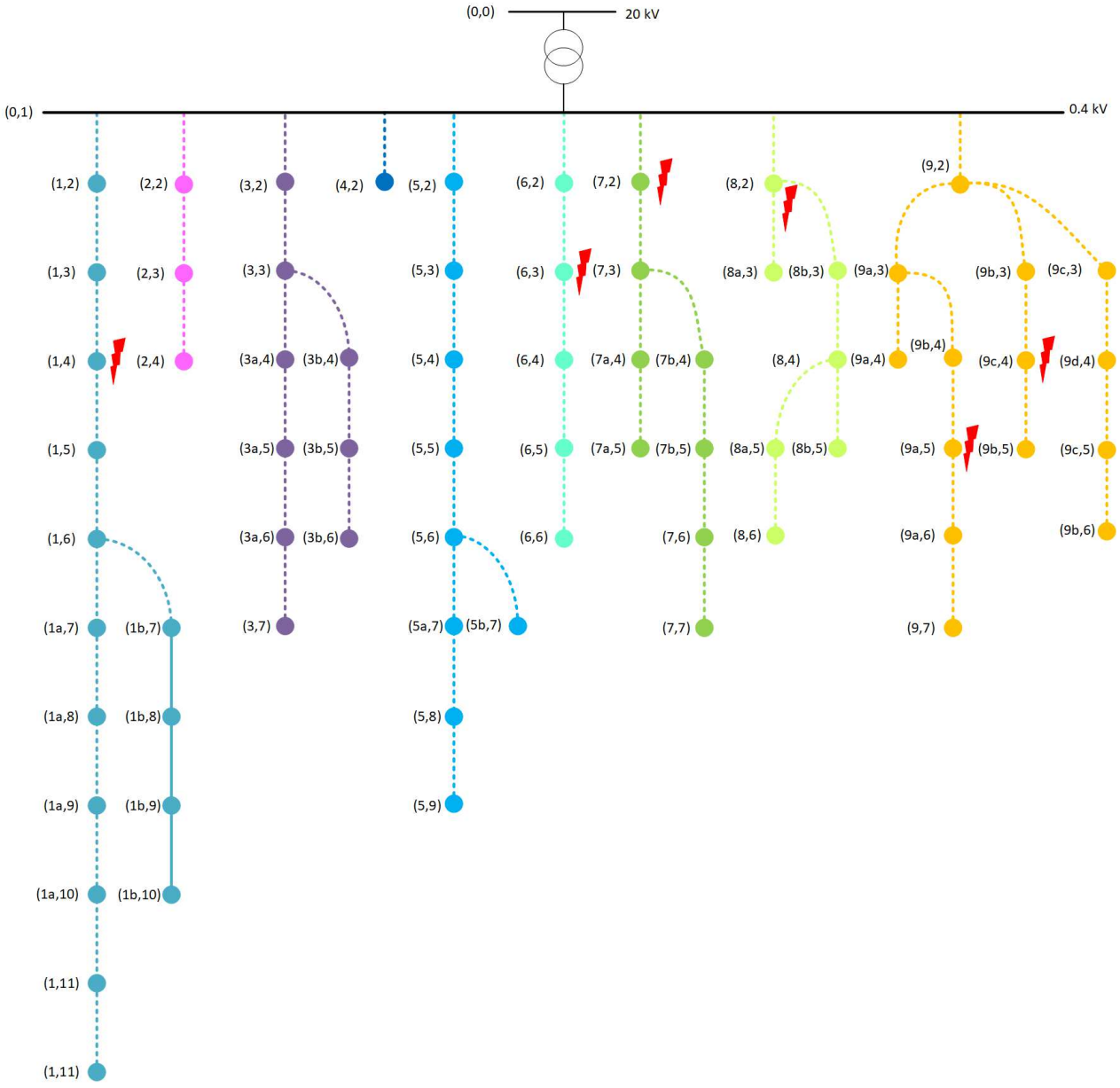

Figure 5.12: Position of voltage violations of the Large Urban Grid-Link at 12:00.

5.2 Impact of the new load nature on the LVG performance

In this section the new load profiles and new ZIP coefficients, which are visualized in Figure 3.6 and table 3.8 are investigated, the main difference is the variation of the power factor and the ZIP coefficients over the day. Due to this the reactive power flow is changing from consumption to production. This could lead to a rise of the reactive power flow in the overlaid Grid-Links. In this section the voltage profiles of both Grid-Links are investigated at three different times. At 12:00 when the voltage violations are highest at 17:00 when the reactive power consumption of the loads are highest and at 22:00 when the reactive power production is at it's peak and the active power consumption is moderate. The different voltage controls by the OLTC-DTR and the LVRs are also investigated and compared with the base case without any voltage control. In the following cases the new load profiles and new ZIP coefficients are used.

5.2.1 Rural Grid-Link

The voltage profiles in the Rural Grid-Link with the new load profiles and new ZIP coefficients are similar to voltage profiles of the base case. The highest voltage level at 12:00 and primary voltage of $v = 1.01$ pu is $v = 1.30$ pu and at primary voltage of $v = 0.96$ pu the highest voltage in the Grid-Link is $v = 1.09$ pu. As Figure 5.13 shows the voltage levels are even slightly lower compared to the base case voltage profiles in Figure 5.1. If the $Q - Autarky$ is also activated the voltage levels are again rising a bit at midday and in the evening. In the night when the residentials are producing reactive power the voltage profiles are lower with activated $Q - Autarky$. The highest voltage level at 12:00 and at primary voltage of $v = 1.06$ pu is $v = 1.138$ pu, with activated $Q - Autarky$ the highest voltage is $v = 1.147$ pu.

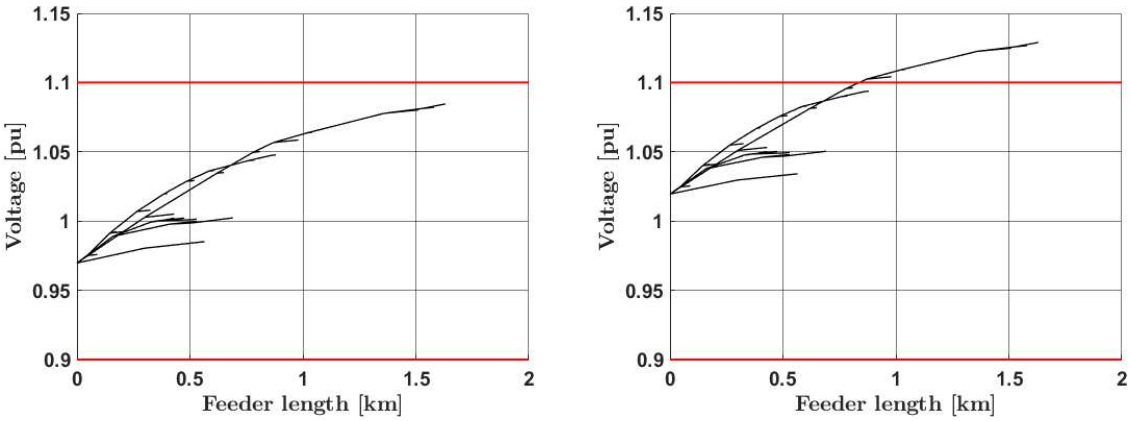

Figure 5.13: Different voltage profiles in the Rural Grid-Link with new load profiles at 12:00 (a) $v = 0.96$ pu (b) $v = 1.01$ pu.

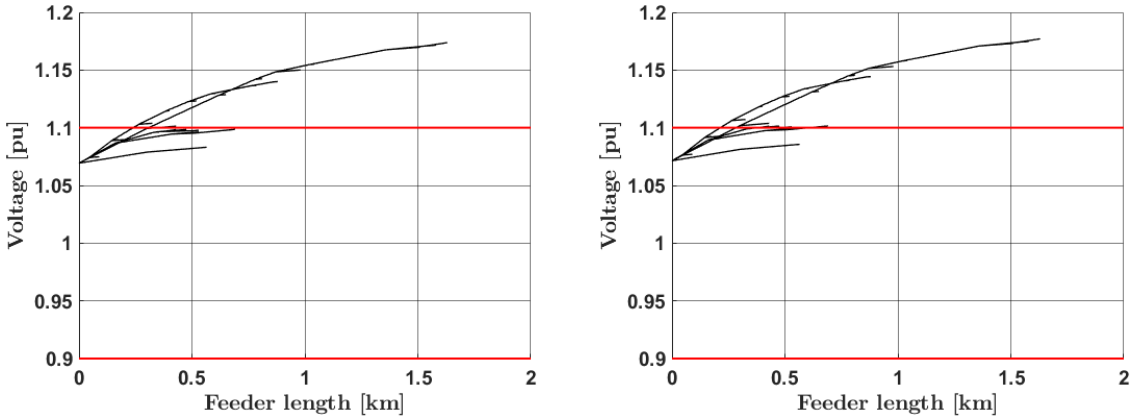

(a) (b)

Figure 5.14: Different voltage profiles in the Rural Grid-Link with new load profiles at 12:00 (a) $v = 1.06$ pu $\neg Q_{Aut}$ (b) $v = 1.06$ pu with Q_{Aut}.

The loading of the DTR is getting significantly lower with the new load profiles compared to the base case in Figure 5.5. If the $Q - Autarky$ is activated the loading of the DTR is getting slightly lower in both cases. Figure 5.15 (a) presents the loading of the DTR in the Rural Grid-Link with new load profiles and new ZIP coefficients. The loading at primary voltage of $v = 1.06$ pu is at 12:00 149.27% and can be reduced with $Q - Autarky$ to 148.71%. The primary voltage is making a significant differencce for the loading at $v = 0.96$ pu the loading is 128.6 % and with $Q - Autarky$ 126.2%. The exchange of reactive power with the overlaid Grid-Link is changing significantly compared to the base case and Figure 5.5.

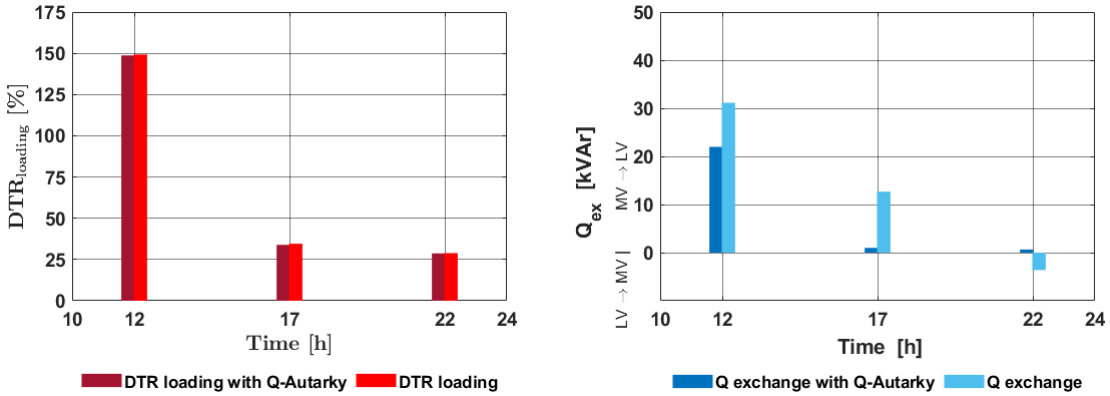

(a) (b)

Figure 5.15: Significant indicators of the Rural Grid-Link with new load profiles at primary DTR voltage of $v = 1.06$ pu (a) loading of the DTR (b) reactive power exchange.

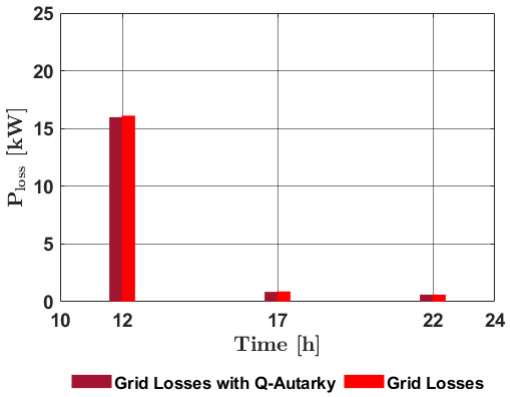

Figure 5.16: Losses of the Rural Grid-Link with new load profiles at primary DTR voltage of $v = 1.06$ pu

The exchange is in all investigated times lower and even changing to production of reactive power for the overlaid Grid-Link in the night. Figure 5.15 (b) presents the exchange of reactive power with the overlaid Grid-Link at different times with the voltage level of $v = 1.06$ pu at the DTR's primary side. The activated $Q - Autarky$ reduces the reactive power exchange in the times of low loading nearly to zero. the exchange of reactive power is getting negative at 22:00. The primary voltage level is also influencing the exchange of reactive power. At 22:00 with $v = 1.06$ the exchange is -3.61 kVAr and with $v = 0.96$ it is -1.97 kVAr. The activated $Q - Autarky$ can reduce the exchange to 0.65 kVAr at 22:00 with $v = 1.06$ and with $v = 0.96$ the exchange is reduced to 0.72 kVAr. The resulting exchange of reactive power is the reactive power of the Grid-Link itself and it's equipment. The losses of the Grid-Link by the equipment is lower due to the lower loading compared to the base case of the Rural Grid-Link in Figure 5.5. Figure 5.16 presents the losses of the Rural Grid-Link at midday in the evening and at night with the voltage level at the primary side of the DTR of $v = 1.06$ pu and compares it with the $Q - Autarky$.

Voltage [pu]	**Time**	DTR_{load}[%]		Q_{ex} [kVAr]		P_{loss} [kW]		$P_{sumLoad}$ [kW]	
		$\neg Q_{Aut}$	Q_{Aut}	$\neg Q_{Aut}$	Q_{Aut}	$\neg Q_{Aut}$	Q_{Aut}	$\neg Q_{Aut}$	Q_{Aut}
0.96	12:00	165.07	164.47	34.87	26.93	19.61	19.46	33.76	33.86
	17:00	33.90	33.30	10.85	0.97	0.85	0.82	54.37	54.61
	22:00	29.33	29.27	-1.97	0.72	0.64	0.64	44.36	44.32
1.01	12:00	156.86	156.27	32.84	24.29	17.75	17.62	35.42	35.52
	17:00	34.20	33.57	11.73	0.98	0.87	0.84	57.42	57.69
	22:00	29.04	28.96	-2.76	0.69	0.62	0.62	46.24	46.18
1.06	12:00	149.27	148.71	31.16	21.97	16.11	15.99	37.16	37.28
	17:00	34.57	33.91	12.66	0.98	0.89	0.85	60.65	60.94
	22:00	28.85	28.74	-3.61	0.65	0.62	0.61	48.18	48.12

Table 5.5: Data from the base case with new load profile of the Rural Grid-Link.

The activated $Q - Autarky$ can reduce those losses at midday, where the impact is at it's peak, like the exchange of reactive power has already shown. The losses of the Grid-Link at 12:00 with the primary voltage of $v = 1.06$ pu are 16.11 kW and with activated $Q - Autarky$ reduced to 8.74 kW. The reduction gets lower with a lower primary voltage, at $v = 0.96$ pu the losses are 15.99 kW and with $Q - Autarky$ 11.44 kW. In table 5.5 the results of the Grid-Link of the loading of the DTR, of the reactive power exchange and the Grid-Link losses are presented.

5.2.2 Large Urban Grid-Link

The new load profiles with the new ZIP coefficients are raising the voltage levels of the voltage profiles slightly in the Large Urban Grid-Link, compared to the base case in Figure 5.7. The control strategy of the $Q - Autarkic$ customers is also raising the voltage levels lightly. Figure 5.17 shows the voltage profiles of the Large Urban Grid-Link with new load profiles and new ZIP coefficients. The highest voltage level in the Large Urban Grid-Link at a primary voltage of $v = 0.96$ pu is 1.06 and the first voltage violation is already with $v = 1.01$ pu primary voltage. The voltage violation is $v = 1.10$ pu, and with $Q - Autarky$ a bit higher at $v = 1.10$ pu. The loading of the DTR is getting lower at the PV-peak production and also in the night, but raising a bit in the evening. The changes are not very big, also the influence of the $Q - Autarky$ control strategy is not very significant to the loading of the DTR. Figure 5.19 (a) shows the loading of the DTR at the investigated times with the maximum voltage on the DTR's primary side of $v = 1.06$. The loading of the DTR in the base case at $v = 1.06$ pu is 107.20 % and with the new load profile the loading is 110.20 % and further reducing with the $Q - Autarky$ to 109.90 %. This time the voltage level has a higher influence as at the primary voltage of $v = 0.96$ pu the loading rises up to 122.00 %. The exchange of reactive power with the overlaid Grid-Link is changing also due to the new load profiles and to the new ZIP coefficients.

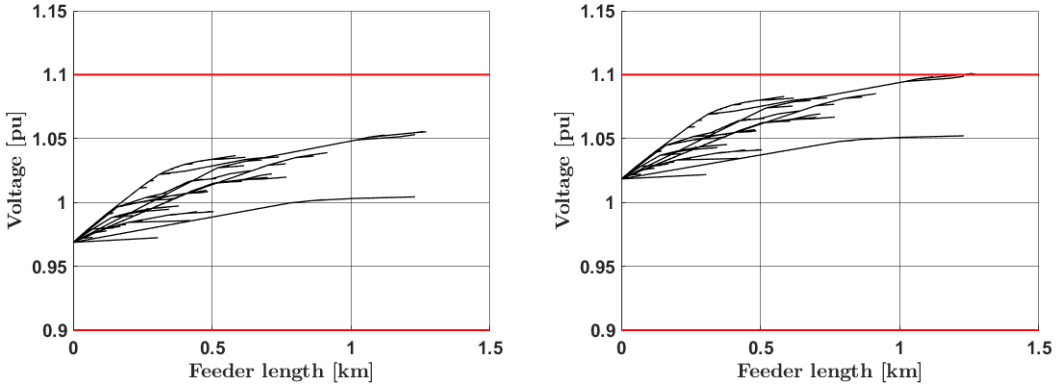

(a) (b)

Figure 5.17: Different voltage profiles in the Large Urban Grid-Link at 12:00 (a) v=0.96pu (b) $v = 1.01$ pu.

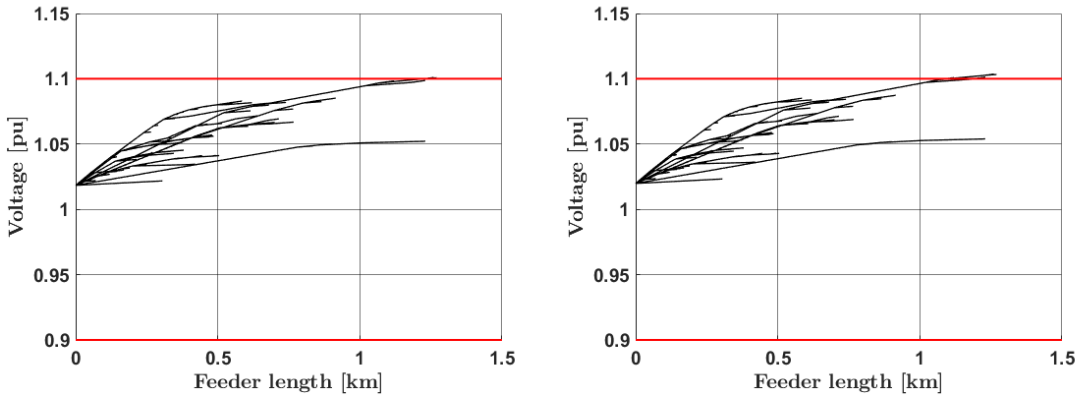

(a) (b)

Figure 5.18: Different voltage profiles in the Large Urban Grid-Link at 12:00 (a) $v = 1.01$ pu $\neg Q_{Aut}$ (b) $v = 1.01$ pu with Q_{Aut}.

Figure 5.19 (b) shows that the Large Urban Grid-Link is even producing reactive power in the night. The reactive power exchange is -11.53 kVAr at 22:00 with primary voltage of $v = 1.06$ pu and can be reduced to 0.87 kVAr with $Q - Autarky$. This change is significant, because especially in the night the equipment of the Grid-Link is not highly loaded and some lines are changing their behaviour from inductive to capacitive. It is assumed that the reactive power balance is getting worse in the night due to this change of the residentials behaviour. Figure 5.19 (b) shows that the $Q-Autarky$ can reduce this exchange to the needs of the Grid-Link itself. The $Q-Autarky$ is presented as a solution to this change. The losses of the Large Urban Grid-Link are changing according to the

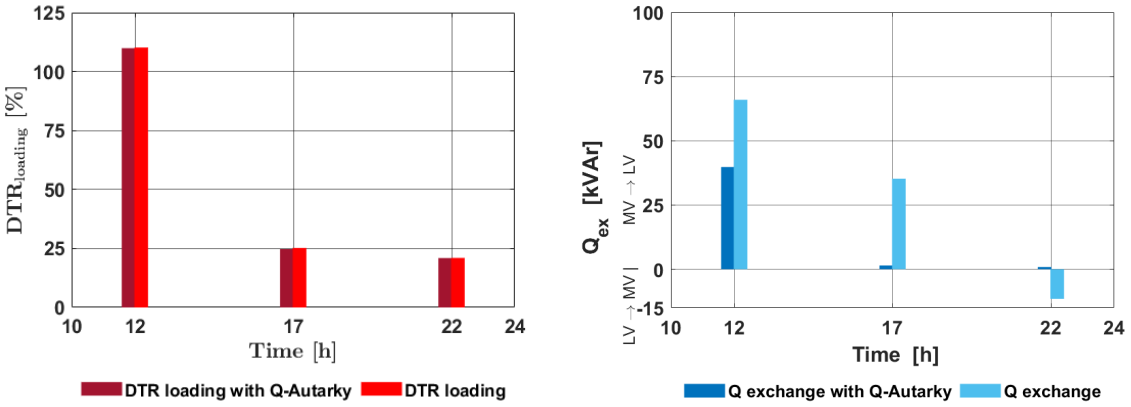

(a) (b)

Figure 5.19: Significant indicators of the Large Urban Grid-Link with new load profiles at primary DTR voltage of $v = 1.06$ pu (a) loading of the DTR (b) reactive power exchange.

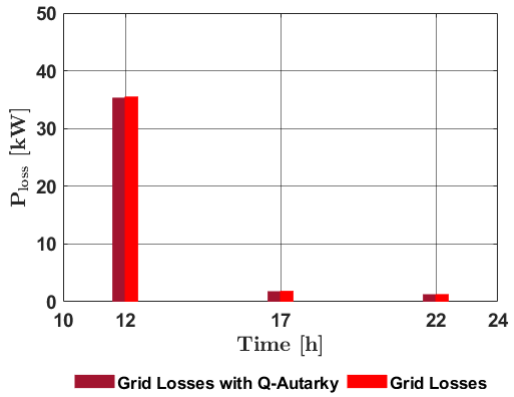

Figure 5.20: Losses of the Large Urban Grid-Link with new load profiles with the voltage level of $v = 1.06$ pu at different times.

loading of the DTR, as the loading is linked to the losses of the Grid-Link. The changes are presented in Figure 5.20 in the night and at midday the losses of the Grid-Link are slightly rising and are getting lower in the evening. The effect of the $Q - Autarky$ is not very high but is lowering the losses as the equipment of the Grid-Link is less loaded. The losses of the Grid-Link at 12:00 with a primary voltage of $v = 1.06$ are 35.54 kW and are reduced by the $Q - Autarky$ to 35.35 kW. In the night at 22:00 with $v = 1.06$ the losses of the Grid-Link are very similar with 1.31 kW and 1.30 kW with activated $Q - Autarky$. The results of the calculations of the Grid-Link with new load profiles of the loading of the DTR, the reactive power exchange and the losses of the Grid-Link are presented in table 5.6.

Voltage [pu]	**Time**	DTR_{load}[%]		Q_{ex} [kVAr]		P_{loss} [kW]		$P_{sumLoad}$ [kW]	
		$\neg Q_{Aut}$	Q_{Aut}	$\neg Q_{Aut}$	Q_{Aut}	$\neg Q_{Aut}$	Q_{Aut}	$\neg Q_{Aut}$	Q_{Aut}
0.96	12:00	122.00	121.70	71.48	49.02	43.49	43.27	95.47	95.65
	17:00	24.72	24.28	30.07	1.49	1.82	1.75	156.93	157.37
	22:00	21.35	21.31	-6.81	1.03	1.36	1.35	127.61	127.53
1.01	12:00	115.90	115.60	68.35	44.09	39.26	39.05	100.23	100.44
	17:00	24.94	24.48	32.57	1.47	1.85	1.78	165.78	166.26
	22:00	21.15	21.09	-9.08	0.95	1.33	1.32	132.96	132.87
1.06	12:00	110.20	109.90	65.93	39.76	35.54	35.35	105.25	105.46
	17:00	25.22	24.73	35.24	1.45	1.89	1.82	175.10	175.61
	22:00	21.02	20.93	-11.53	0.87	1.31	1.30	138.56	138.45

Table 5.6: Data from the base case with new load profile of the Large Urban Grid-Link.

5.3 Effect of LVRs on the LVG performance

In this section the impact of the LVRs on the LVG is investigated and analysed. It is assumed that they can handle the voltage violations of the base cases. The input variable for the control strategy is the last bus bar of the feeder, in which the LVR is controlling the voltage level. So if there is a voltage violation at the end of the feeder the LVR's OLTC are changing the position, to get rid of the violation. In table 5.7 the positions and sizing of the LVRs in the investigated Grid-Links are presented. The positioning and sizing are influencing each another, if the LVR is at the beginning of a line the sizing is way bigger than in the middle or at the end of the feeder. So the optimal position is directly in front of the voltage violation whether the upper limit or the lower limit is violated. They have 13 steps with one neutral position and 6 steps to raise the voltage and reduce the voltage. All voltage steps are equal and can influence the voltage by 4.35 % of the nominal voltage. The control strategy of the tap changer takes the voltage of the end of the feeder and is trying to put the voltage within of 1.08 pu and 0.92 pu. To put the voltage range into narrower voltage limits than allowed is sensible as there is a reserve for the limits before there is a voltage violation by the limits which are given by law. The LVRs placing and sizing is based upon the voltage violations in the base cases.

Grid-Link	**Position [feeder,busbar]**	**Size [kVA]**	**LVR distance [km]**	**Violation distance [km]**
Large Urban	[01,03]	150	0.24	0.24
Large Urban	[06,01]	92	0.41	0.49
Large Urban	[07,00]	92	0.43	0.43
Large Urban	[08,00]	150	0.52	0.52
Large Urban	[09b,04]	69	0.42	0.42
Large Urban	[09b,03]	34	0.41	0.48
Rural	[01,02]	92	0.62	0.62
Rural	[02,03]	69	0.39	0.39

Table 5.7: Placement of the LVR in both Grid-Links.

5.3.1 Rural Grid-Link

The most critical time for the voltage profile is at middays with maximum voltage level on the DTR's primary side. Figure 5.21 shows that the voltage violations are just at the highest voltage level of $v = 1.06$ pu with the control strategy of the LVR's. The activated $Q-Autarky$ is putting the voltage levels again a bit higher, as the comparision of Figure 5.21 and 5.22 shows. The maximum voltage level at 12:00 in the Rural Grid-Link at $v = 0.96$ pu is $v = 1.09$ pu with the primary voltage level of $v = 1.01$ pu the LVRs need to be active. The resulting maximum voltage level is $v = 1.09$ pu. The voltage does not stay within the limits at primary voltage level of $v = 1.06$ pu and is resulting at the maximum voltage of $v = 1.10$ pu and $v = 1.11$ pu with activated $Q - Autarky$.

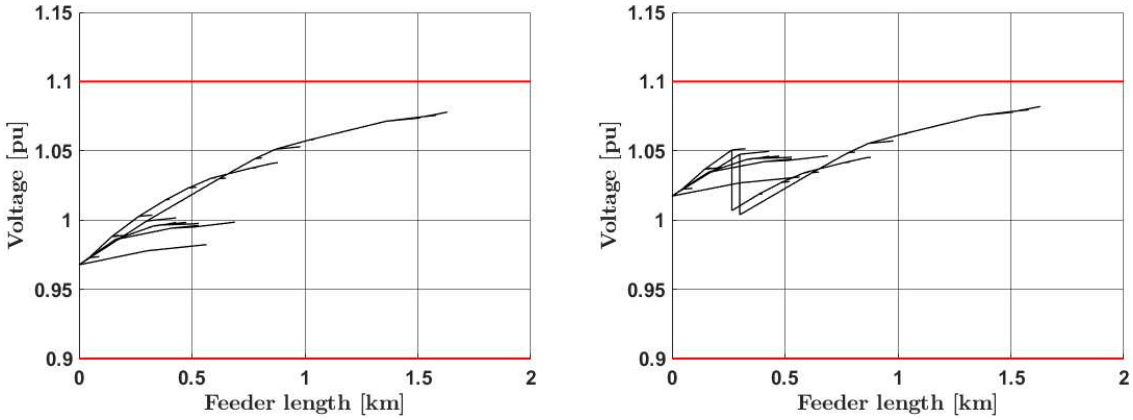

(a) (b)

Figure 5.21: Different voltage profiles in the Rural Grid-Link with LVRs at 12:00 (a) v=0.96pu (b) v = 1.01 pu.

The loading of the DTR in the Rural Grid-Link is a bit higher due to the LVRs. The comparision between the LVR case and the case without LVR but with new load profiles shows that there is nearly no difference. Figure 5.23 (a) presents the DTR loading in the investigated times and also shows the difference to the activated $Q - Autarky$. The activated $Q - Autarky$ is not changing very much to the loading of the DTR. The loading of the DTR in the case with the new load profile is at v = 1.06 pu 149.27 % and in the LVR case it is 149.59 %. The $Q - Autarky$ is reducing the loading of the DTR to 149.09 %. The exchange of the reactive power with the overlaid Grid-Link is changing minimal compared to the case with the new load profiles. Figure 5.23 (b) shows the exchange of reactive power with the overlaid Grid-Link. Figure 5.23 (b) also compares

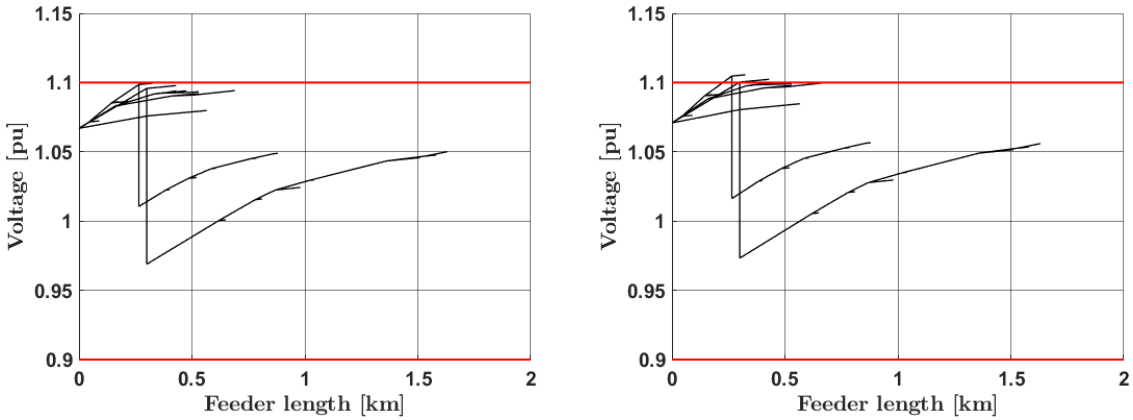

(a) (b)

Figure 5.22: Different voltage profiles in the Rural Grid-Link with LVRs at 12:00 (a) v=1.06pu $\neg Q_{Aut}$ (b) v = 1.06 pu with Q_{Aut}.

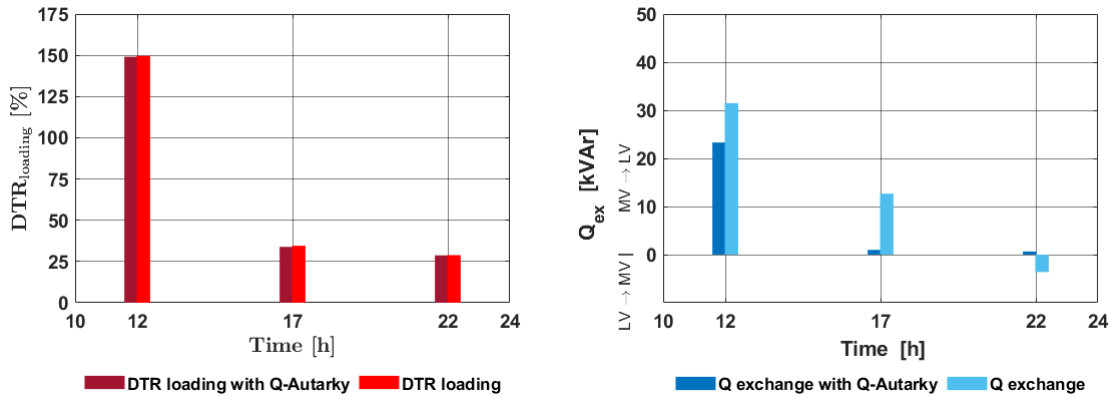

(a) (b)

Figure 5.23: Significant indicators of the Rural Grid-Link with LVRs at primary DTR voltage of $v = 1.06$ pu (a) loading of the DTR (b) reactive power exchange.

Voltage [pu]	Time	DTR_{load}[%]		Q_{ex} [kVAr]		P_{loss} [kW]		$P_{sumLoad}$ [kW]	
		$\neg Q_{Aut}$	Q_{Aut}	$\neg Q_{Aut}$	Q_{Aut}	$\neg Q_{Aut}$	Q_{Aut}	$\neg Q_{Aut}$	Q_{Aut}
0.96	12:00	165.07	164.47	34.87	26.93	19.61	19.46	33.76	33.86
	17:00	33.90	33.30	10.85	0.97	0.85	0.82	54.34	54.61
	22:00	29.33	29.27	-1.97	0.72	0.64	0.64	44.36	44.32
1.01	12:00	156.99	156.43	32.97	24.73	18.35	18.21	34.61	34.72
	17:00	34.20	33.57	11.73	0.98	0.87	0.84	57.42	57.69
	22:00	29.04	28.96	-2.76	0.69	0.63	0.62	46.23	46.18
1.06	12:00	149.59	149.09	31.49	23.32	17.24	17.52	35.52	35.21
	17:00	34.57	33.91	12.66	0.98	0.89	0.85	60.64	60.94
	22:00	28.85	28.74	-3.61	0.65	0.62	0.61	48.18	48.12

Table 5.8: Data from the LVR case with new load profile of the Rural Grid-Link.

with the control strategies of the $Q - Autarkic$ residentials. The changes are similar to the changes in the previous section, the exchange is a bit higher due to the LVRs consumption of reactive power. The reactive power exchange in the new load profile scenario at 12:00 with the primary voltage of $v = 1.06$ pu is 31.16 kVAr and in the LVR scenario it is 31.49 kVAr, the activated $Q - Autarky$ reduces the exchange to 23.32 kVAr. In the night with the primary voltage of $v = 1.06$ pu the reactive power exchange is -3.61 kVAr and can be reduced by the $Q - Autarky$ to 0.65 kVAr. The losses of the Rural Grid-Link are not changing very much, but are a bit higher due to the LVRs in the Grid-Link. Figure 5.24 shows the losses of the Grid-Link in the investigated times and also compares with the activated $Q - Autarky$. The losses with $Q - Autarky$ are a bit lower due to less power which needs to be provided by the Grid-Link. The losses of the Rural Grid-Link with the primary voltage of v=1.06 pu are 19.61 kW and reduced by the $Q - Autarky$ to 19.46 kW at 12:00. The losses in the night at the same primary

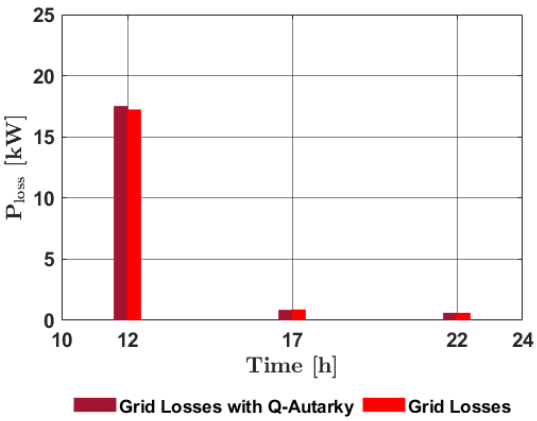

Figure 5.24: Losses of the Rural Grid-Link with LVRs for the voltage level of $v = 1.06$ pu at different times.

voltage level are 0.62 kW and 0.61 kW with $Q - Autarky$. In table 5.8 the results of the DTR loading, the reactive power exchange and the losses of the Rural Grid-Link with LVRs are presented.

5.3.2 Large Urban Grid-Link

In the Large Urban Grid-Link the LVRs cannot eradicate all voltage violations, in Figure 5.25 there are still violations. Those violations are because of the change in the load characteristics, the LVRs are placed in front of the violations in the base case. The highest voltage is no violation because it occurs on the equipment of the DSO right in front of the LVR.

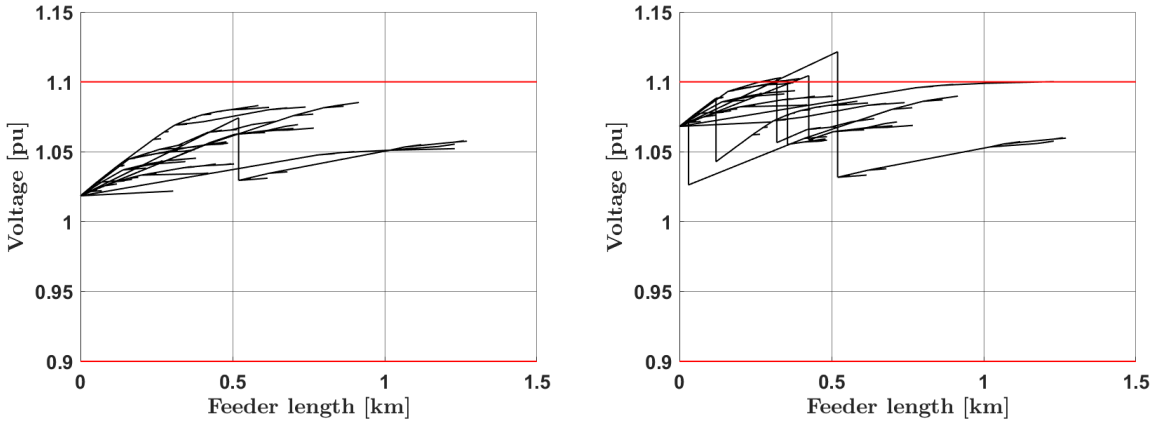

Figure 5.25: Different voltage profiles in the Large Urban Grid-Link with LVRs at 12:00 (a) v=1.01 pu (b) $v = 1.06$ pu.

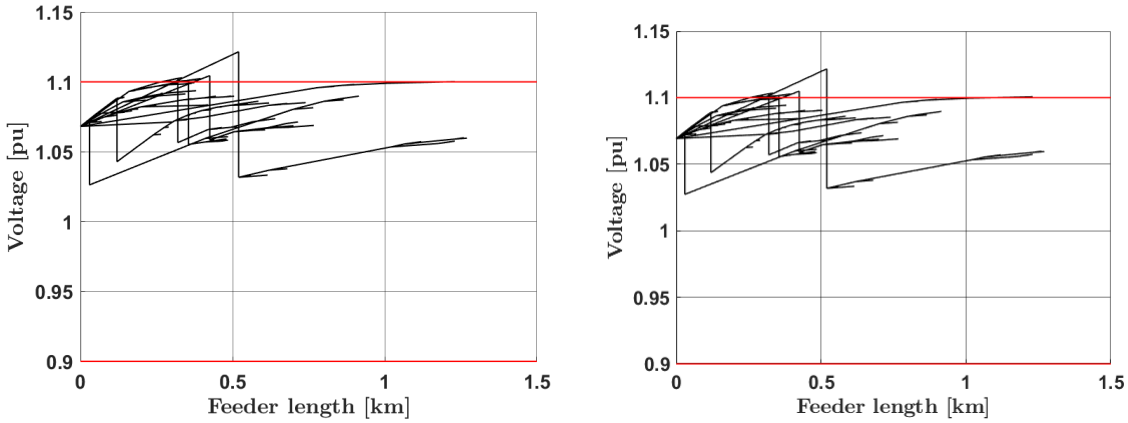

(a) (b)

Figure 5.26: Different voltage profiles in the Large Urban Grid-Link with LVRs at 12:00 (a) v=1.06 pu $\neg Q_{Aut}$ (b) $v = 1.06$ pu with Q_{Aut}.

The highest voltage level at primary voltage $v = 1.01$ pu at 12:00 is $v = 1.085$ pu. If the primary voltage rises to $v = 1.06$ pu the highest voltage violation is at 1.103 pu and rises with the activated $Q - Autarky$ to $v = 1.105$ pu. If the $Q - Autarky$ is activated the voltage levels are again rising a bit and by this there are new voltage violations which also cannot be handled by the LVRs. Figure 5.26 shows the voltage profiles of the Large Urban Grid-Link with activated $Q - Autarky$. The LVR should be placed not exactly in front of the voltage violation to have a bit of a spare range in the voltage control. This way the LVR can react to changes in the load characteristic and the behaviour in general of the Grid-Link.

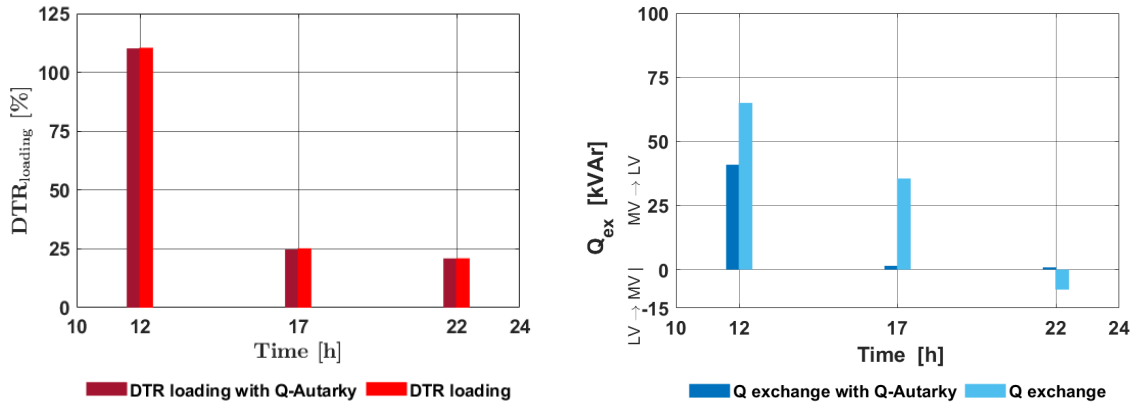

(a) (b)

Figure 5.27: Significant indicators of the Large Urban Grid-Link with LVRs at primary DTR voltage of $v = 1.06$ pu (a) loading of the DTR (b) reactive power exchange.

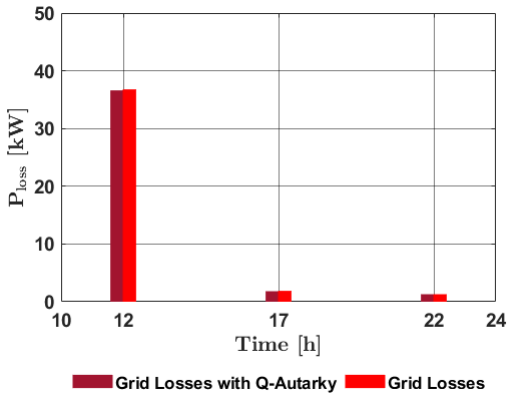

Figure 5.28: Losses of the Large Urban Grid-Link with LVRs for the voltage level of $v = 1.06$ pu at different times.

The loading of the DTR is not changing very much compared to the case with new load profiles and new ZIP coefficients. Figure 5.27 (a) shows the loading of the DTR with $v = 1.06$ pu and also the comparision with the activated $Q - Autarky$. The comparision shows that there is only a slight difference in the loading which was already seen in the base case. In the scenario with new load profile the loading of the DTR is 110.2 % with $v = 1.06$ pu at 12:00. In the LVR case the loading is a bit higher with 110.5 % and can be reduced with the $Q - Autarky$ to 110.2% at 12:00 with $v = 1.06$ pu. The exchange of reactive power with the overlaid Grid-Link is getting a bit less, because of the LVRs need of reactive power. Figure 5.27 (b) shows the reactive power exchange with the overlaid Grid-Link at maximum voltage level of $v = 1.06$ pu. The control strategy of the $Q - Autarkic$ customers is reducing the exchange to the reactive power consumption of the Grid-Link's equipment. The reactive power exchange in the scenario with new load profiles is 65.93 kVAr at 12:00 and primary voltage of $v = 1.06$ pu. In the scenario with LVRs the exchange of reactive power is 64.99 kVAr and can be reduced to 40.91 kVAr with $Q - Autarky$.

Voltage [pu]	**Time**	DTR_{load}[%]		Q_{ex} [kVAr]		P_{loss} [kW]		$P_{sumLoad}$ [kW]	
		$\neg Q_{Aut}$	Q_{Aut}	$\neg Q_{Aut}$	Q_{Aut}	$\neg Q_{Aut}$	Q_{Aut}	$\neg Q_{Aut}$	Q_{Aut}
0.96	12:00	122.00	121.70	70.72	49.02	43.48	43.27	95.48	95.65
	17:00	24.73	24.28	30.30	1.49	1.82	1.75	156.93	157.37
	22:00	21.33	21.31	-4.46	1.03	1.35	1.35	127.59	127.53
1.01	12:00	115.90	115.60	67.52	44.29	39.43	39.24	99.70	99.88
	17:00	24.95	24.48	32.83	1.47	1.85	1.78	165.78	166.26
	22:00	21.12	21.09	-6.07	0.95	1.33	1.32	132.92	132.87
1.06	12:00	110.50	110.20	64.99	40.91	36.79	36.61	102.04	102.23
	17:00	25.23	24.73	35.52	1.45	1.89	1.82	175.10	175.61
	22:00	20.97	20.93	-7.81	0.87	1.31	1.30	138.52	138.45

Table 5.9: Data from the LVR case with new load profile of the Large Urban Grid-Link.

In the night the exchange is -7.81 kVAr at $v = 1.06$ pu and can be reduced to 0.87 kVAr with activated $Q-Autarky$. The losses of the Large Urban Grid-Link are slightly higher. The difference is clearly seen if the Grid-Link is highly loaded like midday. Figure 5.28 shows the losses of the Grid-Link and compares them to the activated $Q - Autarky$. The losses are getting lower with the activated $Q - Autarky$ because of a lower loading of the Grid-Link. In the Grid-Link without LVRs but new load profiles the losses are 35.54 kW at 12:00 and $v = 1.06$ pu. The losses are rising to 36.79 kW and with activated $Q - Autarky$ the losses are 36.61 kW. In table 5.9 the calculated results of the DTR loading the reactive power exchange and the losses of the Grid-Link are presented.

5.4 Effect of the OLTC-DTR on the LVG performance

In this section the impact of an OLTC-DTR is investigated and compared to the base case with new load profiles. The DTR's OLTC can only regulate the whole Grid-Link, this is no problem if the Grid-Link is behaving equally. If the Grid-Link is partly equipped with DGs, which are raising the voltage levels only on some feeders the OLTC of the DTR cannot act freely. It is possible that a voltage spreading occurs between different feeders. This problem can occur in the transition time of a LVG-Link to a equally Grid-Link with the same amount of DGs per residential in all feeders. To prevent this voltage spreading the feeders can be seperated between two DTRs, one with an OLTC and the other one without. This solution has some advantages like the n-1 security and at the end of the transition time the DTR without an OLTC, which is expected to be an older one does not need to be exchanged anymore. Another advantage is that the extra equipment is just the OLTC with the DTR and not one extra equipment per feeder. Figure **??** presents the suggested solution for the problem of a not equally behaving Grid-Link due to voltage violations. The OLTC is controlling the voltages in the Grid-Link. The tap changer is changing it's position if the bus bar which has the highest voltage levels is just before a voltage violation. The OLTC-DTR has a control range of 9 steps and one neutral position, each step has a voltage step of 2%, so the range is from 0.92 pu to 1.08 pu of the nominal voltage level. The transformer parameters are not changed, only the OLTC is applied with the already told parameters. The OLTC voltage control is based upon the voltage violations in the base case with common load profiles.

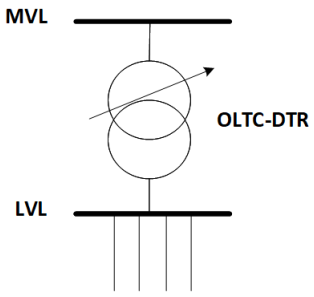

Figure 5.29: Combination of a DTR and a RDT as Link-Link between LVL and MVL.

5.4.1 Rural Grid-Link

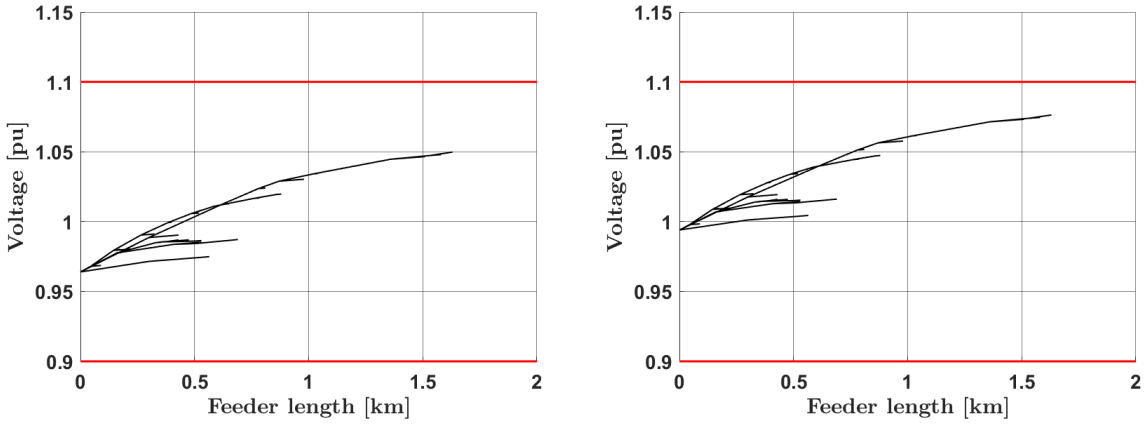

Figure 5.30: Different voltage profiles in the Rural Grid-Link with OLTC-DTR at 12:00 (a) v=0.96 pu (b) v = 1.01 pu.

In the Rural Grid-Link the OLTC can just not eradicate the voltage violations. Figure 5.30 shows the voltage profile of the Rural Grid-Link at midday and with the maximum voltage level on the DTR's primary side of v = 1.06 pu. The maximum voltage level at v = 0.96 pu is v = 1.07 pu at 12:00 and with the primary voltage level of v = 1.01 pu the highest voltage level is v = 1.08 pu in the Grid-Link. Figure 5.31 presents the voltage profiles of the Rural Grid-Link with activated $Q - Autarky$. To prevent violations the control range of the OLTC must have enough spare range to handle changes in the Grid-Link.

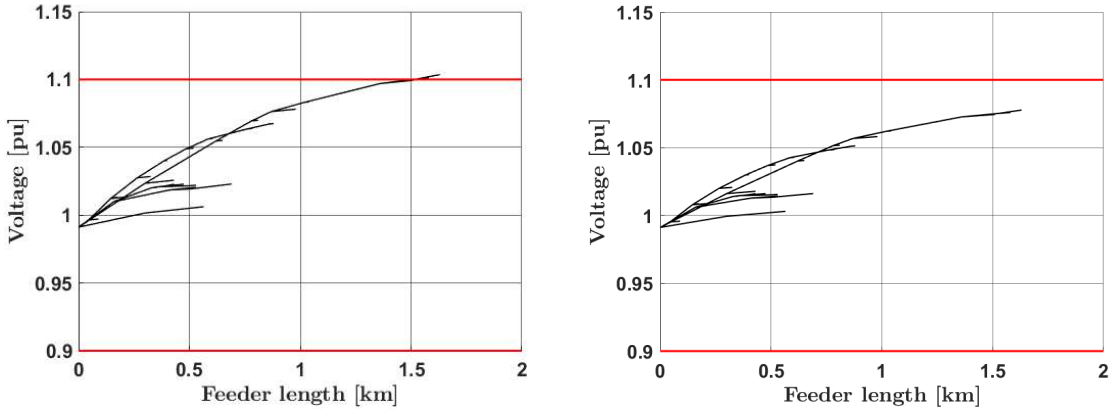

Figure 5.31: Different voltage profiles in the Rural Grid-Link with OLTC-DTR at 12:00 (a) v=1.06 pu $\neg Q_{Aut}$ (b) v = 1.06 pu with Q_{Aut}.

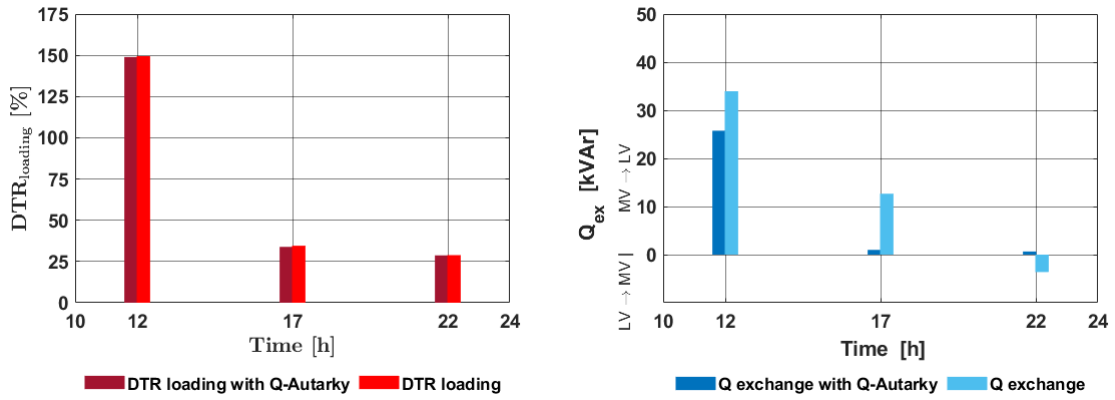

(a) (b)

Figure 5.32: Significant indicators of the Grid-Link with OLTC-DTR for primary DTR voltage of $v = 1.06$ pu (a) loading of the DTR (b) reactive power exchange.

The suggested control range needs to be at least the minimum of the maximal voltage violation. The spare range of the OLTC should be another step to prevent voltage violations. The loading of the DTR is slightly higher due to the lower voltage level. The control strategy of the $Q - Autarkic$ residentials is reducing the loading of the DTR slightly at midday and has nearly no effect in the evening or at night to the loading of the DTR. The loading of the DTR in the new profile scenario is 149.27% at midday with the primary voltage of $v = 1.06$ pu. In the scenario with the OLTC-DTR the loading is 149.50 % at midday with primary voltage level of $v = 1.06$ pu and is reduced by the $Q-Autarky$ to 148.95 %. Figure 5.32 (a) presents the loading of the DTR at midday. In the evening and at night with $Q - Autarky$ with the voltage level of the DTR primaries side of $v = 1.06$ pu. The exchange of reactive power with the overlaid Grid-Link is a bit higher due to the lower voltage levels.

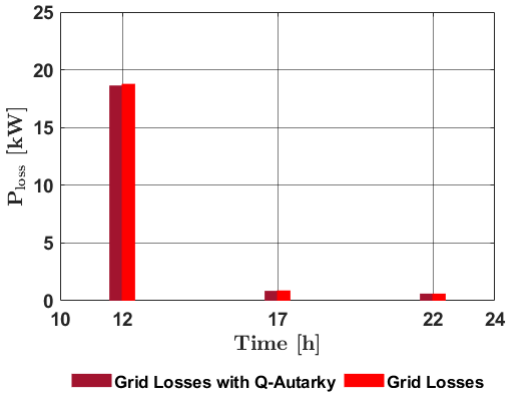

Figure 5.33: Losses of the Rural Grid-Link with OLTC-DTR for the voltage level of $v = 1.06$ pu at different times.

The reactive power is 33.95 kVAr at midday with a primary voltage level of $v = 1.06$ pu and is reduced by the $Q - Autarky$ to 25.76 kVAr. In the night when the reactive power exchange reverses and injects into the overlaid Grid-Link the exchange of reactive power can be reduced from -3.61 kVAr to 0.65 kVAr at $v = 1.06$ pu. The losses of the Rural Grid-Link are higher with the OLTC-DTR due to the lower voltage levels. The losses of the Grid-Link at 12:00 and with a primary voltage level of $v = 1.06$ pu are 18.78 kW and can be reduced to 18.64 kW with $Q - Autarky$. The losses of the new profile scenario are 16.11 kW and with $Q - Autarky$ 15.99 kW. The losses are correlating with the current and if the voltage is getting lower the currents are rising to hold the needed power of the customers. Figure 5.33 shows the losses at different times with the DTR voltage level of $v = 1.06$ pu. The activated $Q - Autarky$ is reducing the losses a bit but not significant. In table 5.10 the calculated results of the DTR loading the reactive power exchange and the losses of the Grid-Link are presented. Figure 5.32 (b) shows the exchange of the reactive power with the overlaid Grid-Link at the investigated times with the maximum voltage level at the DTR's primary side and compares it with the control strategy of the $Q - Autarkic$ residentials.

Voltage [pu]	**Time**	DTR_{load}[%]		Q_{ex} [kVAr]		P_{loss} [kW]		$P_{sumLoad}$ [kW]	
		$\neg Q_{Aut}$	Q_{Aut}	$\neg Q_{Aut}$	Q_{Aut}	$\neg Q_{Aut}$	Q_{Aut}	$\neg Q_{Aut}$	Q_{Aut}
0.96	12:00	158.45	164.45	35.64	28.02	20.29	20.22	33.22	33.26
	17:00	33.90	33.30	10.85	0.97	0.85	0.82	54.37	54.61
	22:00	29.33	29.27	-1.97	0.72	0.64	0.64	44.36	44.32
1.01	12:00	156.90	156.30	35.20	28.37	19.90	20.47	33.52	33.07
	17:00	34.20	33.57	11.73	0.98	0.87	0.84	57.42	57.69
	22:00	29.04	28.96	-2.76	0.69	0.63	0.62	46.23	46.18
1.06	12:00	149.50	148.95	33.95	25.76	18.78	18.64	34.46	34.56
	17:00	34.57	33.91	12.66	0.98	0.89	0.85	60.69	60.90
	22:00	28.85	28.74	-3.61	0.65	0.62	0.61	48.18	48.12

Table 5.10: Data from the OLTC-DTR case with new load profile of the Rural Grid-Link.

5.4.2 Large Urban Grid-Link

In the Large Urban Grid-Link the OLTC can eradicate all the voltage violations by setting the voltage levels down. Figure 5.34 shows the voltage profile of the Grid-Link at midday with the voltage level of the primary side of the DTR of $v = 1.06$ pu. The highest voltage levels at the primary voltage level of $v = 0.96$ pu is $v = 1.055$ pu at 12:00. At the primary voltage level of $v = 1.01$ pu the highest voltage level is $v = 1.08$ in the Grid-Link. In this case the control strategy of the $Q - Autarkic$ customers is again raising the voltage levels but not as far as there are voltage violations again. At the primary voltage level of $v = 1.06$ pu the highest voltage level is $v = 1.08$ and is not changing with the $Q - Autarky$. Figure 5.35 shows the voltage profiles of the Large Urban Grid-Link with an DTR equipped with an OLTC and activated $Q - Autarky$. The loading of the DTR is changing, compared to the base case with new load profiles

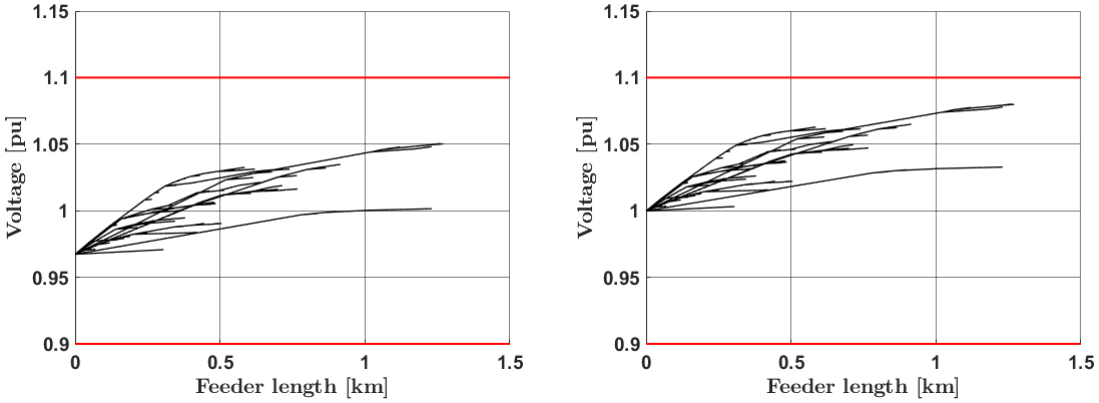

(a) (b)

Figure 5.34: Different voltage profiles in the Large Urban Grid-Link with OLTC-DTR at 12:00 (a) $v = 0.96$ pu (b) $v = 1.01$ pu.

and new ZIP coefficients, not very much it is slightly getting higher but the change can almost not be seen. The loading of the DTR in the Large Urban Grid-Link is 110.5 % and can be reduced to 110.2 % with the activated $Q - Autarky$ at 12:00 and with the primary voltage level of $v = 1.06$. The compared loading of the new profile scenario is 110.2 % and with activated $Q - Autarky$ 109.9 %. Figure 5.36 shows the loading of the DTR at maximum voltage level at the primary side of the DTR at all investigated times. The $Q - Autarky$ control strategy is also changing not very much for the loading of the DTR. The exchange of reactive power in the Large Urban Grid-Link is getting a bit higher by the lower voltage levels. At midday with the primary voltage level of $v = 1.06$ pu the exchange of reactive power is 69.69 kVAr and can be reduced 46.54 kVAr with the $Q - Autarky$.

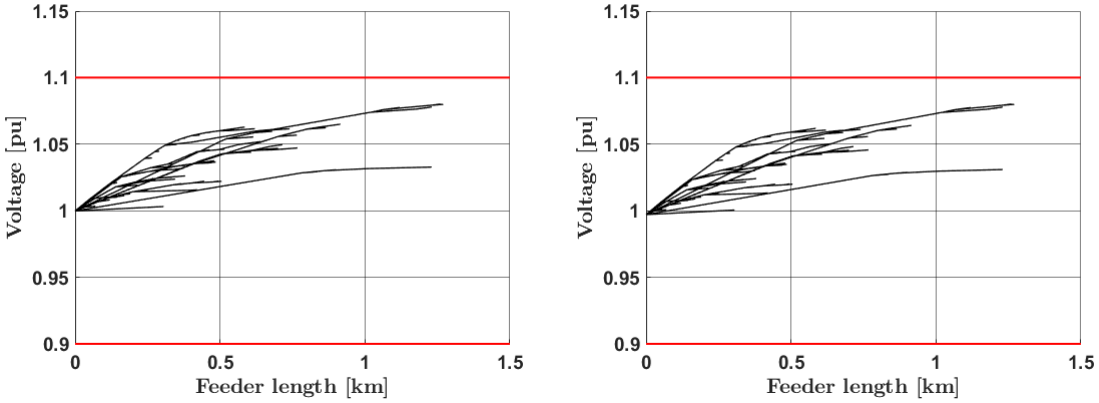

(a) (b)

Figure 5.35: Different voltage profiles in the Large Urban Grid-Link OLTC-DTR at 12:00 (a) $v = 1.06$ pu $\neg Q_{Aut}$(b) $v = 1.06$ pu with Q_{Aut}.

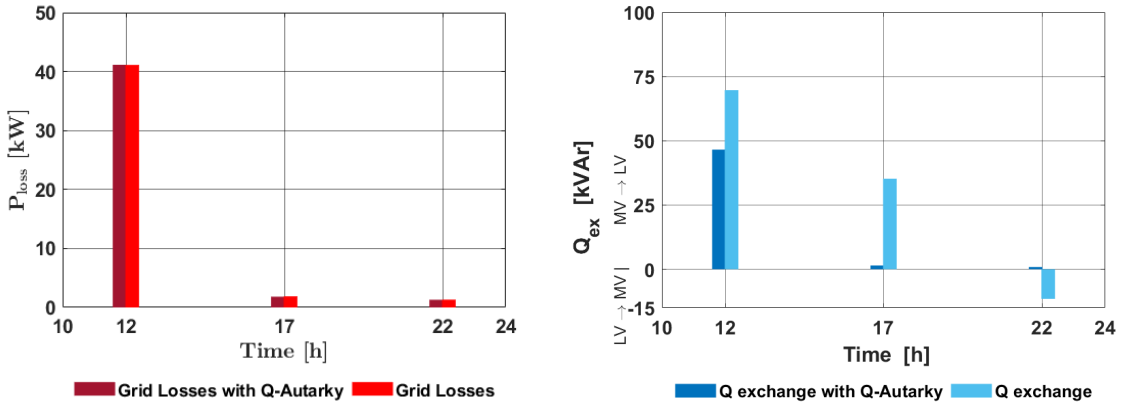

(a) (b)

Figure 5.36: Significant indicators of the Large Urban Grid-Link with OLTC-DTR for primary DTR voltage of $v = 1.06$ pu (a) loading of the DTR (b) reactive power exchange.

At 22:00 and again with the primary voltage level of $v = 1.06$ pu the reactive power exchange is -11.53 kVAr and can be reduced to 0.87 kVAr. If the voltage is getting lower the current is rising and so the thermal losses within the equipment of the Grid-Link are rising. Figure 5.37 shows the losses of the Large Urban Grid-Link. In table 5.11 the calculated results of the DTR loading the reactive power exchange and the losses of the Grid-Link are presented. Figure 5.36 shows the exchange of reactive power with the overlaid Grid-Link at all investigated times and at the voltage level on the primary side of the DTR of $v = 1.06$ pu. The losses in the Large Urban Grid-Link with the OLTC-DTR are getting higher due to the lower voltage levels. The losses of the Grid-Link with an OLTC-DTR are 41.13 kW at 12;00 with $v = 1.06$ pu and are rising with the $Q - Autarky$ to 41.15 kW. The losses of the scenario with the new load profile are 35.54 kVAr and with activated $Q - Autarky$ 35.35 kVAr.

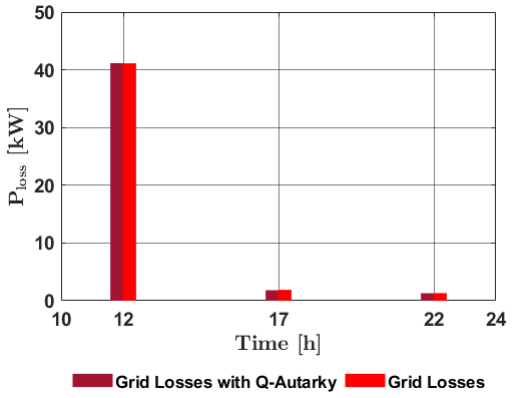

Figure 5.37: Losses of the Large Urban Grid-Link with OLTC-DTR for the voltage level of v=1.06 pu at different times.

Voltage [pu]	Time	DTR_{load}[%]		Q_{ex} [kVAr]		P_{loss} [kW]		$P_{sumLoad}$ [kW]	
		$\neg Q_{Aut}$	Q_{Aut}	$\neg Q_{Aut}$	Q_{Aut}	$\neg Q_{Aut}$	Q_{Aut}	$\neg Q_{Aut}$	Q_{Aut}
0.96	12:00	122.00	121.70	71.48	49.02	43.49	43.27	95.47	95.65
	17:00	24.72	24.28	30.07	1.49	1.82	1.75	156.93	157.37
	22:00	21.35	21.31	-6.81	1.03	1.36	1.35	127.60	127.53
1.01	12:00	115.90	115.70	69.69	46.54	41.13	41.15	98.02	97.95
	17:00	24.94	24.48	32.57	1.47	1.85	1.78	165.78	166.26
	22:00	21.15	21.09	-9.08	0.95	1.33	1.32	132.96	132.87
1.06	12:00	110.50	110.20	69.69	46.54	41.13	41.15	98.02	97.95
	17:00	25.22	24.73	35.24	1.45	1.89	1.82	175.10	175.61
	22:00	21.02	20.93	-11.53	0.87	1.31	1.30	138.56	138.45

Table 5.11: Data from the OLTC-DTR case with new load profile of the Large Urban Grid-Link.

5.5 Voltage control capabilities of OLTC-DTR vs. LVR

This sections discusses the differences between the LVR and a DTR by their physical structure and their performance in the investigated Grid-Links. Figure 5.38 shows the differences of the topology of the two possible voltage control strategies by transformers. This concludes to, a LVR is just for the same voltage levels useful and a normal power transformer is better between different voltage levels. It is possible to install an OLTC at the DTR. If an OLTC-DTR is used, all the feeders of the whole Grid-Link which are beneath are influenced. This might be reasonable, as in some Grid-Links nearly all feeders are affected by voltage violations. In those Grid-Links which have only few feeders affected by voltage violations, it is not wise to use an OLTC-DTR. If only few feeders of the LVG-Link are affected by voltage violations the OLTC-DTR can lead to voltage spreading of the feeders. The voltage spreading of the feeders of a Grid-Link is a voltage violation of the upper limit on one feeder and of the lower limit on another feeder. An OLTC-DTR can correct a voltage violation, but it can also lead to a voltage violation on another feeder by the correction of the former voltage violation. So if only few feeders are affected by voltage violations it is reasonable to use LVRs. The advantage of a LVR is, it can influence only one feeder of a Grid-Link. In the Large Urban Grid-Link the use of an OLTC-DTR would be best, as the majority of the feeders are affected by voltage violations. In the Rural Grid-Link it may be reasonable to use a LVR, because there are only two feeders affected by voltage violations, an OLTC equipped DTR is also possible, as all voltage profiles of the feeders are nearly acting the same. Both scenarios use equal Grid-Links, but the DSOs are not having equally Grid-Links until nearly all residentials have PVs installed, this is taking time. During this transition time of the Grid-Links, it may be reasonable to use the LVRs until the voltage profiles of the different feeders of the Grid-Link are behaving in a similar way. If the transition time of the Grid-Link concludes, it is wise to install an OLTC-DTR instead of seperate LVRs to have fewer electrical equipment in the Grid-Link. Fewer electrical equipment is sensible for the

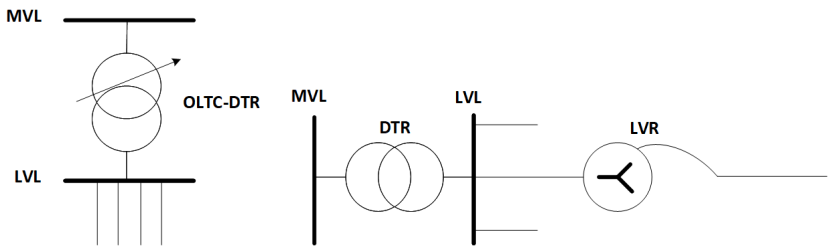

(a) (b)

Figure 5.38: Exemplary topology of (a) OLTC-DTR and (b) LVR.

DSO, as this also means less equipment, which needs to be maintained, less possibilities to have an outage by failure of equipment and also less losses by the Grid-Link due to lower loading. Another possible solution may be to install an OLTC-DTR, as already presented in the previous section. Figure 5.38 demonstrates the presented solution with the OLTC-DTR. In the end both solutions the LVR and the OLTC-DTR are possible solutions for the investigated Grid-Links with few differences. One big advantage of the OLTC-DTR is the position is absolut clear, compared to the LVR. It may be that the OLTC-DTR is the more expensive solution but it can also be the easier solution to install.

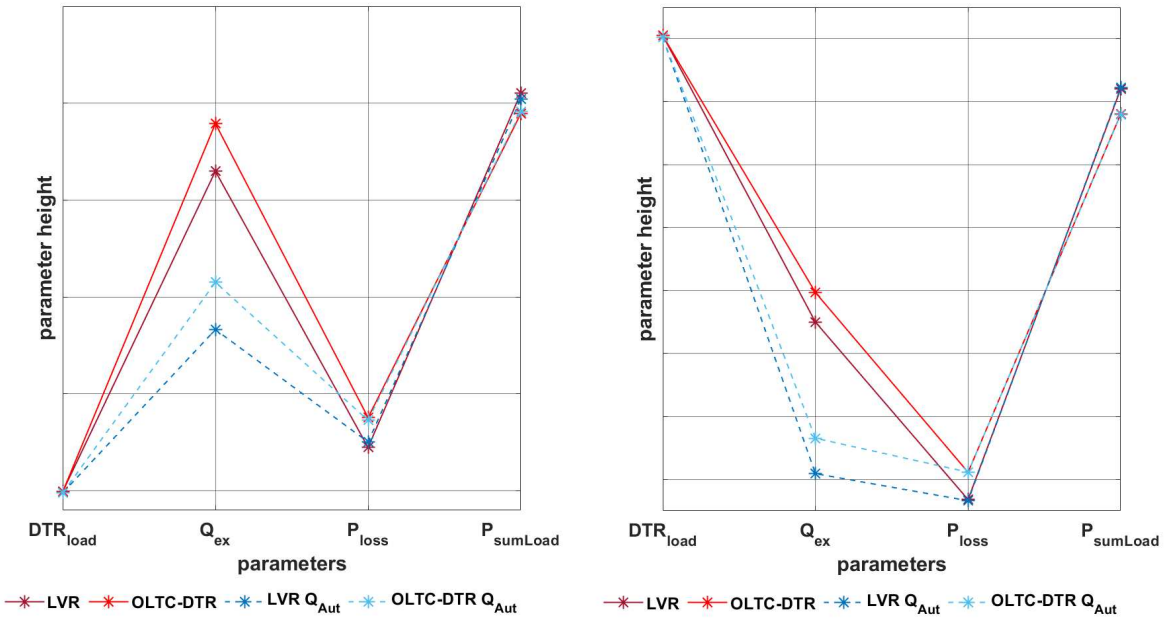

(a) (b)

Figure 5.39: Parameters at 12:00 and $v = 1.06$ pu of the (a) Rural Grid-Link and (b) Large Urban Grid-Link.

The OLTC-DTR is better in long terms as it can be installed parallel to the regular DTR and if the transition time is concluded the DTR can be deinstalled. It changes not very much for the behaviour of the Grid-Link. In all cases the $Q - Autarky$ was raising the voltage levels at midday and getting the situation worse for the Grid-Links. The cable share in the distribution grids are raising on the LVL and the MVL due to this the Grid-Links are turning to get capacitive. If the consumption of reactive power by the costumers is no more the voltages are also rising. In the evening and the night the reactive power flow is nearly zero with the $Q - Autarky$. This is positive for the DSO as the low loading of the lines and cables are raising the voltages not only for the DSO but also for the TSO. If the customers are producing reactive power too the voltages are rising further to the limits of the breakers in Grid-Links above. The suggestion for the reactive power flow is that the consumption of reactive power is allowed but the injection should be forbidden as it concludes in an expensive reconstruction of the power grid. Figure 5.39 shows the comparision of the Grid-Link parameters at 12:00 and $v = 1.06$ pu. Tendencies of the different solutions can be seen in Figure 5.39. The $Q - Autarky$ is reducing the exchange of reactive power and the grid losses. The loads are changing lightly due to the different voltage levels by the control strategy or the $Q - Autarky$. The DTR loading is changing not significant but is also getting lower. The effects of the $Q - Autarky$ are mainly positive on the behaviour of the LV_Grid-Links.

6 Conclusion

The installation of PVs on the roofs of houses in an LV_Grid-Link area causes the violation of the upper voltage limit. Under others, LVRs or an OLTC-DTR are used to prevent those violations. Additionally, the use of modern equipment in customer plants changes their behaviour mainly in the evening from inductive to capacitive. The active power demand of modern equipment is less than that of the conventional ones.
The placement and sizing of LVRs based on the conventional load behaviour, proves to be inadequate, as the new load profile at midday is characterized by values lower than conventional ones. Therefore, the active power injected back into the MV_Grid-Link is larger and the voltage violations appear closer to the feeder begin. The grater the back feed active power, the closer to the beginning of the feeder occur the voltage violations. In the case of high PV share, the LVRs placement results mainly close to the feeders begin (near the low voltage bus bar of the DTR).
The integration of rooftop PVs in large scale and the penetration of the new modern equipment in customer plants provoke higher voltages. The resulting violations occur closer and closer to the beginning of the feeder. In these conditions the effect of a DTR upgraded with OLTC is investigated.
Results show that in both cases (use of LVRs or OLTC-DTR) the loading of the DTR in the rural and large urban grid slightly increases. This increase is a bit larger for OLTC-DTR than for LVR. In all cases the reactive power exchange and loss results higher when using the OLTC-DTR.
In all cases the use of $Q - Autarky$ significantly reduces the reactive power demand of the LV_Grid-Link from MV_Grid-Link. It also meets the needs for capacitive power demand of the modern equipment thus relieves the MV_Grid-Link in the evening hours. At this time interval, the voltages in the grid decrease, while the voltages of the grid increase slightly during the rest of the day.
The placement of LVR should be investigated further, because the place where the voltage violation occur on the feeder depends on the magnitude of the backfeed current. The latter depends on the number of prosumer plant injecting into the grid, as well as on the actual sun radiation. Their positioning close to the feeder head makes their practical use questionable. On the other hand the use of OLTC-DTRs may fail when only one part of the customer plants supplied from the same DTR have implemented rooftop PVs. In this case, there is a considerable spread between the voltage profiles of the different feeders. A parallel shift of the voltage profiles through the OLTC-DTR may lead to the violation of the low voltage limit.

References

[1] European Commission, "A roadmap for moving to a competitive low carbon economy in 2050," Mar. 2011.

[2] International Energy Agency, "Key world energy statistics," 2017.

[3] G. Brauner, *Energiesysteme: regenerativ und dezentral*. Springer Fachmedien Wiesbaden, 2016. http://dx.doi.org/10.1007/978-3-658-12755-8

[4] Bundesministerium für Nachhaltigkeit und Tourismus, "Energie in Österreich," Bundesministerium für Nachhaltigkeit und Tourismus, 2018.

[5] International Energy Agency, "Key world energy statistics," 2018.

[6] F. Katiraei and J. R. Aguero, "Solar pv integration challenges," *IEEE Power and Energy Magazine*, vol. 9, no. 3, pp. 62–71, May 2011. http://dx.doi.org/10.1109/MPE.2011.940579

[7] Bundesminister für Digitalisierung und Wirtschaftsstandort, "Elektrotechnikerverordnung 2002," www.ris.bka.gv.at, 2002.

[8] D.-L. Schultis, A. Ilo, and C. Schirmer, "Overall performance evaluation of reactive power control strategies in low voltage grids with high prosumer share," *Electric Power Systems Research*, Dec. 2018.

[9] A. Ilo, "" Link "— the smart grid paradigm for a secure decentralized operation architecture," *Electric Power Systems Research*, vol. 131, pp. 116–125, Feb. 2016. http://dx.doi.org/10.1016/j.epsr.2015.10.001

[10] ENTSO-E. (2018, May) Entso-e annual report.

[11] W. Raldow, "Smart grids from a european perspective," in *2012 IEEE PES Innovative Smart Grid Technologies (ISGT)*, Jan. 2012, pp. 1–2. http://dx.doi.org/10.1109/ISGT.2012.6175582

[12] W. Gawlik and G. Brauner. Energieübertragung und hochspannungstechnik skriptum zur vorlesung 370.028. ESEA - TU Wien. Oct, 2016.

[13] V. Crastan, *Elektrische Energieversorgung 1*. Springer Berlin Heidelberg, Mar. 2012. http://dx.doi.org/10.1007/978-3-642-22346-4

[14] D.-L. Schultis, "Volt/var behaviour of low voltage grid-link in european grid type," Master's thesis, Technische Universität Wien, Nov. 2017.

[15] A. Ilo, "Effects of the reactive power injection on the grid—the rise of the volt/var interaction chain," *Smart Grid and Renewable Energy*, vol. 07, no. 07, pp. 217–232, Jul. 2016. http://dx.doi.org/10.4236/sgre.2016.77017

[16] P. Schäfer, "Analysis of strategies limiting the reactive power flow between power distribution and transmission networks," *International ETG Congress Bonn Germany*, pp. 1–7, Nov. 2015.

[17] W. Gawlik. Energieversorgung skriptum zur vorlesung 370.002. ESEA - TU Wien. 2018, Sep.

[18] E-Control. (2009, Sep.) Technische und organisatorische regeln für betreiber und benutzer von netzen mit nennspannung <110kv.

[19] C. Winter, M. Heidl, B. Bletterie, S. Kadam, and A. Abart. morepv2grid: Spannungsregelung von pv- wechselrichtern - ergebnisse aus einem feldtest. 13. Symposium Energieinnovation Graz Austria. 13. Symposium Energieinnovation. 2014, Feb.

[20] E-Control. Technische und organisatorische regeln für betreiber und benutzer von netzen hauptabschnitt d4: Parallelbetrieb von erzeugungsanlagen mit verteilernetzen. 2016, Jul.

[21] A. P. Tellez, "Modelling aggregate loads in power systems," Master's thesis, KTH Royal Intitute of Technology, 2017.

[22] C. Winter, R. Schwalbe, M. Heidl, and W. Prüggler. Harnessing pv inverter controls for increased hosting capacities of smart low voltage grids. 2014, Nov. Solar Integration Workshop Berlin Germany.

[23] M. Holt, G. Grosse-Holz, and C. Rehtanz. Line voltage regulation in low voltage grids. 2018, Jun. CIRED.

[24] N. Efkarpidis, T. De Rybel, and J. Driesen, "Optimal placement and sizing of active in-line voltage regulators in flemish lv distribution grids," in *2015 International Conference on Renewable Energy Research and Applications (ICRERA)*, Nov. 2015, pp. 408–413. http://dx.doi.org/10.1109/ICRERA.2015.7418446

[25] Walcher GmbH&Co.KG. Voltage regulator 28.7.2019. https://www.walcher.com//files/netzregler_2011_engl.pdf

[26] A. Bokhari, A. Alkan, R. Dogan, M. Diaz-Aguiló, F. de León, D. Czarkowski, Z. Zabar, L. Birenbaum, A. Noel, and R. E. Uosef, "Experimental determination of the zip coefficients for modern residential, commercial, and industrial loads," *IEEE Transactions on Power Delivery*, vol. 29, no. 3, pp. 1372–1381, Jun. 2014. http://dx.doi.org/10.1109/TPWRD.2013.2285096

[27] D.-L. Schultis and A. Ilo. Adaption of the current load model to consider residential customers having turned to led lighting. IEEE APPEEC, Macao China, 2.-4. Dec. 2019 for publication.

[28] D.-L. Schultis, "Daily load profiles and zip models of current and new residential customers," 2019. https://data.mendeley.com/datasets/7gp7dpvw6b/1 http://dx.doi.org/10.17632/7GP7DPVW6B.1

[29] P. Austria. Förderungen 28.7.2019. https://www.pvaustria.at/forderungen/

A Test grids

A.1 Rural topologies

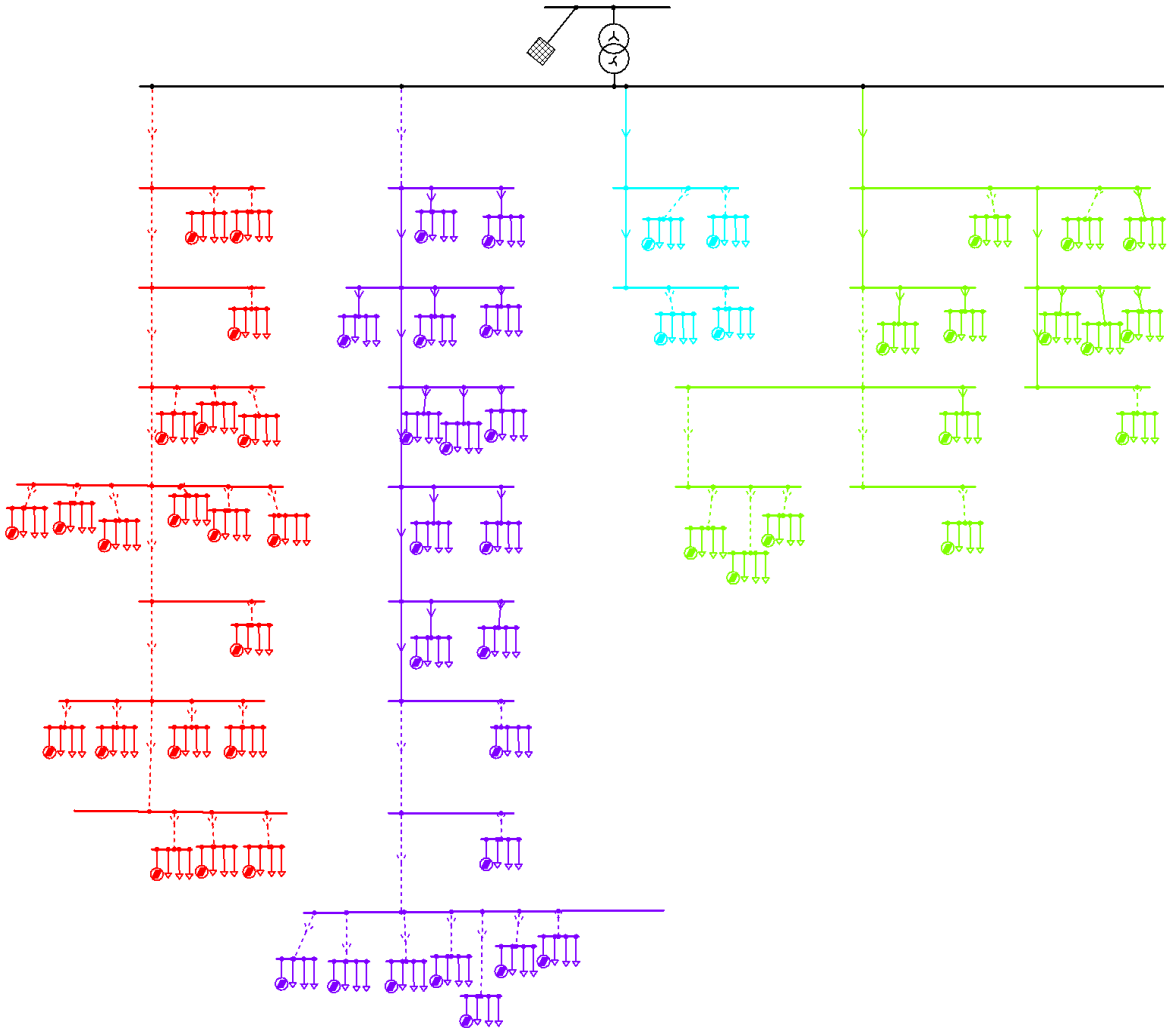

Figure A.1: Rural Grid-Link topology of the base case and OLTC-DTR case.

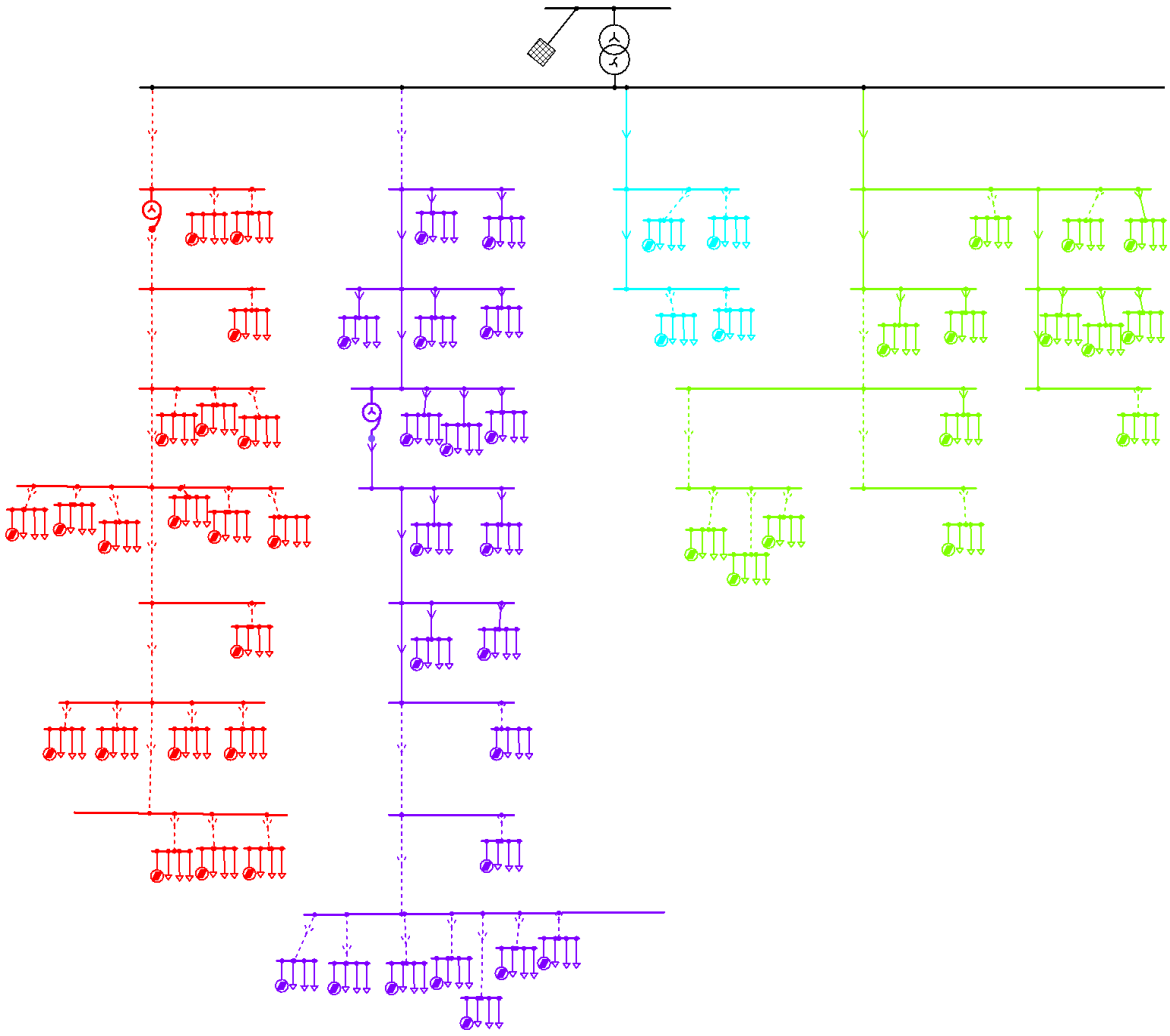

Figure A.2: Rural Grid-Link topology of the LVR case.

A.2 Large Urban topologies

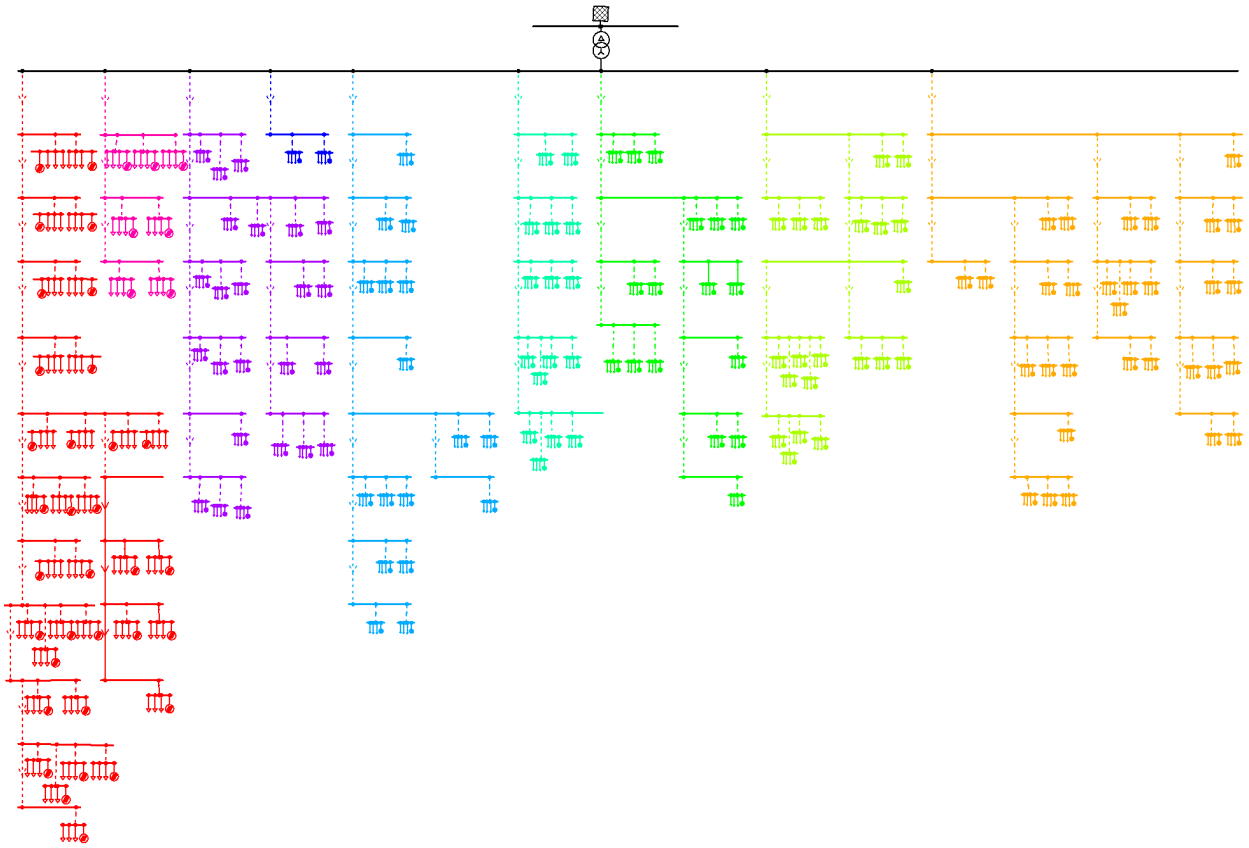

Figure A.3: Large Urban Grid-Link topology of the base case and OLTC-DTR.

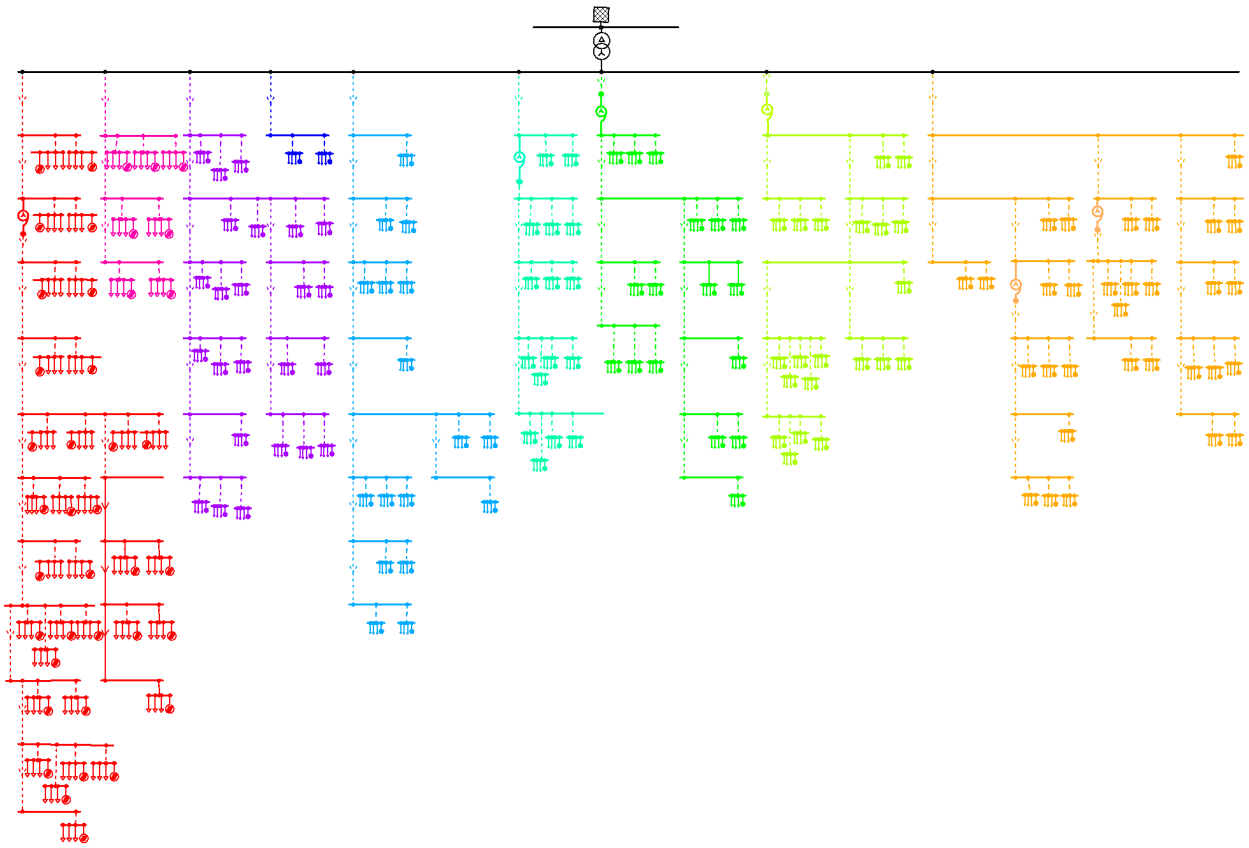

Figure A.4: Large Urban Grid-Link topology of the LVR case.

B Powerflow results

B.1 Voltage profiles

B.1.1 Base case

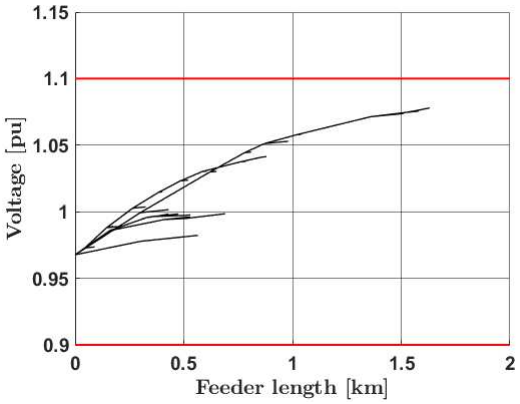

(a) Voltage profile $v = 0.96$ pu at 12:00

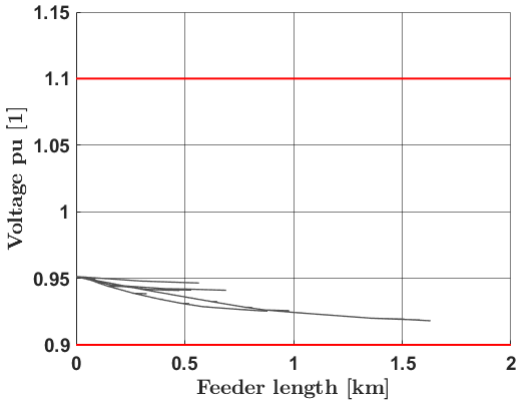

(b) Voltage profile $v = 0.96$ pu at 22:00

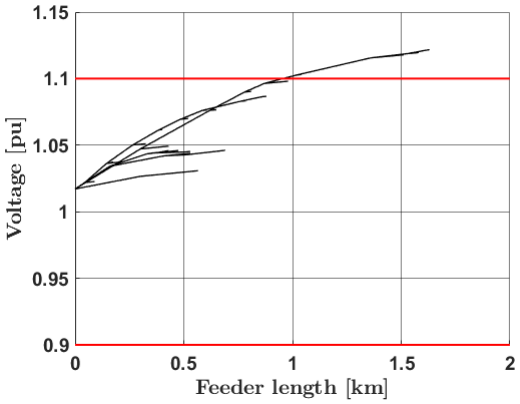

(c) Voltage profile $v = 1.01$ pu at 12:00

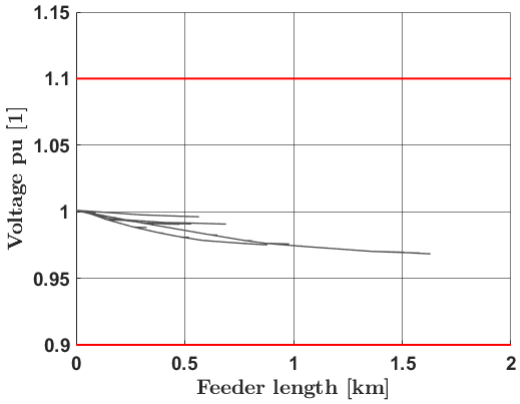

(d) Voltage profile $v = 1.01$ pu at 22:00

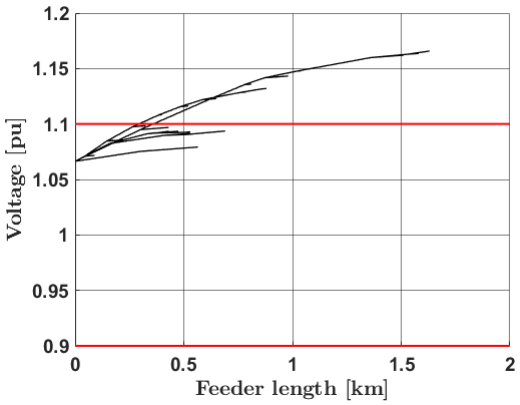

(e) Voltage profile $v = 1.06$ pu at 12:00

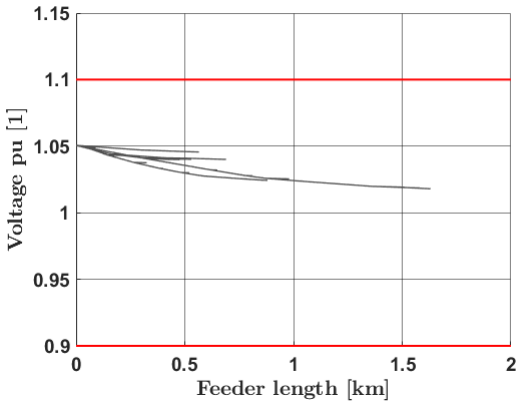

(f) Voltage profile $v = 1.06$ pu at 22:00

Figure B.1: Different voltage profiles of the base cases in the Rural Grid-Link.

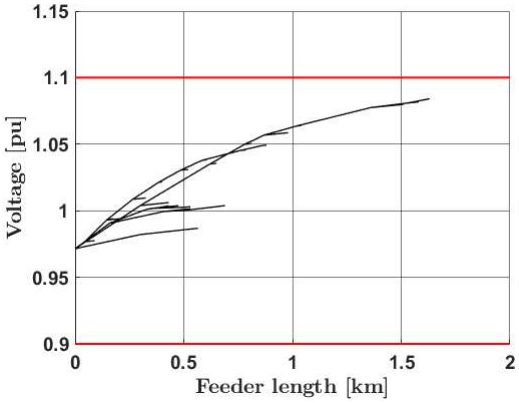

(a) Voltage profile $v = 0.96$ pu at 12:00

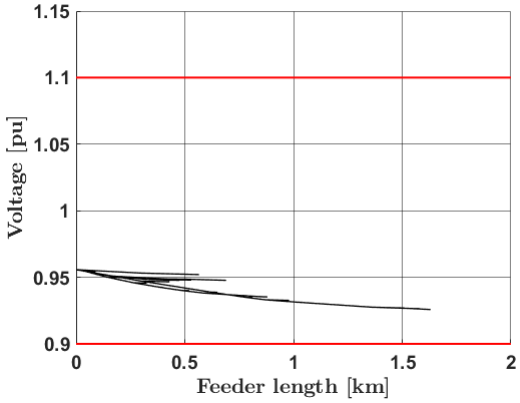

(b) Voltage profile $v = 0.96$ pu at 22:00

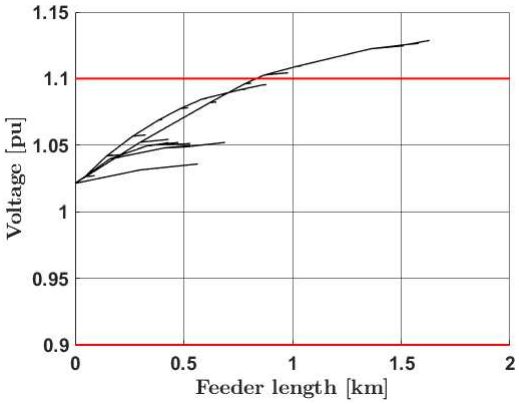

(c) Voltage profile $v = 1.01$ pu at 12:00

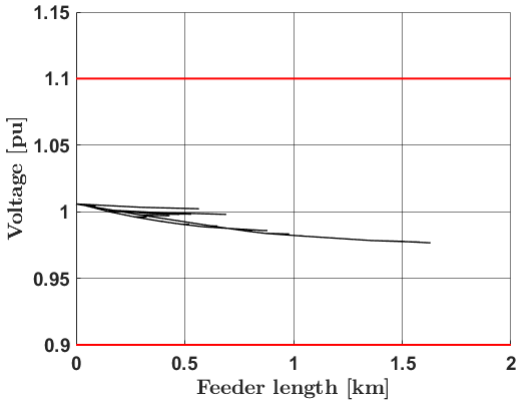

(d) Voltage profile $v = 1.01$ pu at 22:00

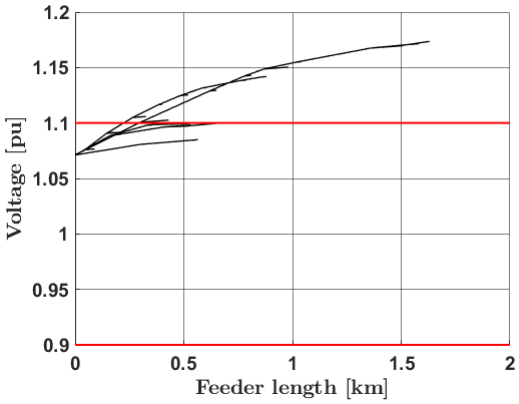

(e) Voltage profile $v = 1.06$ pu at 12:00

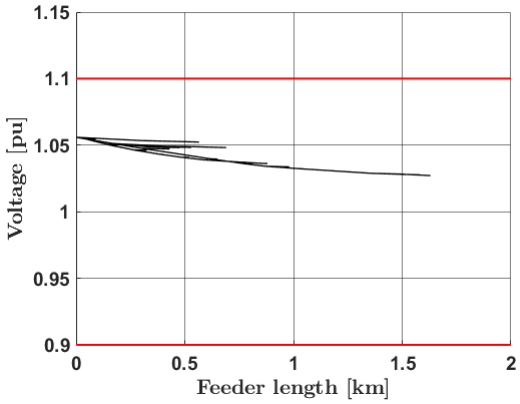

(f) Voltage profile $v = 1.06$ pu at 22:00

Figure B.2: Different voltage profiles of the base cases in the Rural Grid-Link with Q_{aut}.

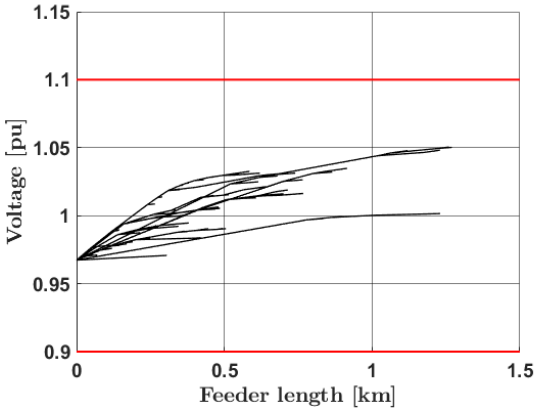

(a) Voltage profile $v = 0.96$ pu at 12:00

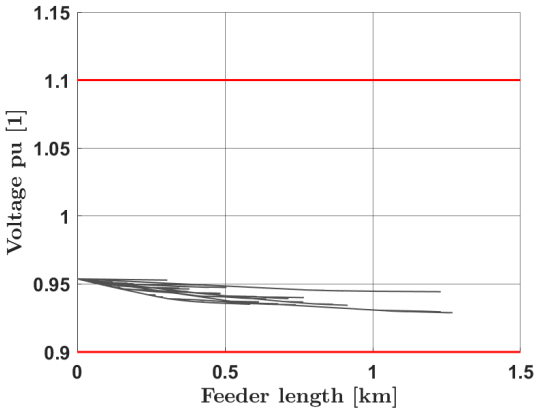

(b) Voltage profile $v = 0.96$ pu at 22:00

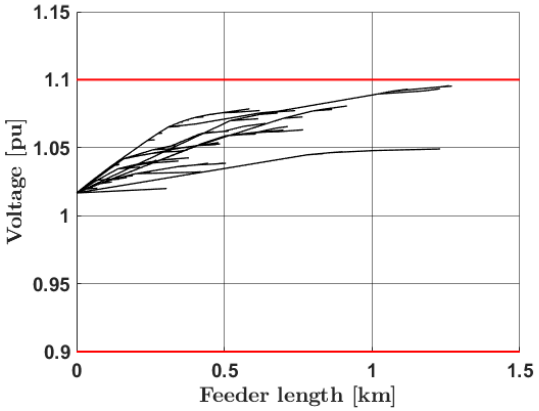

(c) Voltage profile $v = 1.01$ pu at 12:00

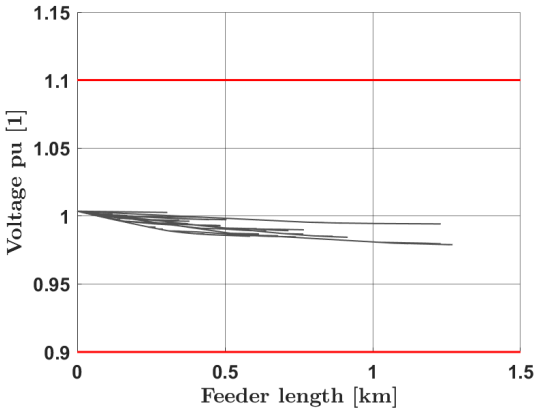

(d) Voltage profile $v = 1.01$ pu at 22:00

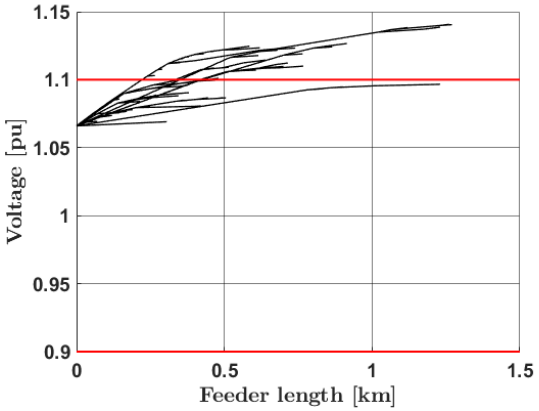

(e) Voltage profile $v = 1.06$ pu at 12:00

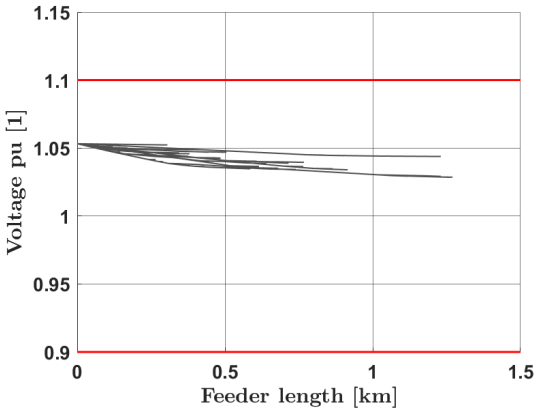

(f) Voltage profile $v = 1.06$ pu at 22:00

Figure B.3: Different voltage profiles of the base case in the Large Urban Grid-Link.

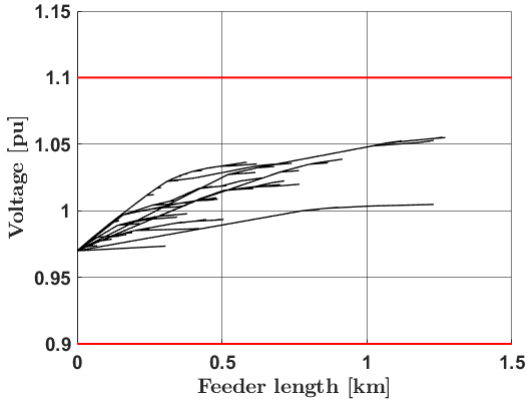

(a) Voltage profile $v = 0.96$ pu at 12:00

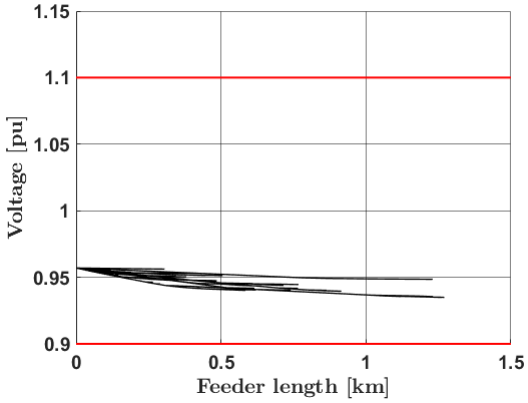

(b) Voltage profile $v = 0.96$ pu at 22:00

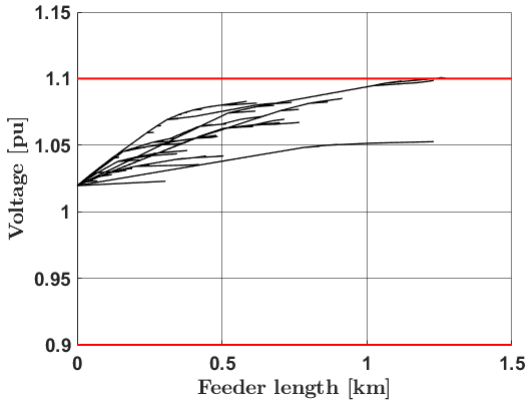

(c) Voltage profile $v = 1.01$ pu at 12:00

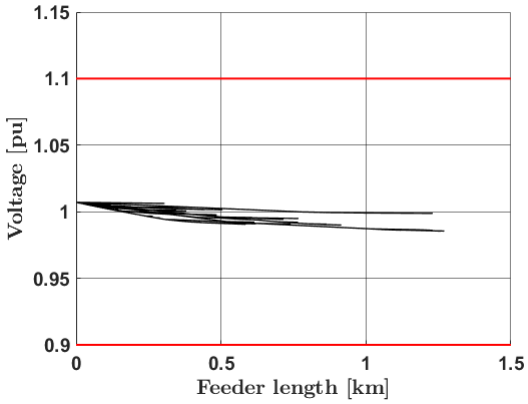

(d) Voltage profile $v = 1.01$ pu at 22:00

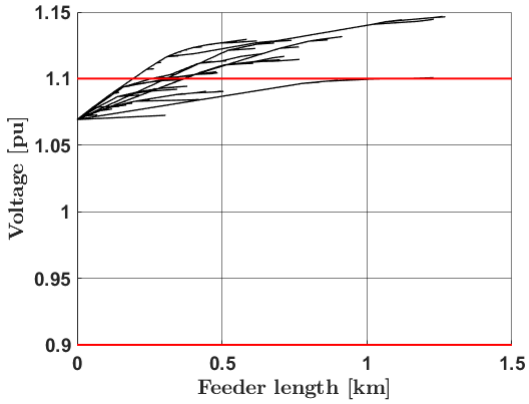

(e) Voltage profile $v = 1.06$ pu at 12:00

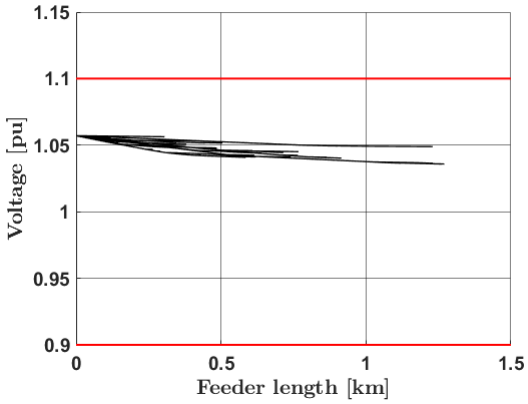

(f) Voltage profile $v = 1.06$ pu at 22:00

Figure B.4: Different voltage profiles of the base case in the Large Urban Grid-Link with Q_{aut}.

B.1.2 New load profiles

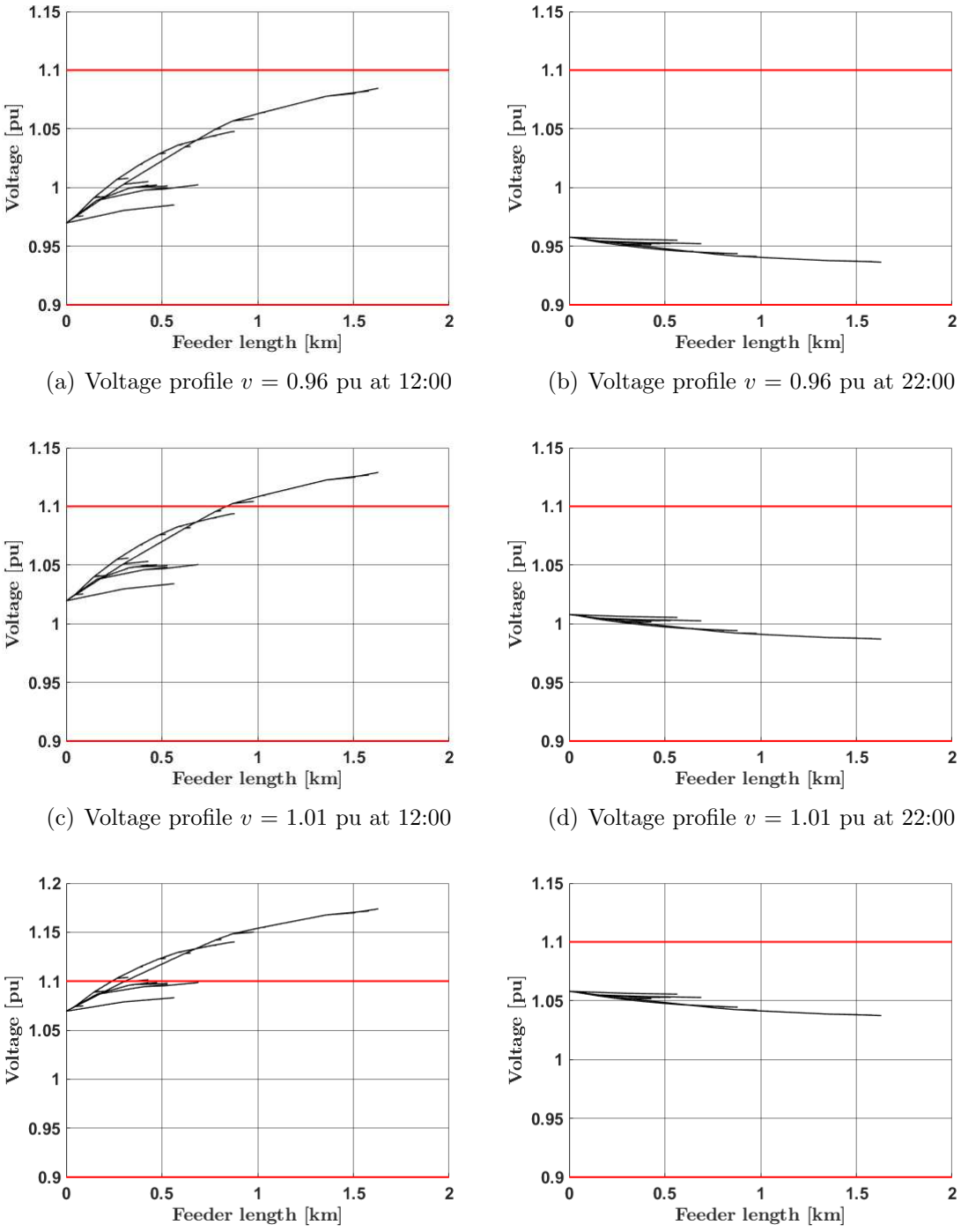

(a) Voltage profile $v = 0.96$ pu at 12:00

(b) Voltage profile $v = 0.96$ pu at 22:00

(c) Voltage profile $v = 1.01$ pu at 12:00

(d) Voltage profile $v = 1.01$ pu at 22:00

(e) Voltage profile $v = 1.06$ pu at 12:00

(f) Voltage profile $v = 1.06$ pu at 22:00

Figure B.5: Different voltage profiles with new ZIP coefficients in the Rural Grid-Link.

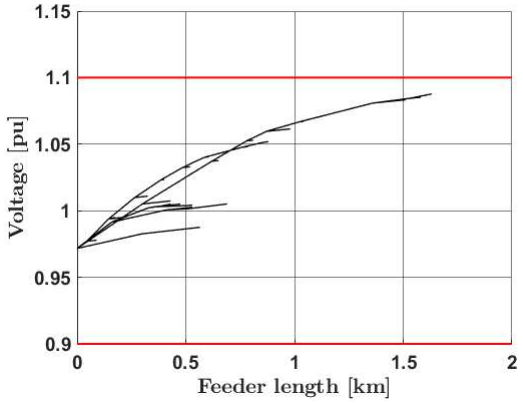

(a) Voltage profile $v = 0.96$ pu at 12:00

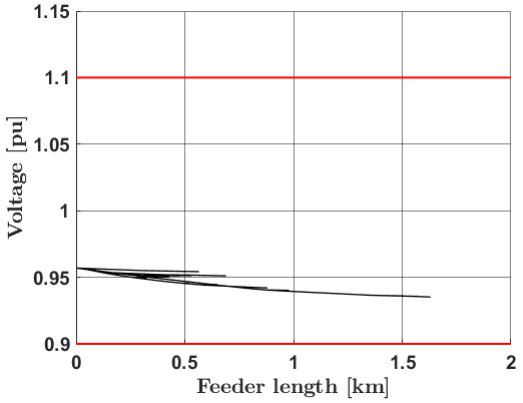

(b) Voltage profile $v = 0.96$ pu at 22:00

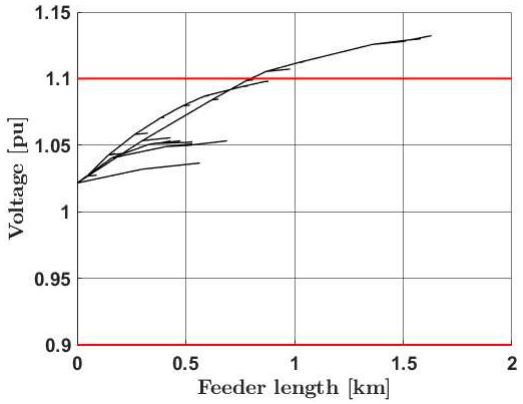

(c) Voltage profile $v = 1.01$ pu at 12:00

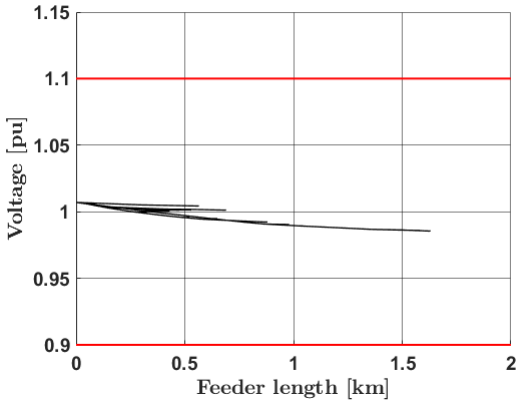

(d) Voltage profile $v = 1.01$ pu at 22:00

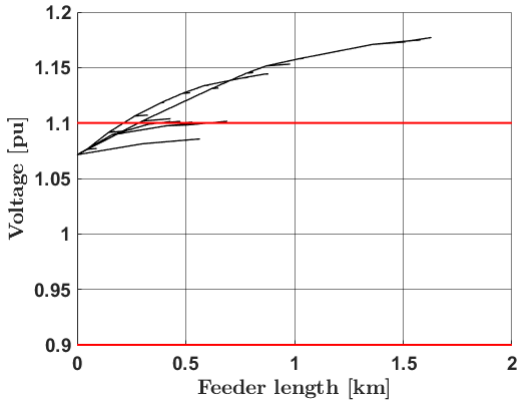

(e) Voltage profile $v = 1.06$ pu at 12:00

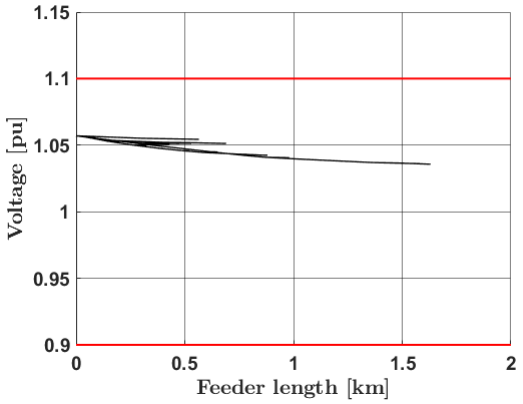

(f) Voltage profile $v = 1.06$ pu at 22:00

Figure B.6: Different voltage profiles with new ZIP coefficients in the Rural Grid-Link with Q_{aut}.

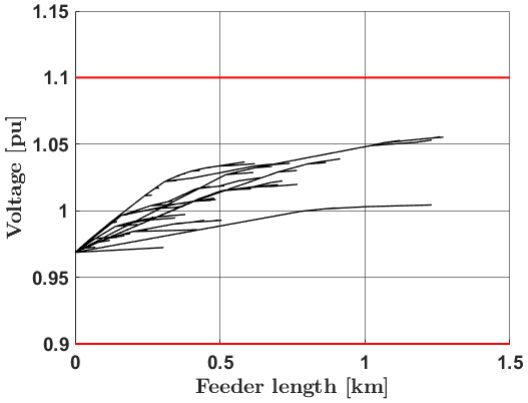

(a) Voltage profile $v = 0.96$ pu at 12:00

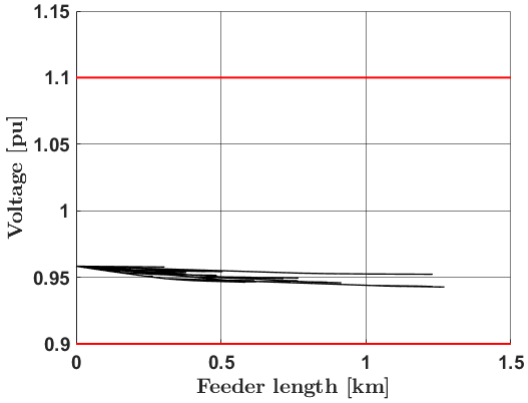

(b) Voltage profile $v = 0.96$ pu at 22:00

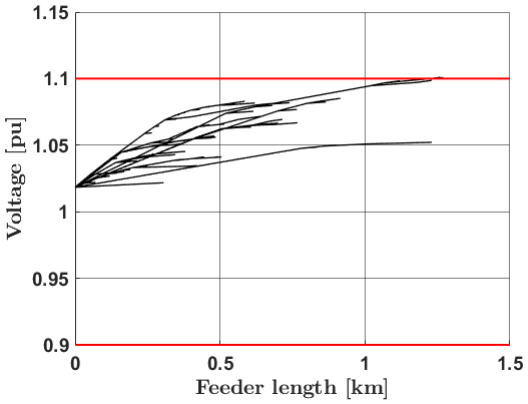

(c) Voltage profile $v = 1.01$ pu at 12:00

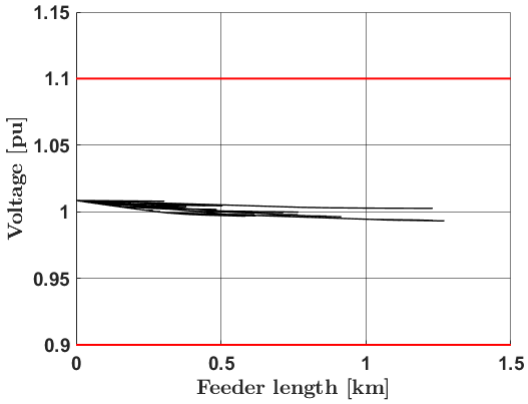

(d) Voltage profile $v = 1.01$ pu at 22:00

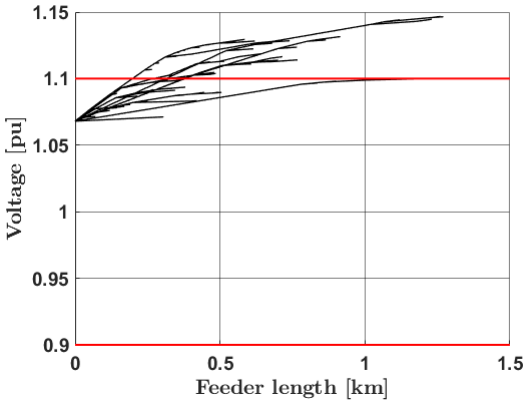

(e) Voltage profile $v = 1.06$ pu at 12:00

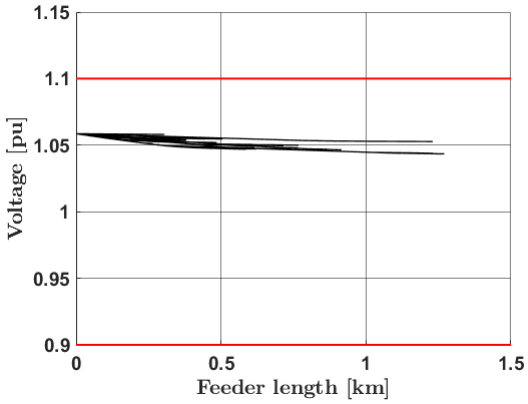

(f) Voltage profile $v = 1.06$ pu at 22:00

Figure B.7: Different voltage profiles with new ZIP coefficients in the Large Urban Grid-Link.

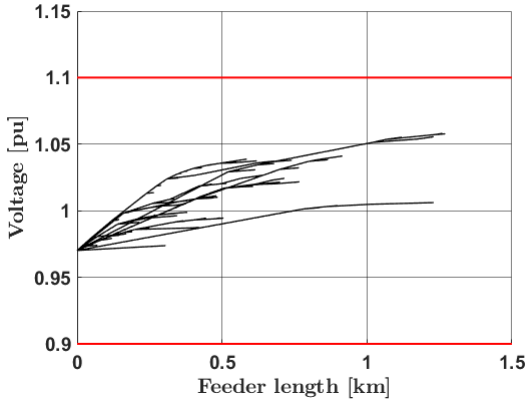

(a) Voltage profile $v = 0.96$ pu at 12:00

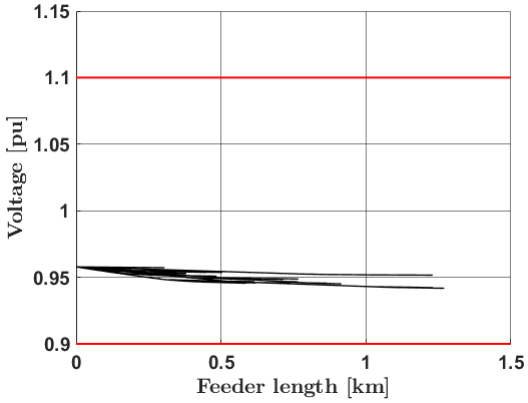

(b) Voltage profile $v = 0.96$ pu at 22:00

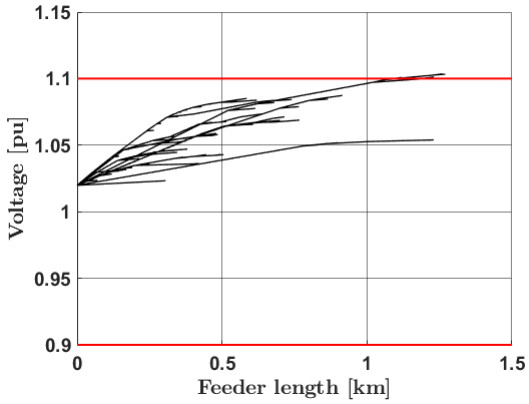

(c) Voltage profile $v = 1.01$ pu at 12:00

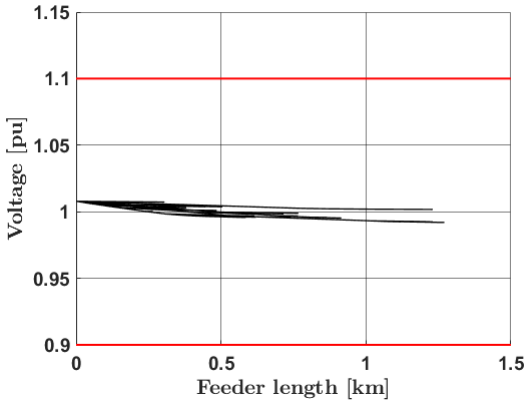

(d) Voltage profile $v = 1.01$ pu at 22:00

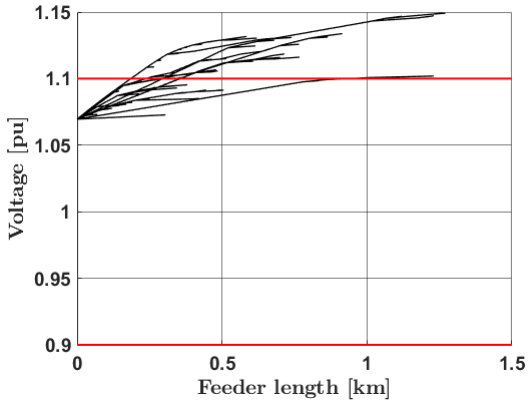

(e) Voltage profile $v = 1.06$ pu at 12:00

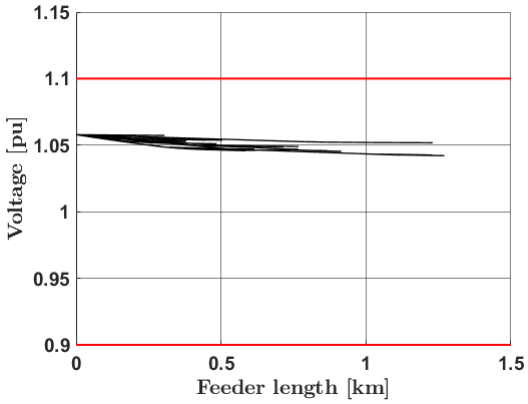

(f) Voltage profile $v = 1.06$ pu at 22:00

Figure B.8: Different voltage profiles with new ZIP coefficients in the Large Urban Grid-Link with Q_{aut}.

B.1.3 LVR case

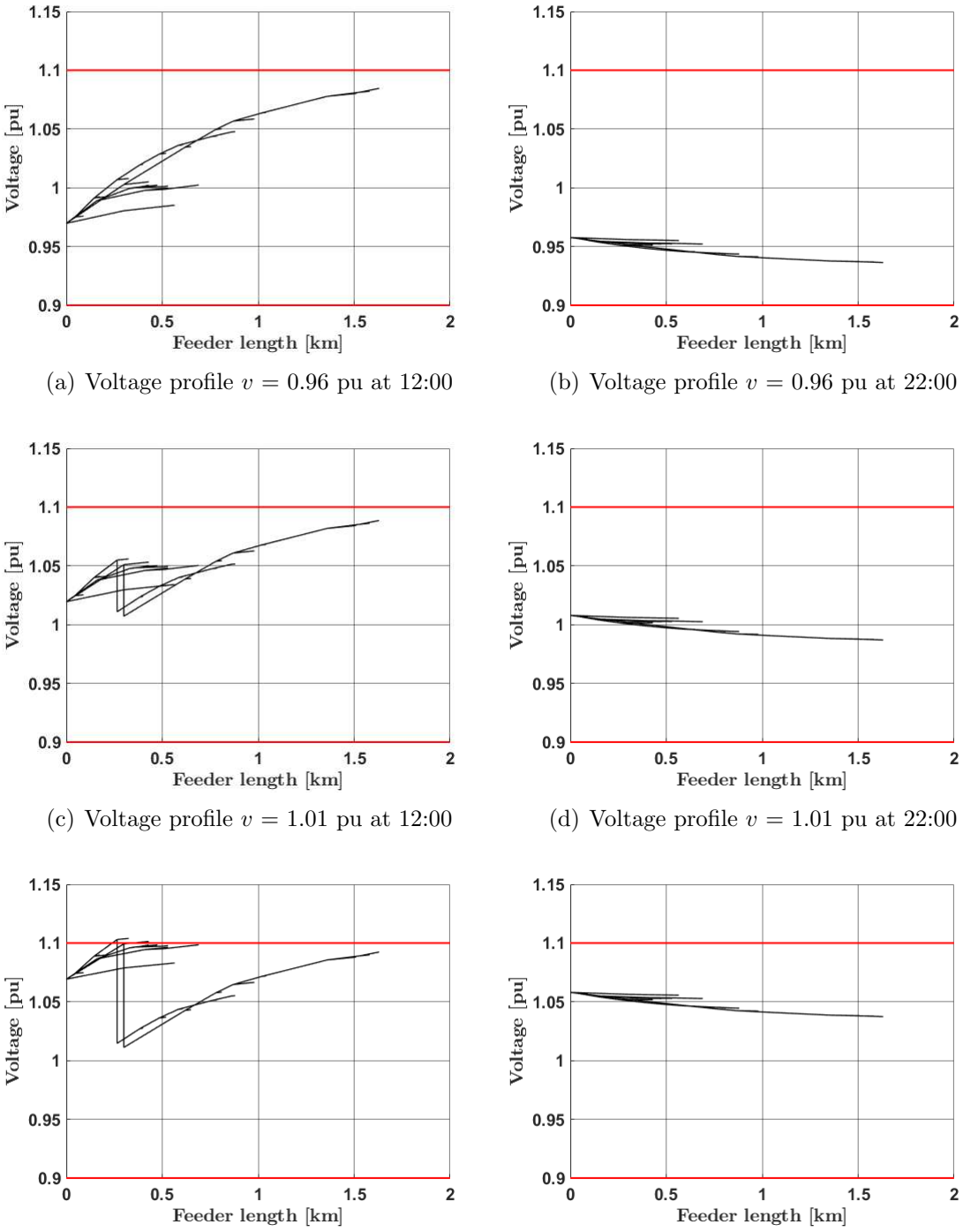

(a) Voltage profile $v = 0.96$ pu at 12:00

(b) Voltage profile $v = 0.96$ pu at 22:00

(c) Voltage profile $v = 1.01$ pu at 12:00

(d) Voltage profile $v = 1.01$ pu at 22:00

(e) Voltage profile $v = 1.06$ pu at 12:00

(f) Voltage profile $v = 1.06$ pu at 22:00

Figure B.9: Different voltage profiles with LVRs and new ZIP coefficients in the Rural GridLink.

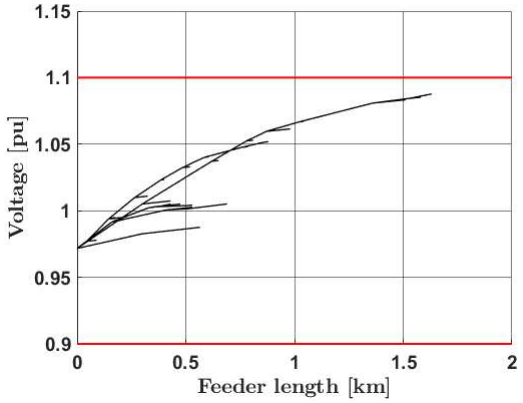

(a) Voltage profile $v = 0.96$ pu at 12:00

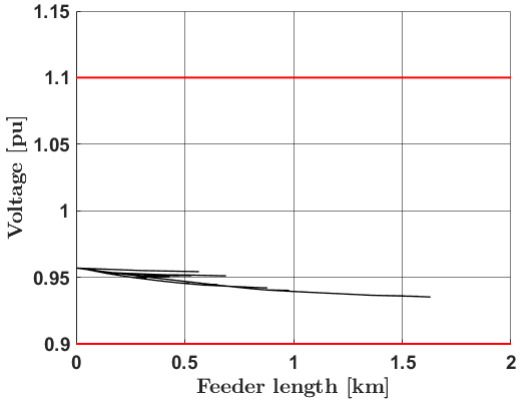

(b) Voltage profile $v = 0.96$ pu at 22:00

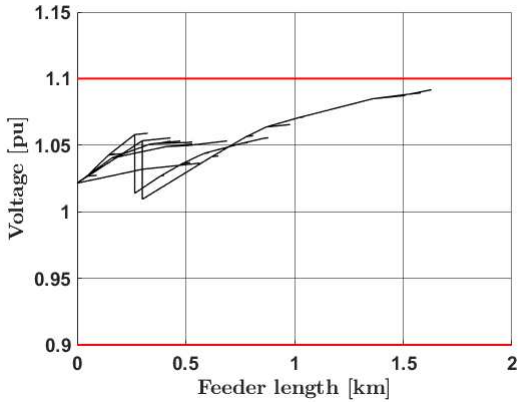

(c) Voltage profile $v = 1.01$ pu at 12:00

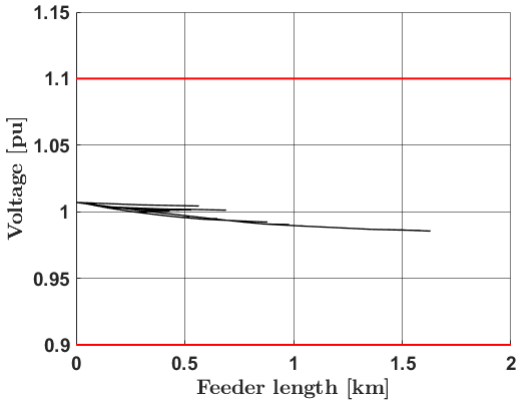

(d) Voltage profile $v = 1.01$ pu at 22:00

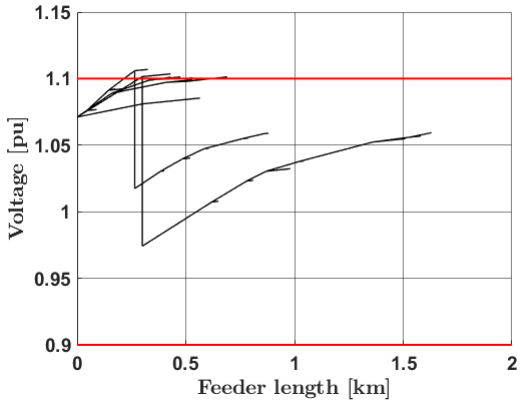

(e) Voltage profile $v = 1.06$ pu at 12:00

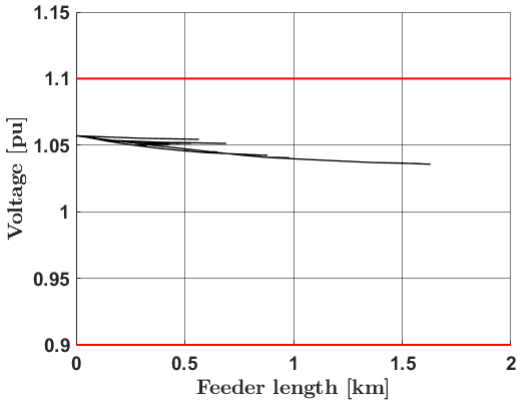

(f) Voltage profile $v = 1.06$ pu at 22:00

Figure B.10: Different voltage profiles with LVRs and new ZIP coefficients in the Rural Grid-Link with Q_{aut}.

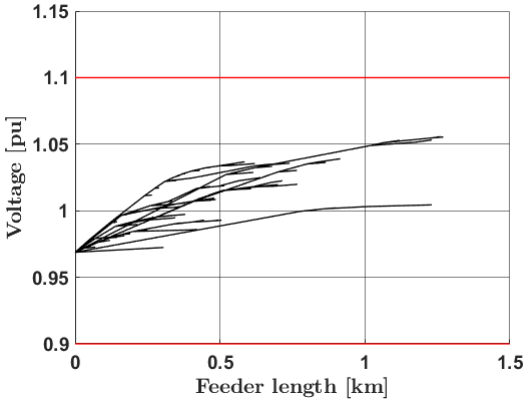

(a) Voltage profile $v = 0.96$ pu at 12:00

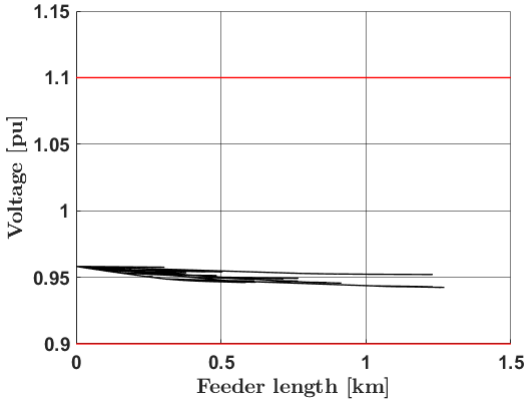

(b) Voltage profile $v = 0.96$ pu at 22:00

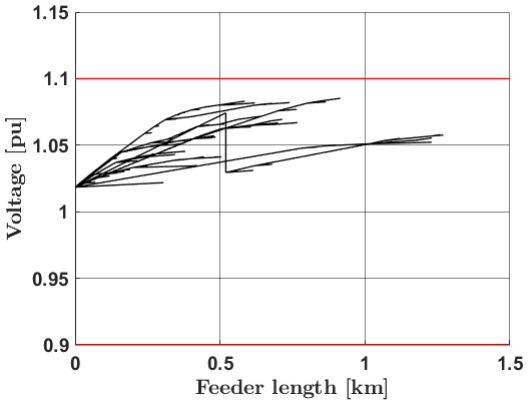

(c) Voltage profile $v = 1.01$ pu at 12:00

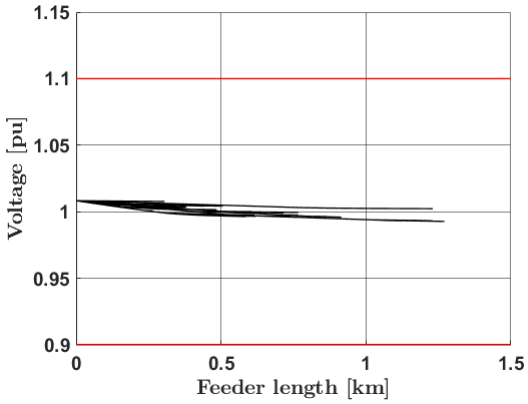

(d) Voltage profile $v = 1.01$ pu at 22:00

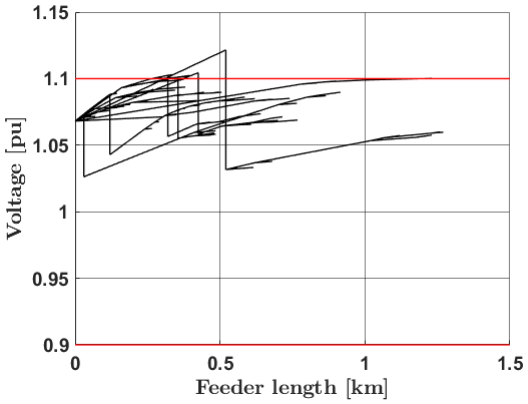

(e) Voltage profile $v = 1.06$ pu at 12:00

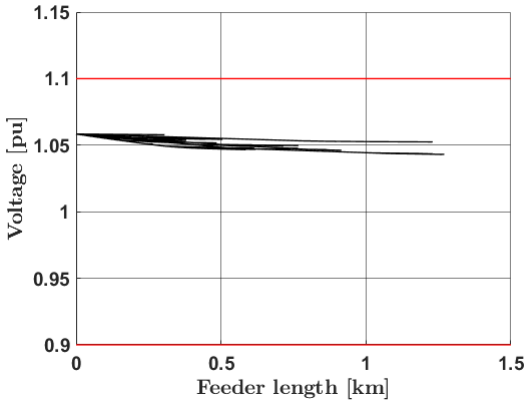

(f) Voltage profile $v = 1.06$ pu at 22:00

Figure B.11: Different voltage profiles with LVRs and new ZIP coefficients in the Large Urban Grid-Link.

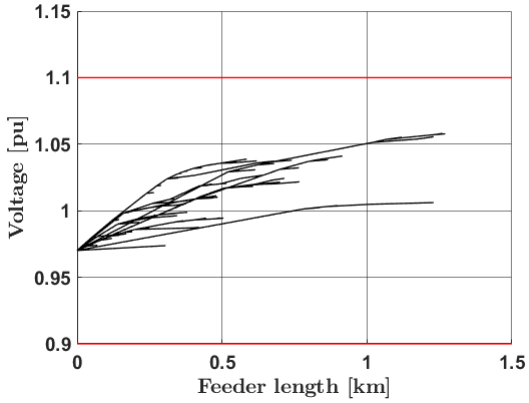

(a) Voltage profile $v = 0.96$ pu at 12:00

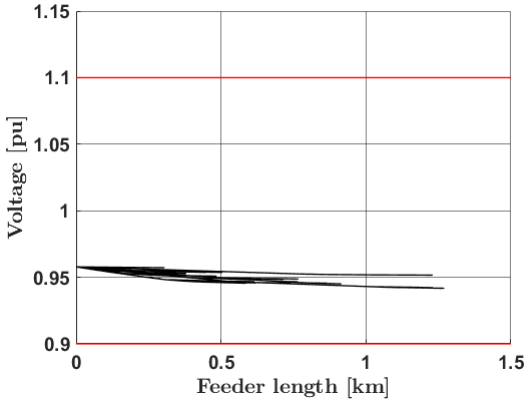

(b) Voltage profile $v = 0.96$ pu at 22:00

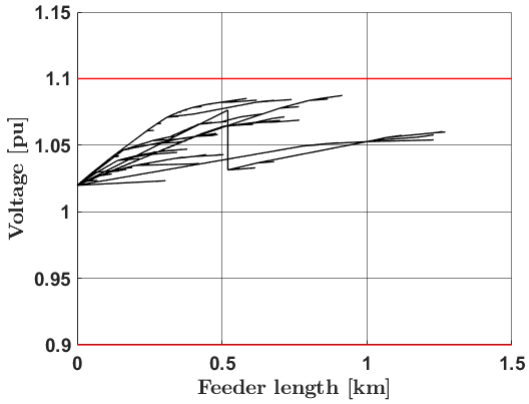

(c) Voltage profile $v = 1.01$ pu at 12:00

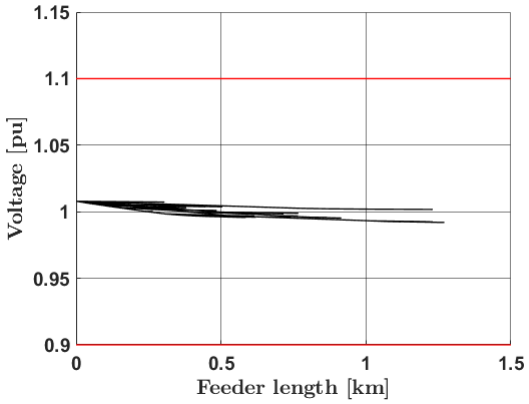

(d) Voltage profile $v = 1.01$ pu at 22:00

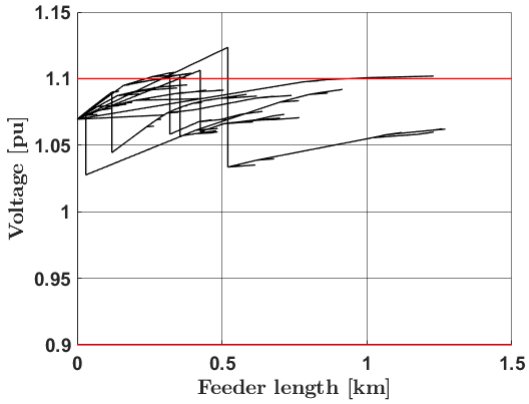

(e) Voltage profile $v = 1.06$ pu at 12:00

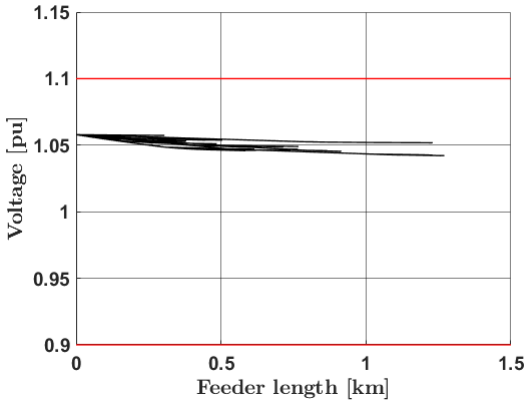

(f) Voltage profile $v = 1.06$ pu at 22:00

Figure B.12: Different voltage profiles with LVRs and new ZIP coefficients in the Large Urban Grid-Link with Q_{aut}.

B.1.4 OLTC-DTR case

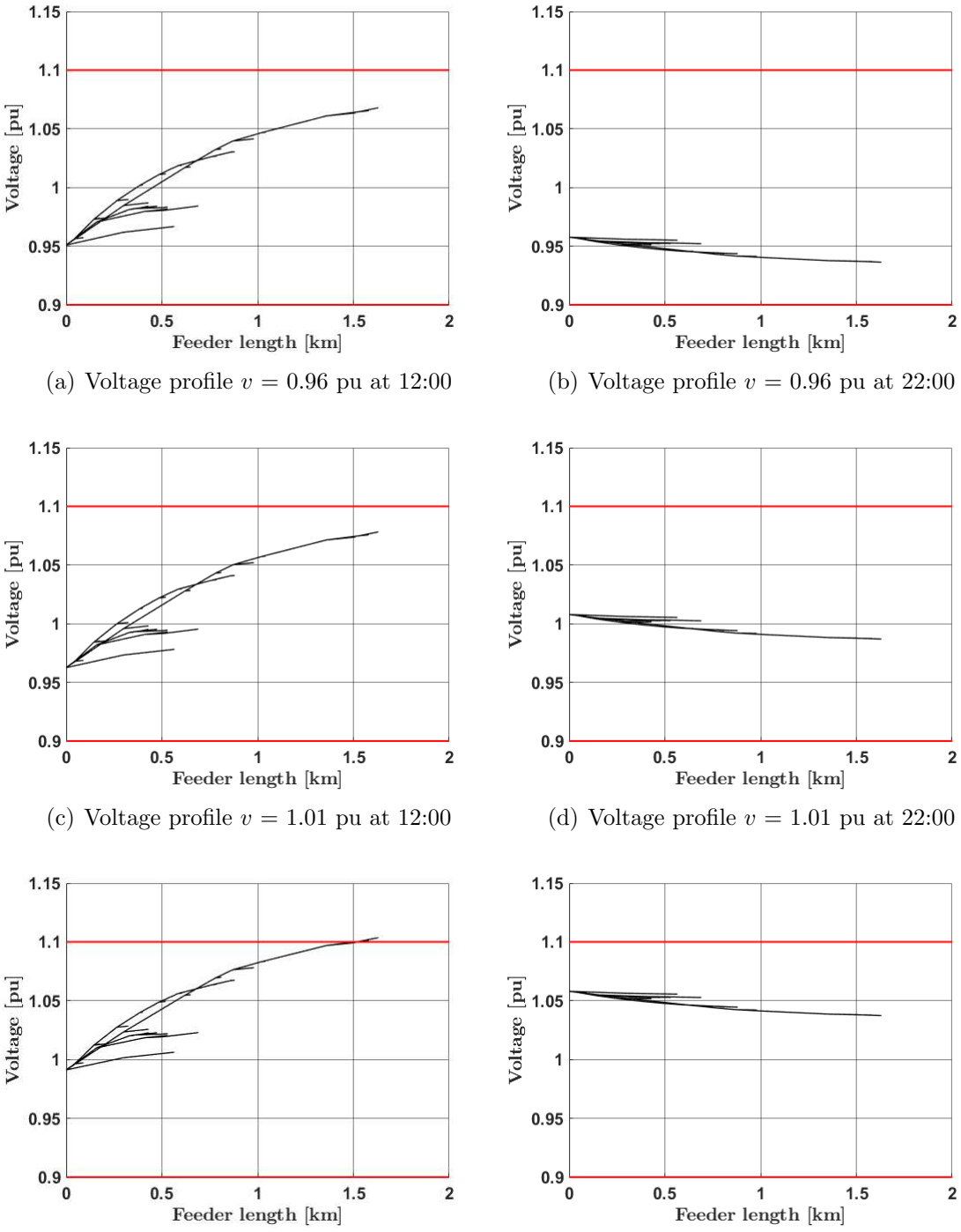

(a) Voltage profile $v = 0.96$ pu at 12:00

(b) Voltage profile $v = 0.96$ pu at 22:00

(c) Voltage profile $v = 1.01$ pu at 12:00

(d) Voltage profile $v = 1.01$ pu at 22:00

(e) Voltage profile $v = 1.06$ pu at 12:00

(f) Voltage profile $v = 1.06$ pu at 22:00

Figure B.13: Different voltage profiles with OLTC-DTR in the Rural Grid-Link.

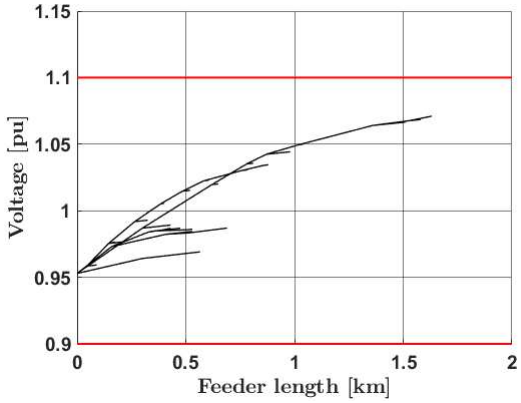

(a) Voltage profile $v = 0.96$ pu at 12:00

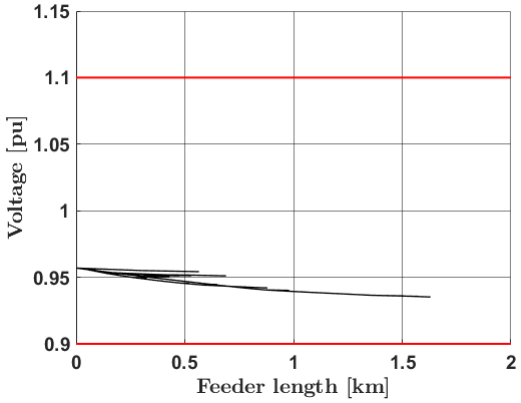

(b) Voltage profile $v = 0.96$ pu at 22:00

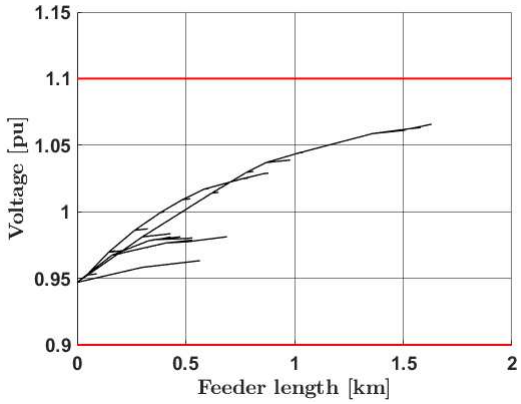

(c) Voltage profile $v = 1.01$ pu at 12:00

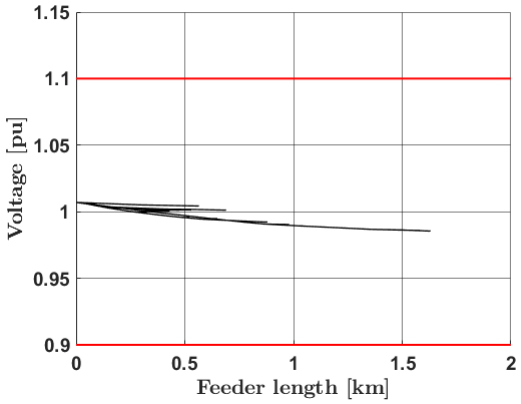

(d) Voltage profile $v = 1.01$ pu at 22:00

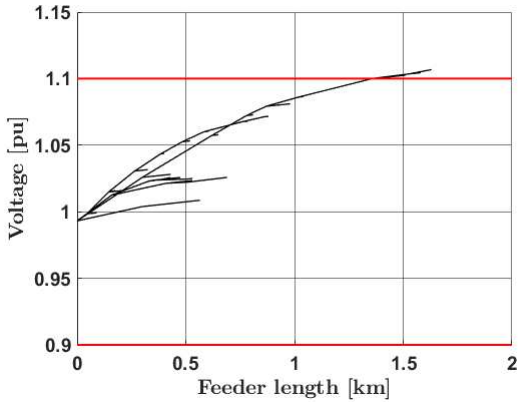

(e) Voltage profile $v = 1.06$ pu at 12:00

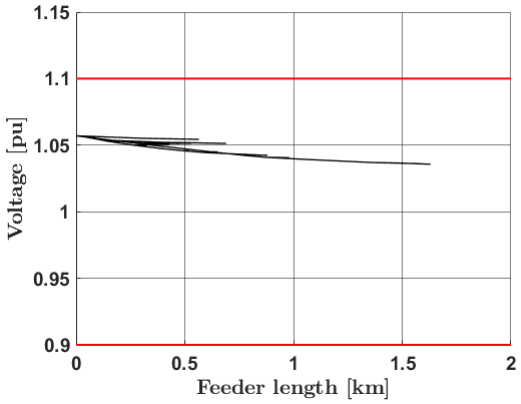

(f) Voltage profile $v = 1.06$ pu at 22:00

Figure B.14: Different voltage profiles with OLTC-DTR in the Rural Grid-Link with Q_{aut}.

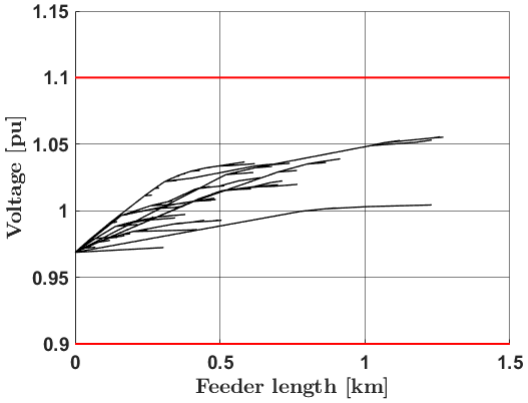

(a) Voltage profile $v = 0.96$ pu at 12:00

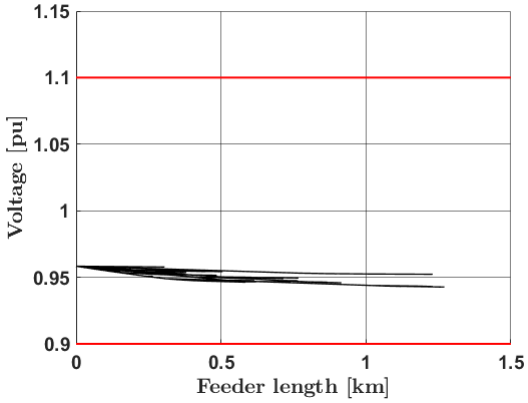

(b) Voltage profile $v = 0.96$ pu at 22:00

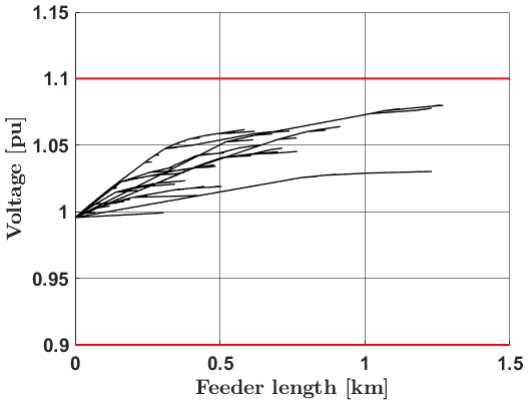

(c) Voltage profile $v = 1.01$ pu at 12:00

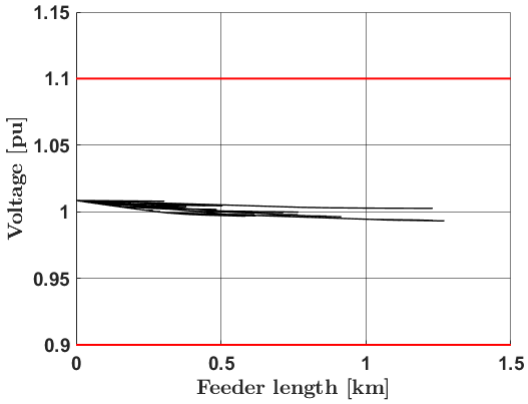

(d) Voltage profile $v = 1.01$ pu at 22:00

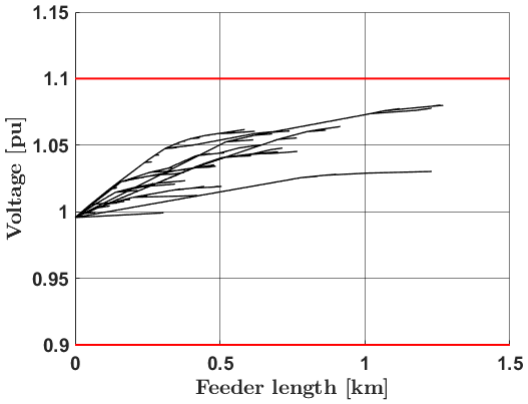

(e) Voltage profile $v = 1.06$ pu at 12:00

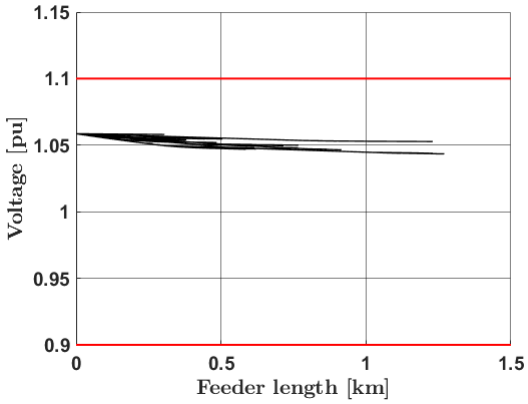

(f) Voltage profile $v = 1.06$ pu at 22:00

Figure B.15: Different voltage profiles with OLTC-DTR in the Large Urban Grid-Link.

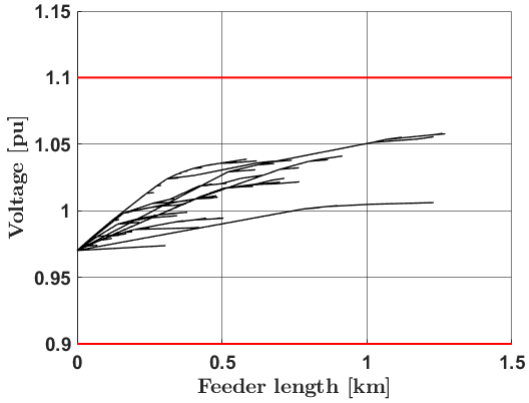

(a) Voltage profile $v = 0.96$ pu at 12:00

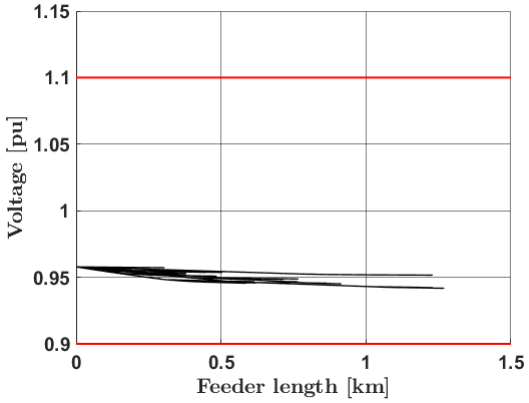

(b) Voltage profile $v = 0.96$ pu at 22:00

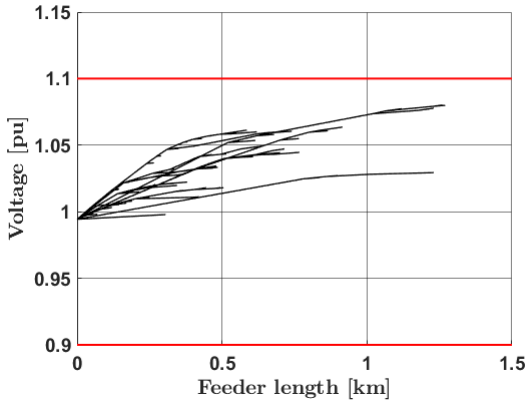

(c) Voltage profile $v = 1.01$ pu at 12:00

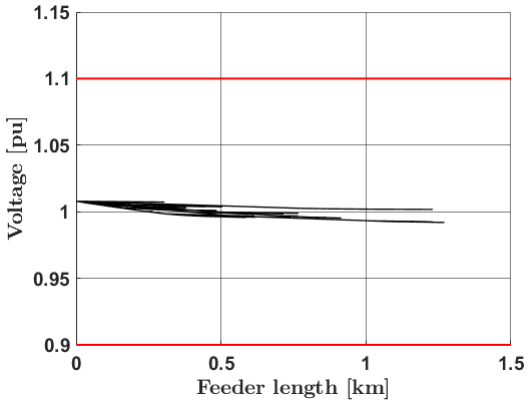

(d) Voltage profile $v = 1.01$ pu at 22:00

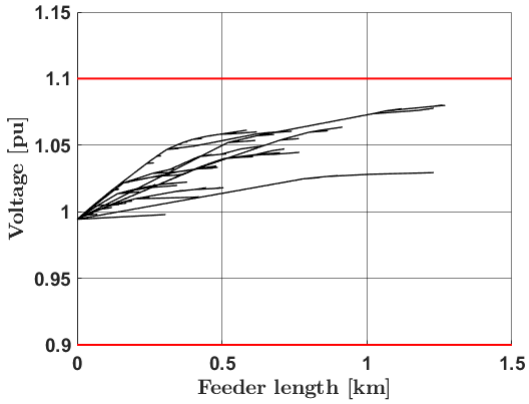

(e) Voltage profile $v = 1.06$ pu at 12:00

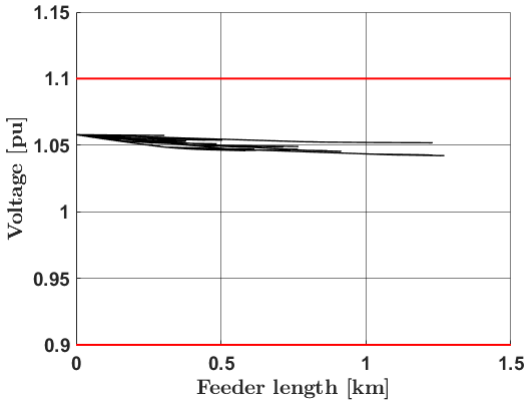

(f) Voltage profile $v = 1.06$ pu at 22:00

Figure B.16: Different voltage profiles with OLTC-DTR in the Large Urban Grid-Link with Q_{aut}.

B.2 Reactive power exchange, losses and DTR loading

B.2.1 Rural Grid-Link base case

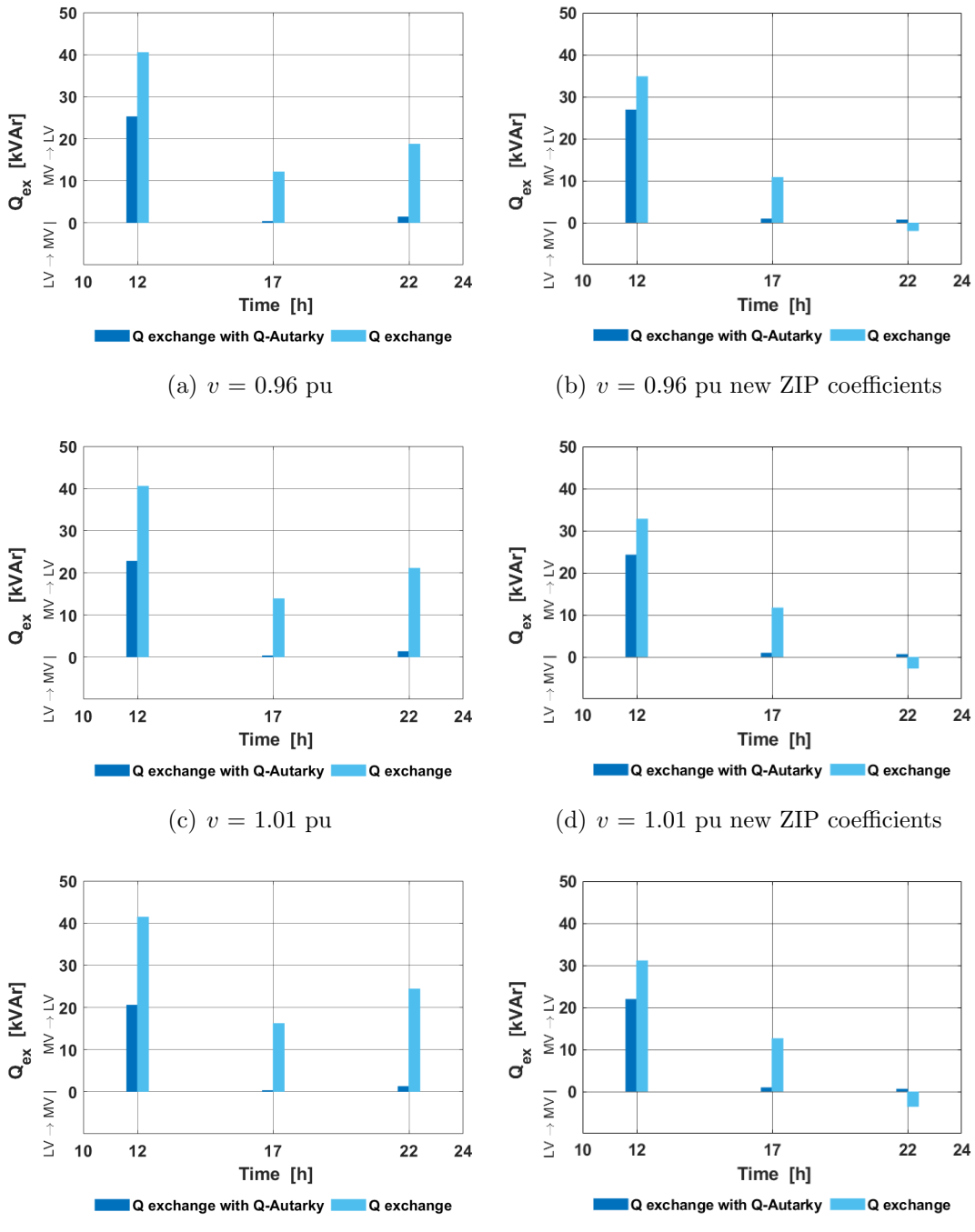

(a) $v = 0.96$ pu

(b) $v = 0.96$ pu new ZIP coefficients

(c) $v = 1.01$ pu

(d) $v = 1.01$ pu new ZIP coefficients

(e) $v = 1.06$ pu

(f) $v = 1.06$ pu new ZIP coefficients

Figure B.17: Different reactive power exchanges in the Rural Grid-Link.

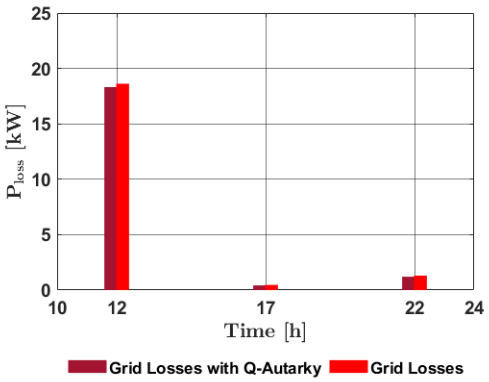

(a) $v = 0.96$ pu

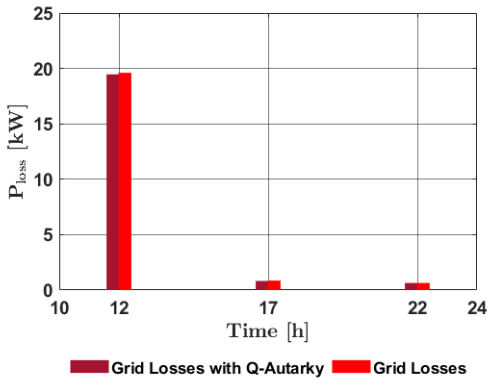

(b) $v = 0.96$ pu new ZIP coefficients

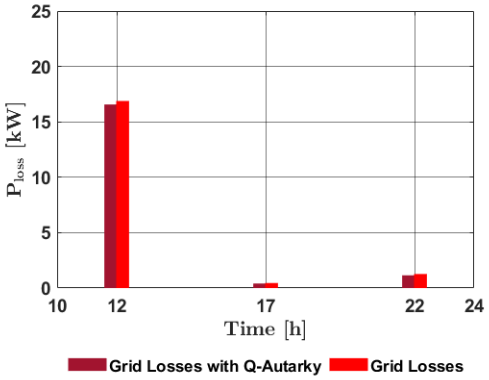

(c) $v = 1.01$ pu

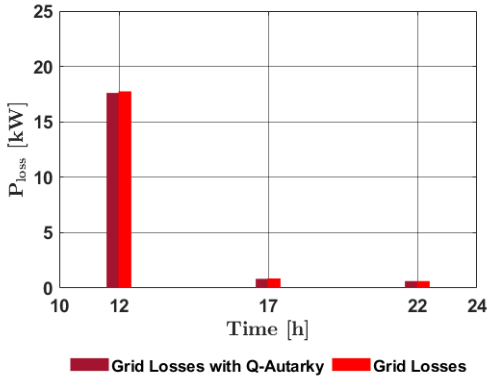

(d) $v = 1.01$ pu new ZIP coefficients

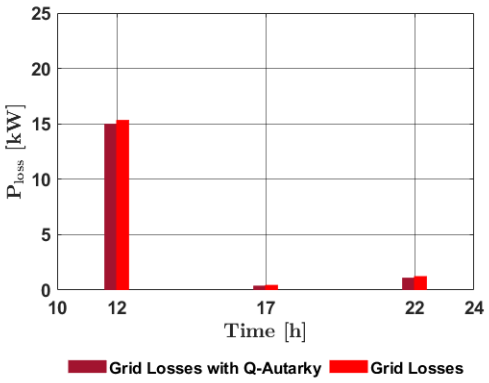

(e) $v = 1.06$ pu

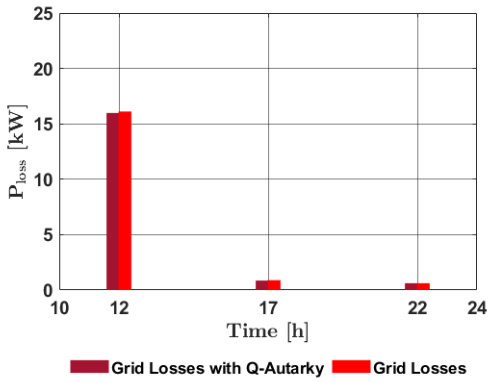

(f) $v = 1.06$ pu new ZIP coefficients

Figure B.18: Different losses in the Rural Grid-Link.

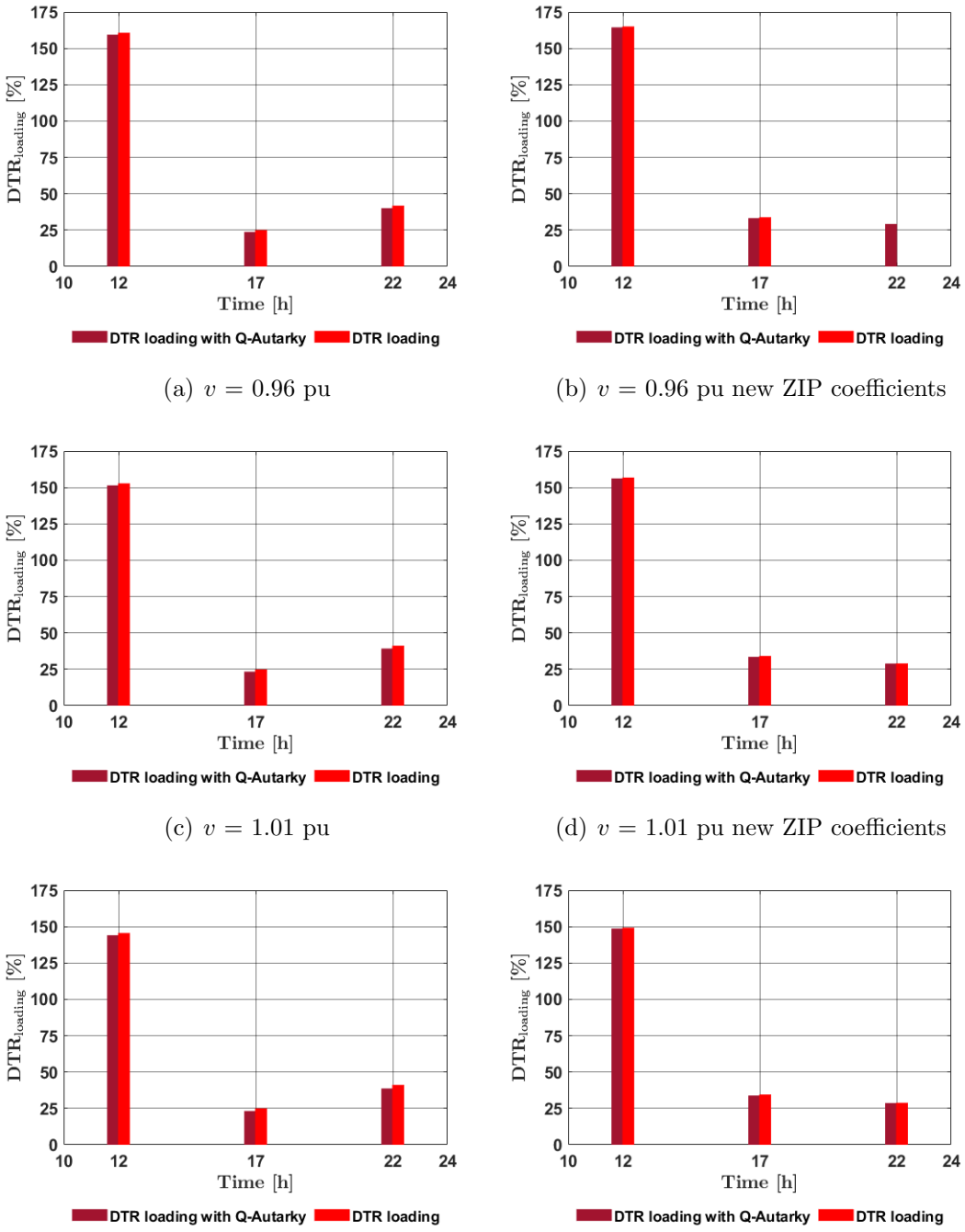

(a) $v = 0.96$ pu

(b) $v = 0.96$ pu new ZIP coefficients

(c) $v = 1.01$ pu

(d) $v = 1.01$ pu new ZIP coefficients

(e) $v = 1.06$ pu

(f) $v = 1.06$ pu new ZIP coefficients

Figure B.19: Different loading of the DTR in the Rural Grid-Link.

B.2.2 Rural Grid-Link LVR

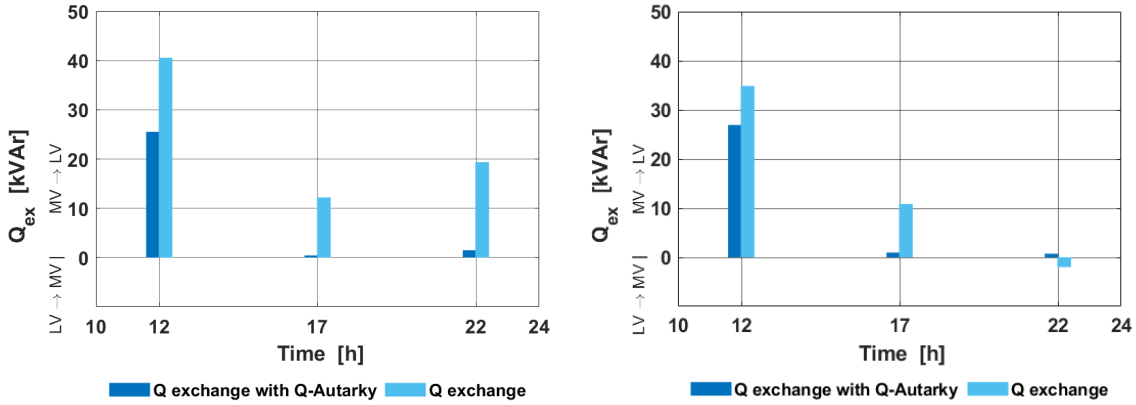

(a) $v = 0.96$ pu

(b) $v = 0.96$ pu new ZIP coefficients

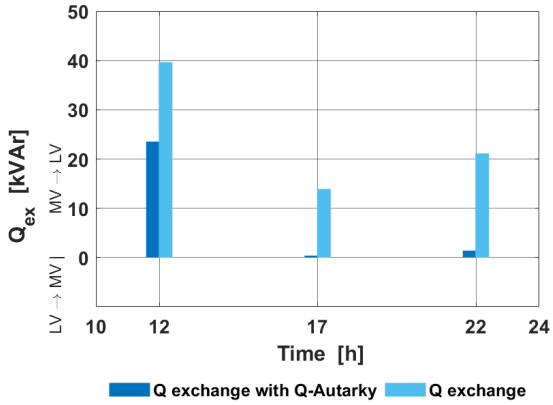

(c) $v = 1.01$ pu

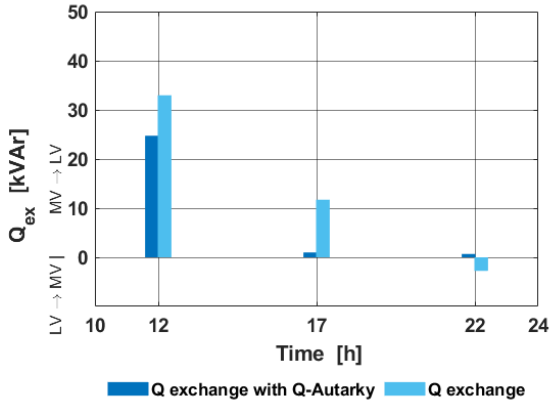

(d) $v = 1.01$ pu new ZIP coefficients

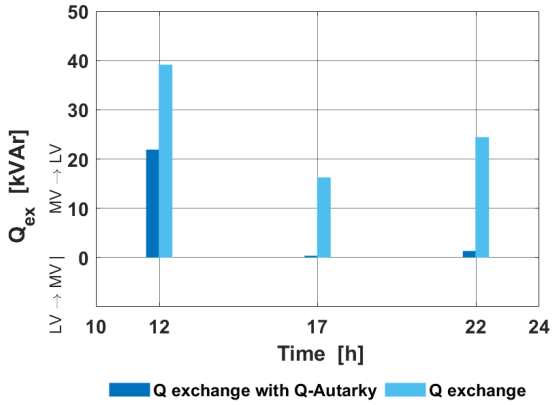

(e) $v = 1.06$ pu

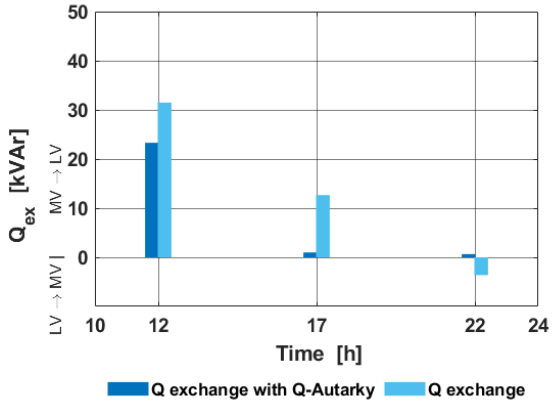

(f) $v = 1.06$ pu new ZIP coefficients

Figure B.20: Different reactive power exchanges with LVRs in the Rural Grid-Link.

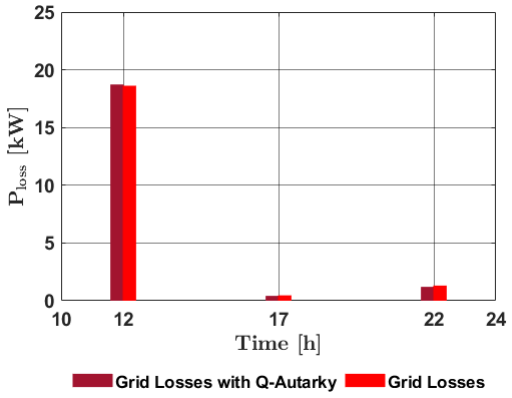

(a) $v = 0.96$ pu

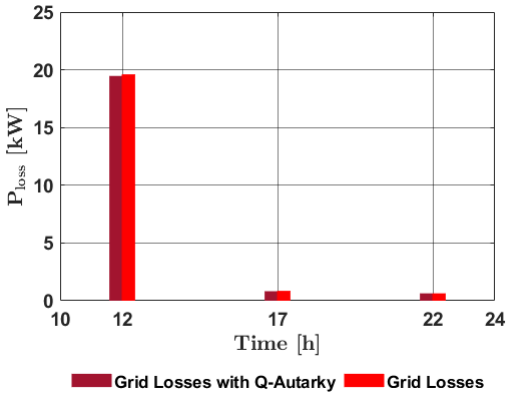

(b) $v = 0.96$ pu new ZIP coefficients

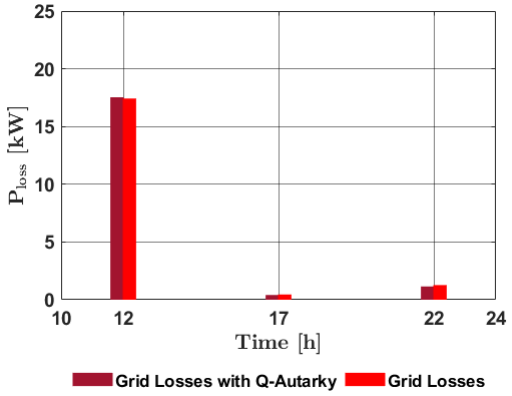

(c) $v = 1.01$ pu

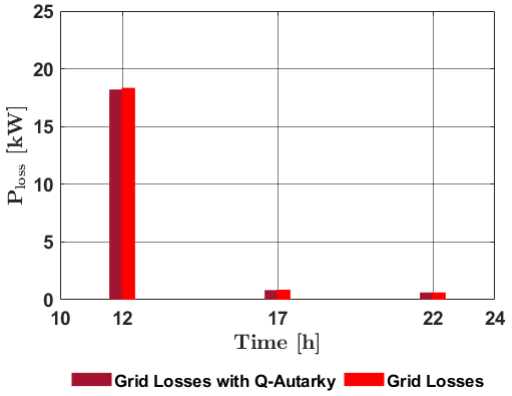

(d) $v = 1.01$ pu new ZIP coefficients

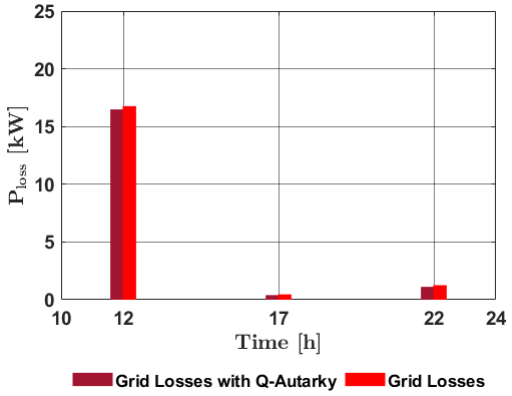

(e) $v = 1.06$ pu

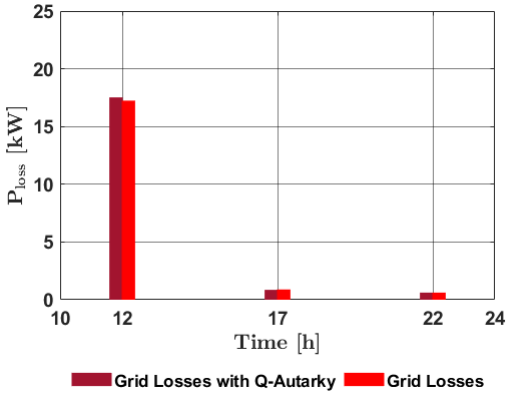

(f) $v = 1.06$ pu new ZIP Coefficients

Figure B.21: Different losses with LVRs in the Rural Grid-Link.

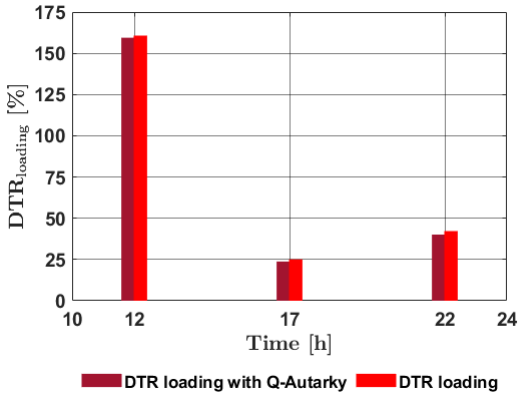

(a) $v = 0.96$ pu

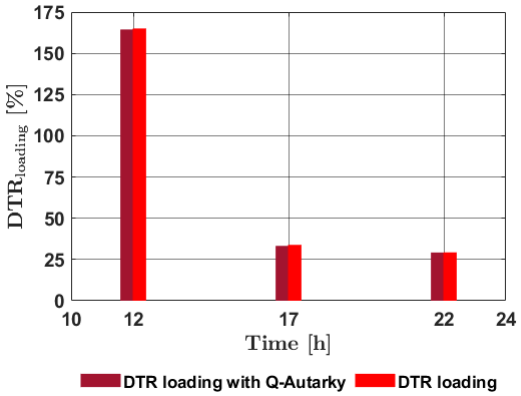

(b) $v = 0.96$ pu new ZIP coefficients

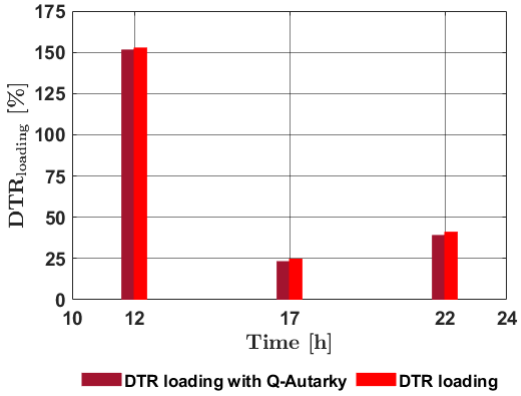

(c) $v = 1.01$ pu

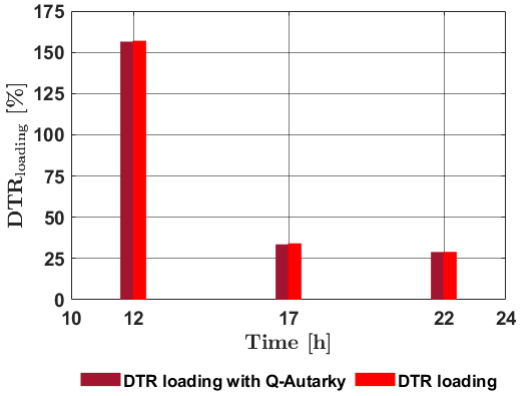

(d) $v = 1.01$ pu new ZIP coefficients

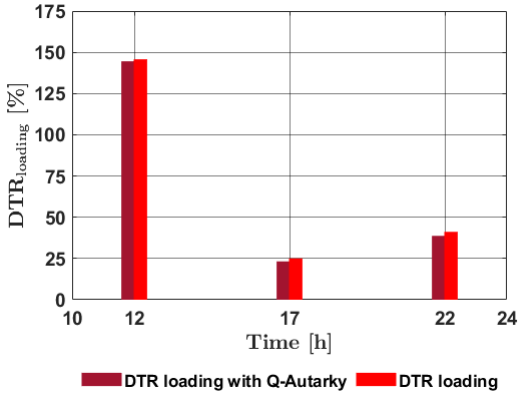

(e) $v = 1.06$ pu

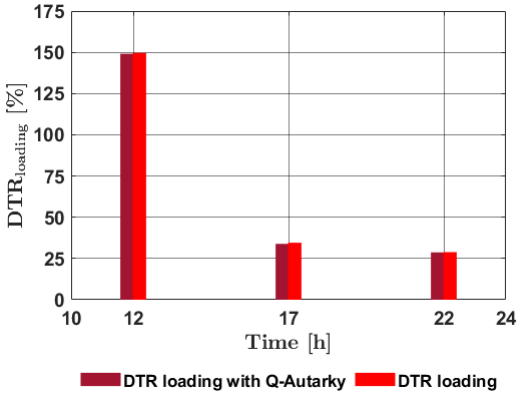

(f) $v = 1.06$ pu new ZIP coefficients

Figure B.22: Different loading of the DTR with LVRs in the Rural Grid-Link.

B.2.3 Rural Grid-Link OLTC-DTR

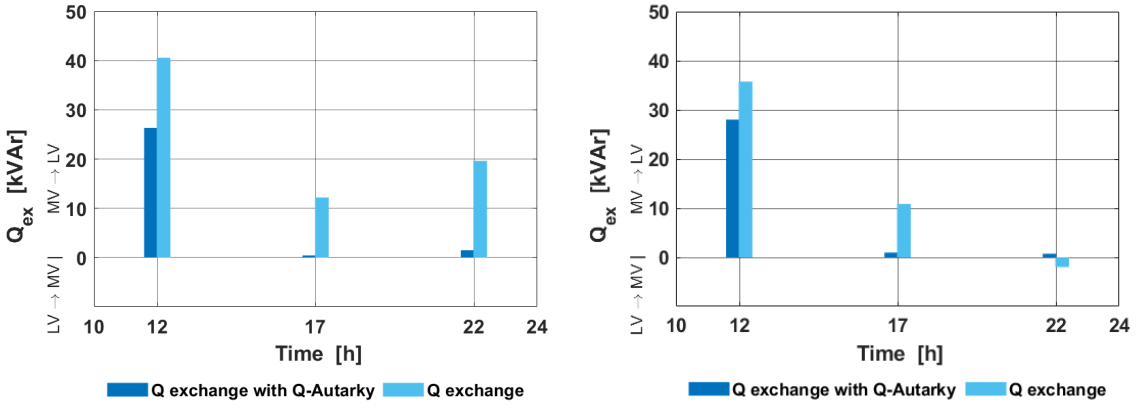

(a) $v = 0.96$ pu

(b) $v = 0.96$ pu new ZIP coefficients

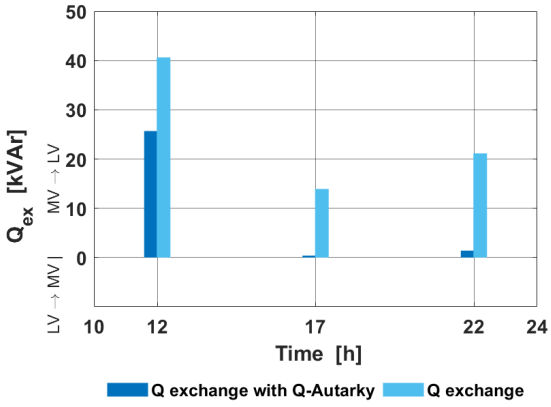

(c) $v = 1.01$ pu

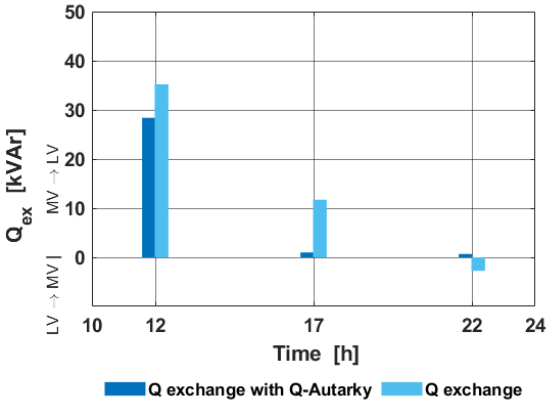

(d) $v = 1.01$ pu new ZIP coefficients

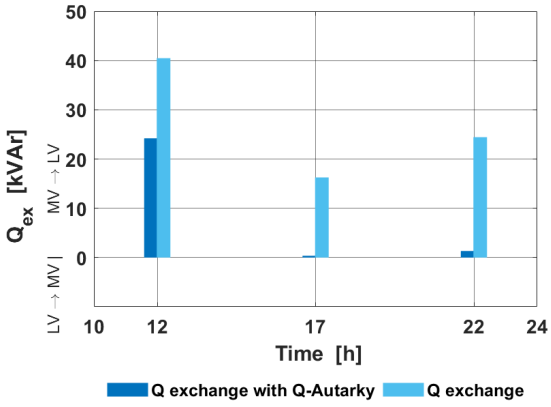

(e) $v = 1.06$ pu

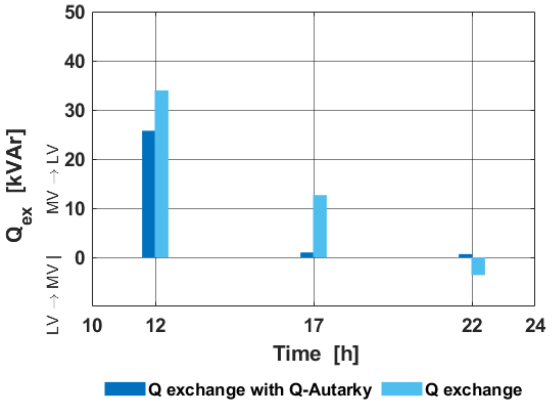

(f) $v = 1.06$ pu new ZIP coefficients

Figure B.23: Different reactive power exchanges with OLTC-DTR in the Rural Grid-Link.

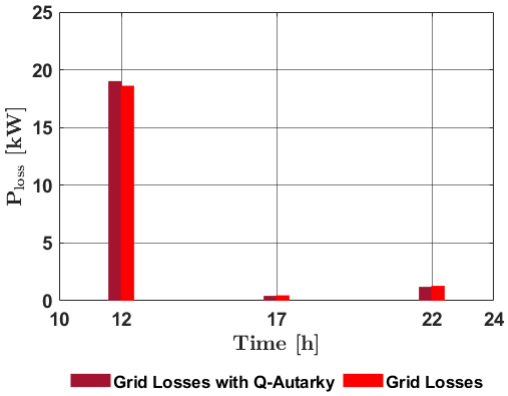

(a) $v = 0.96$ pu

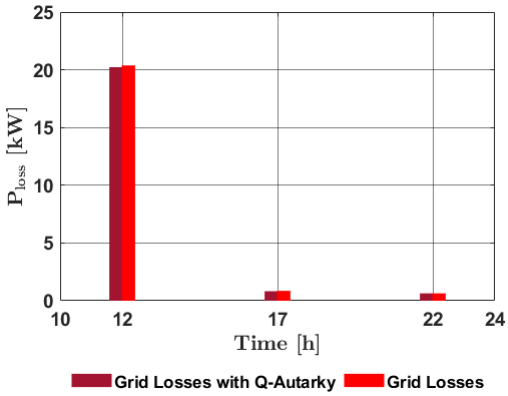

(b) $v = 0.96$ pu new ZIP coefficients

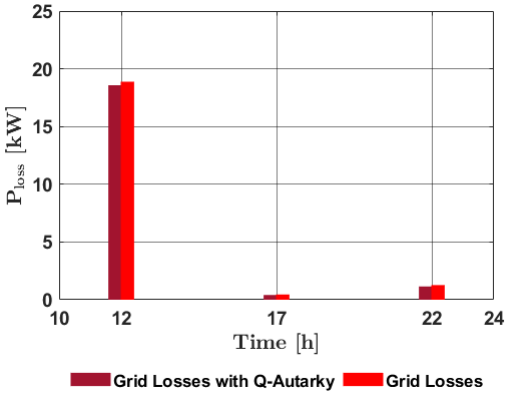

(c) $v = 1.01$ pu

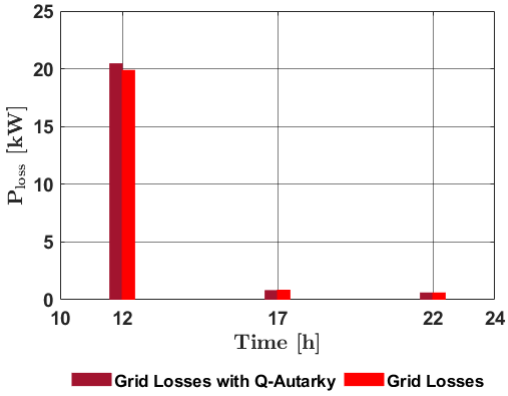

(d) $v = 1.01$ pu new ZIP coefficients

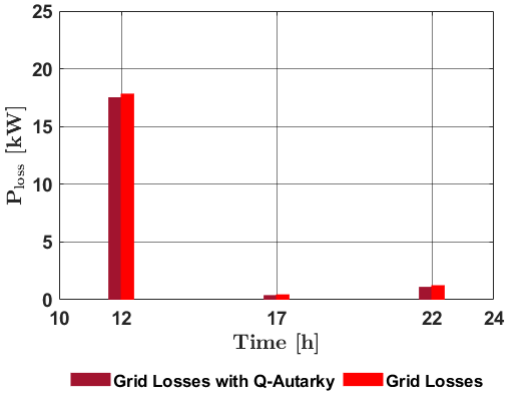

(e) $v = 1.06$ pu

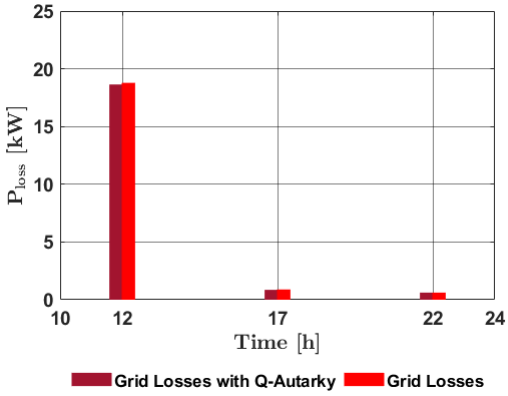

(f) $v = 1.06$ pu new ZIP coefficients

Figure B.24: Different losses with OLTC-DTR in the Rural Grid-Link.

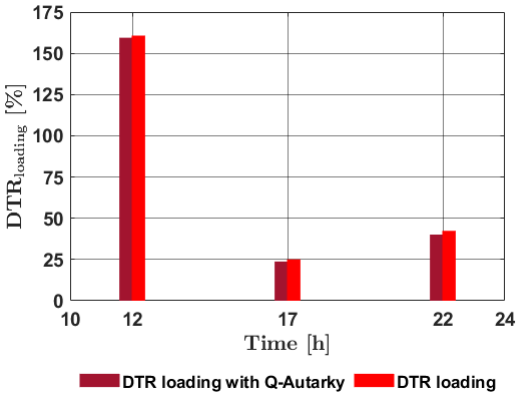

(a) $v = 0.96$ pu

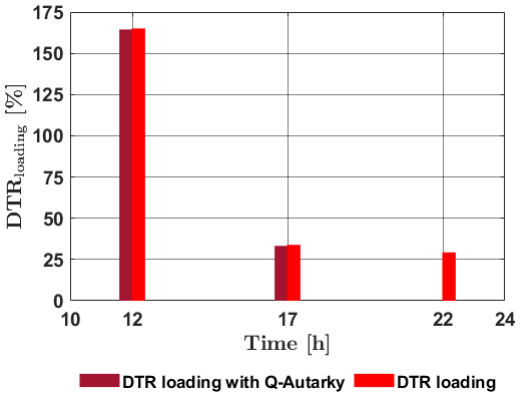

(b) $v = 0.96$ pu new ZIP coefficients

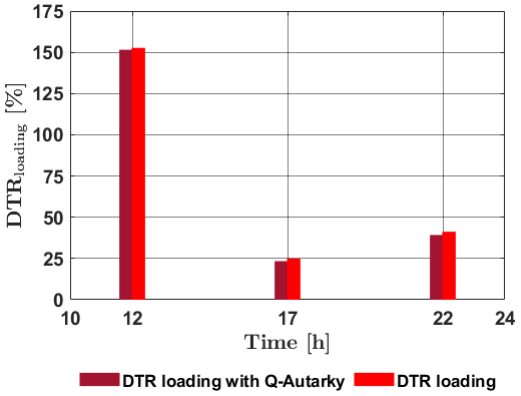

(c) $v = 1.01$ pu

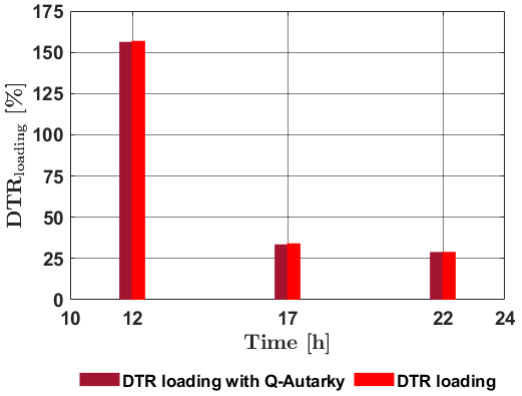

(d) $v = 1.01$ pu new ZIP coefficients

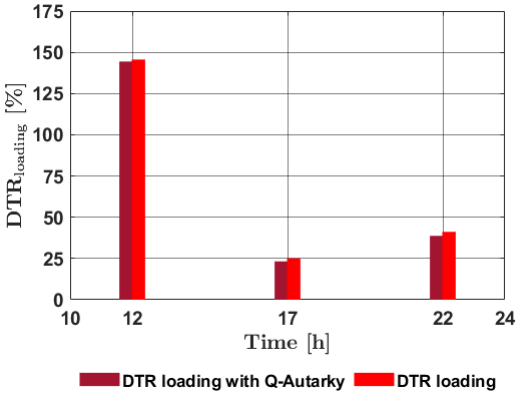

(e) $v = 1.06$ pu

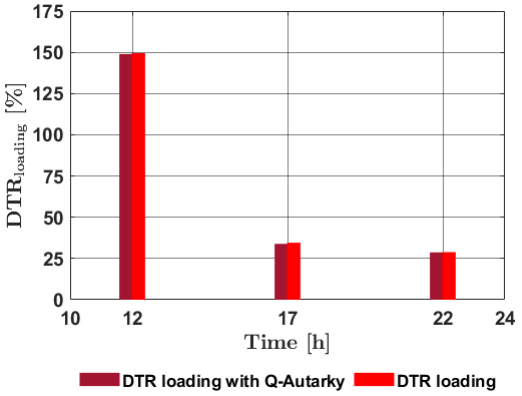

(f) $v = 1.06$ pu new ZIP coefficients

Figure B.25: Different loading of the DTR with OLTC-DTR in the Rural Grid-Link.

B.2.4 Large Urban Grid-Link base case

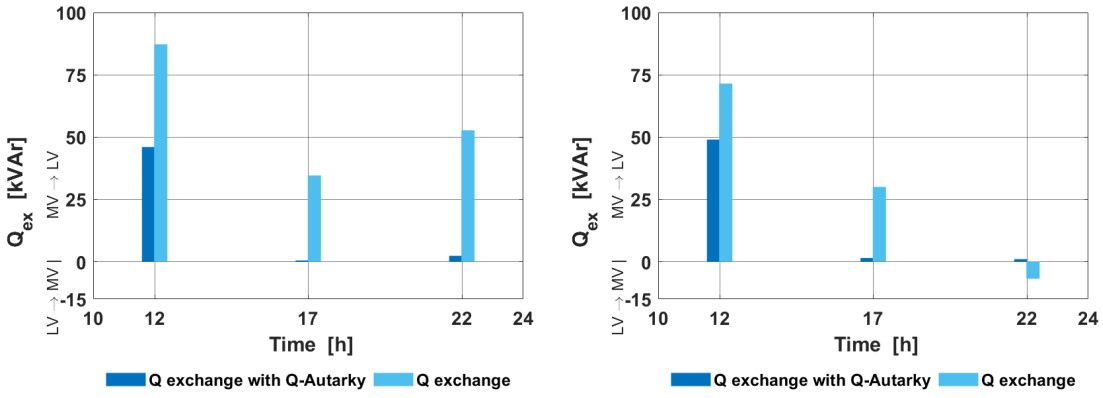

(a) $v = 0.96$ pu

(b) $v = 0.96$ pu new ZIP coefficients

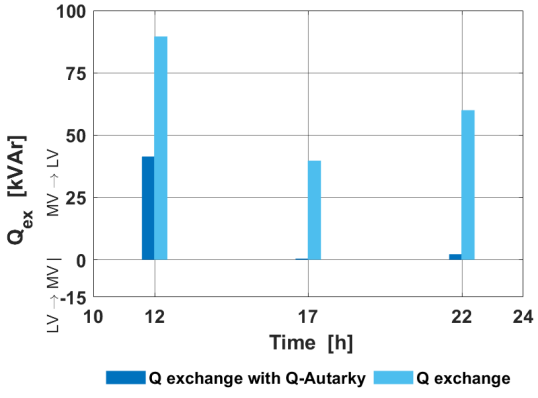

(c) $v = 1.01$ pu

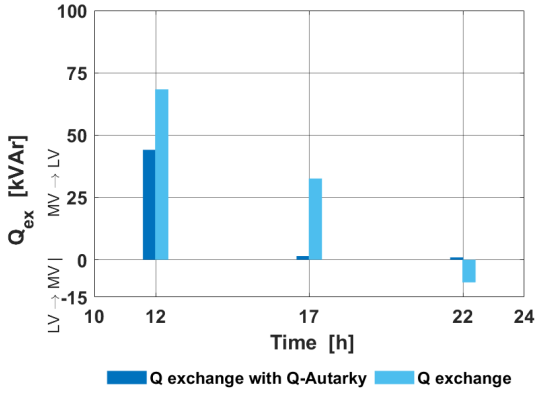

(d) $v = 1.01$ pu new ZIP coefficients

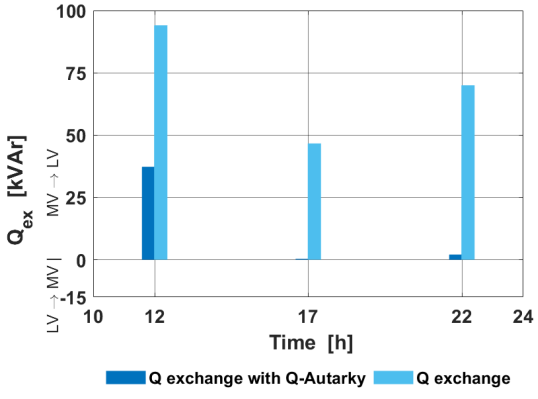

(e) $v = 1.06$ pu

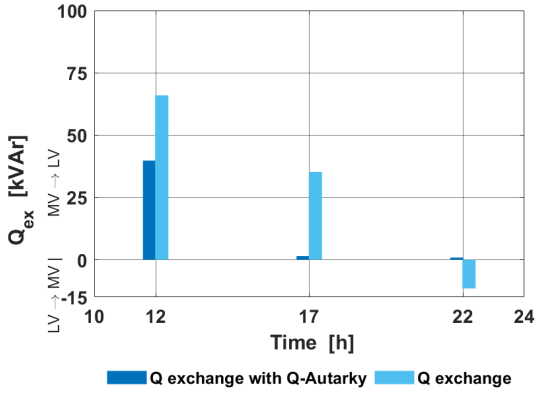

(f) $v = 1.06$ pu new ZIP coefficients

Figure B.26: Different reactive power exchanges in the Large Urban Grid-Link.

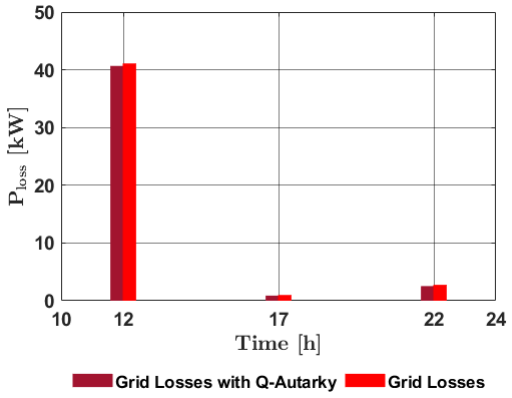

(a) $v = 0.96$ pu

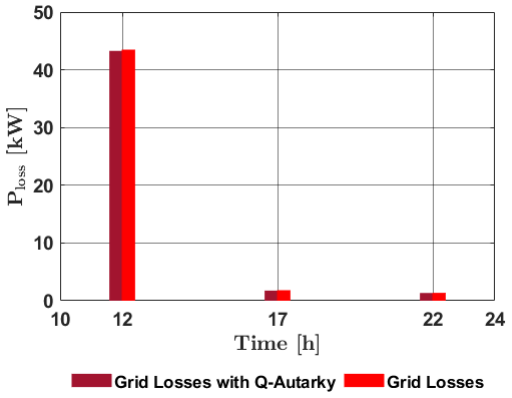

(b) $v = 0.96$ pu new ZIP coefficients

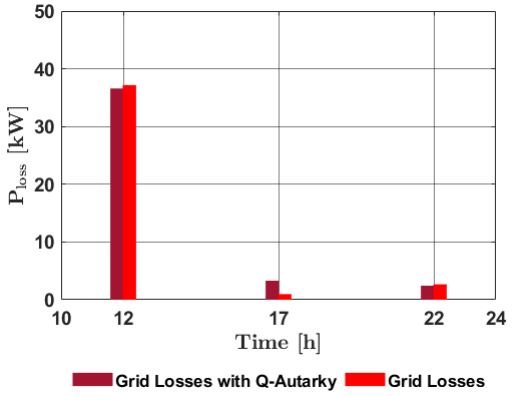

(c) $v = 1.01$ pu

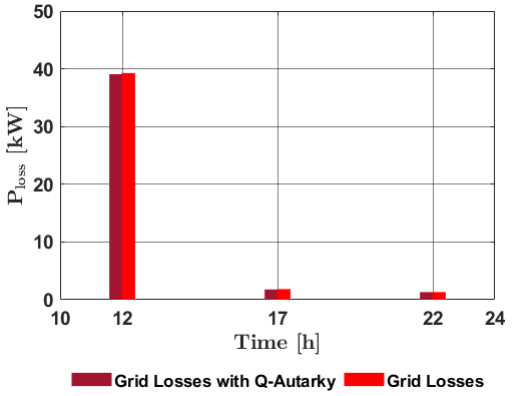

(d) $v = 1.01$ pu new ZIP coefficients

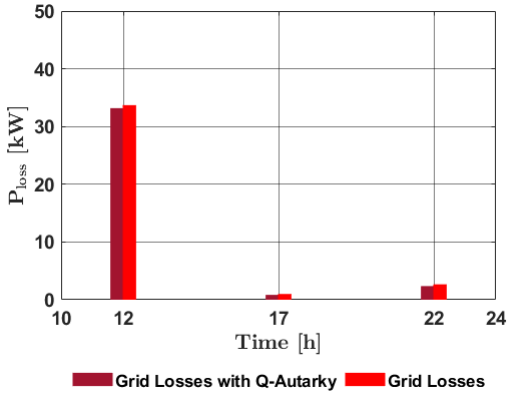

(e) $v = 1.06$ pu

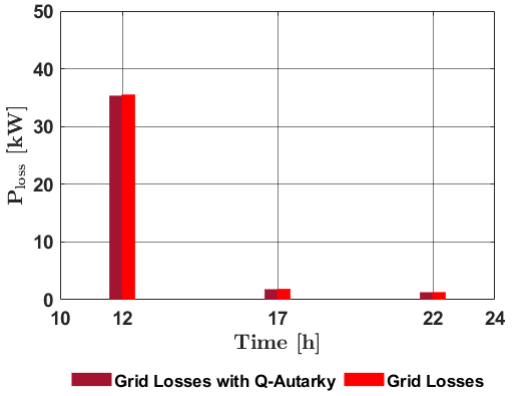

(f) $v = 1.06$ pu new ZIP coefficients

Figure B.27: Different losses in the Large Urban Grid-Link.

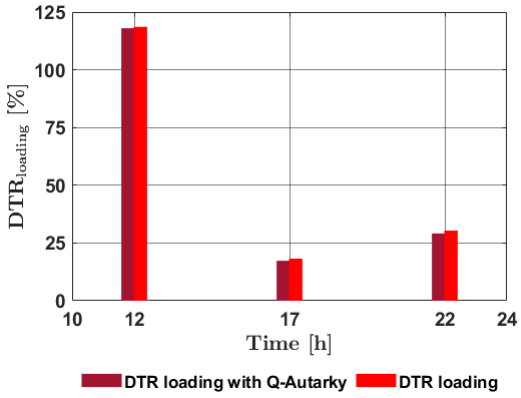

(a) $v = 0.96$ pu

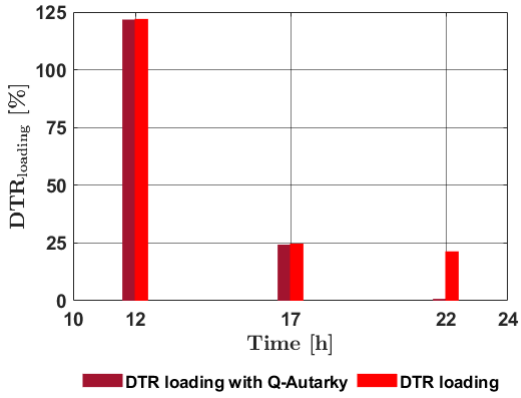

(b) $v = 0.96$ pu new ZIP coefficients

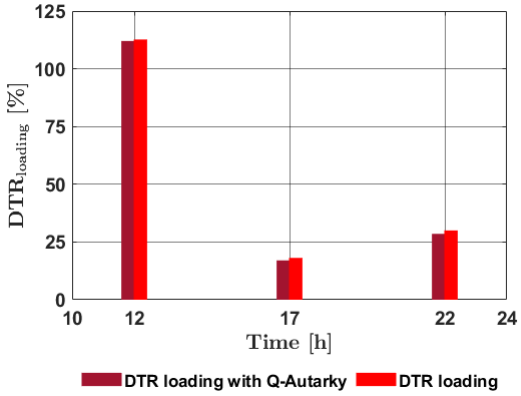

(c) $v = 1.01$ pu

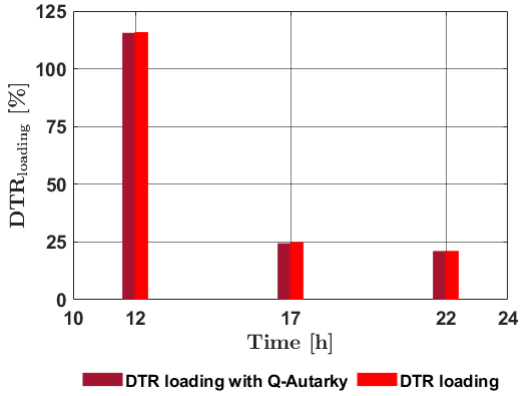

(d) $v = 1.01$ pu new ZIP coefficients

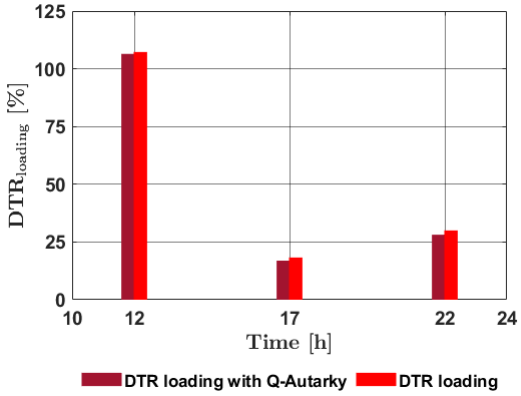

(e) $v = 1.06$ pu

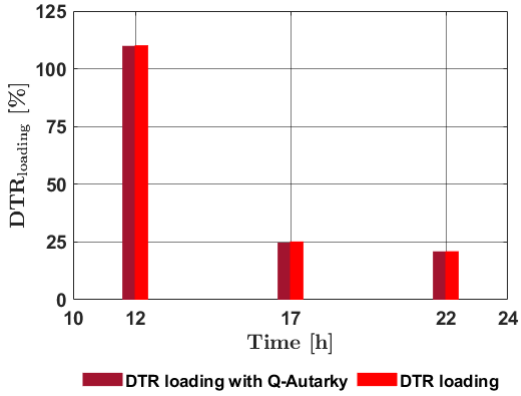

(f) $v = 1.06$ pu new ZIP coefficients

Figure B.28: Different loading of the DTR in the Large Urban Grid-Link.

B.2.5 Large Urban Grid-Link LVR

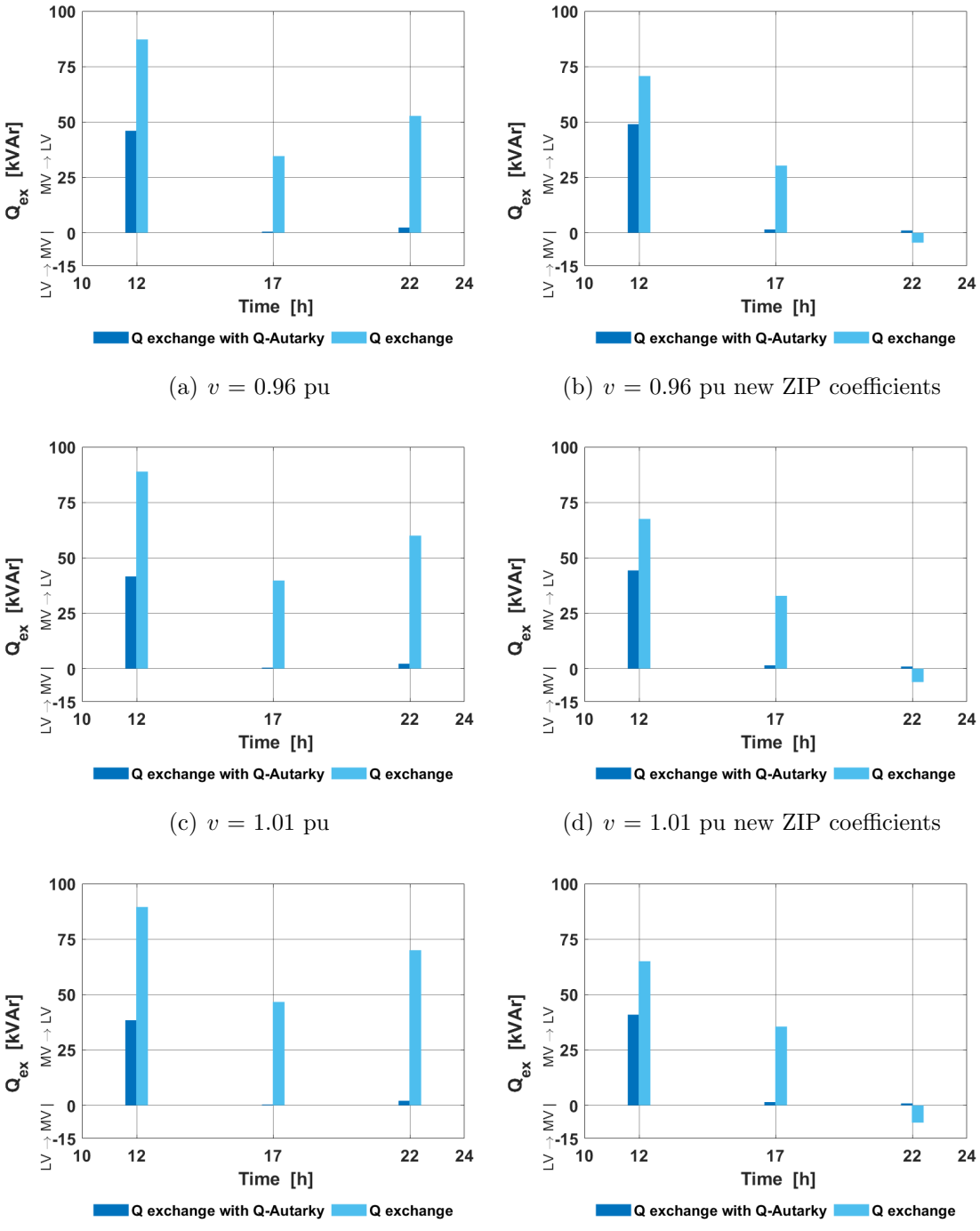

(a) $v = 0.96$ pu

(b) $v = 0.96$ pu new ZIP coefficients

(c) $v = 1.01$ pu

(d) $v = 1.01$ pu new ZIP coefficients

(e) $v = 1.06$ pu

(f) $v = 1.06$ pu new ZIP coefficients

Figure B.29: Different reactive power exchanges with LVRs in the Large Urban Grid-Link.

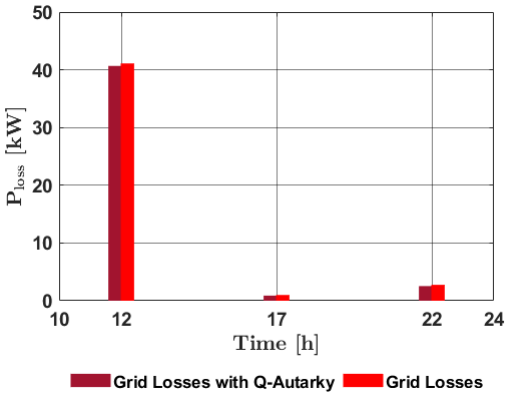

(a) $v = 0.96$ pu

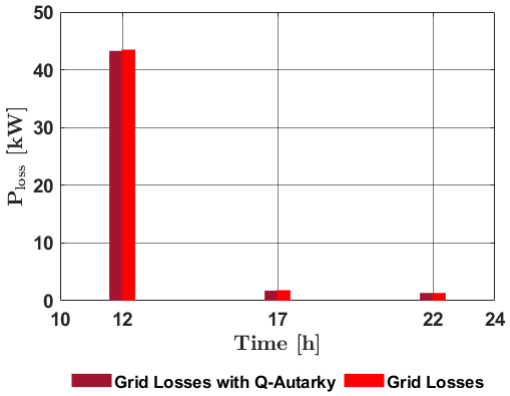

(b) $v = 0.96$ pu new ZIP coefficients

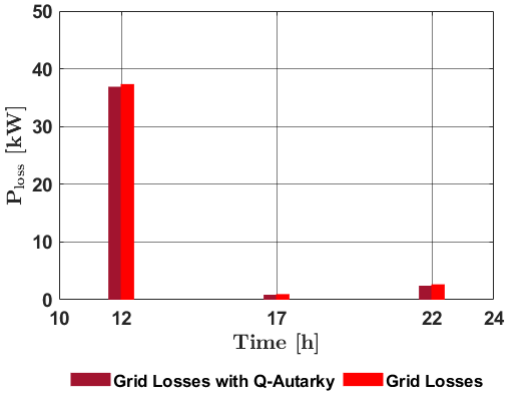

(c) $v = 1.01$ pu

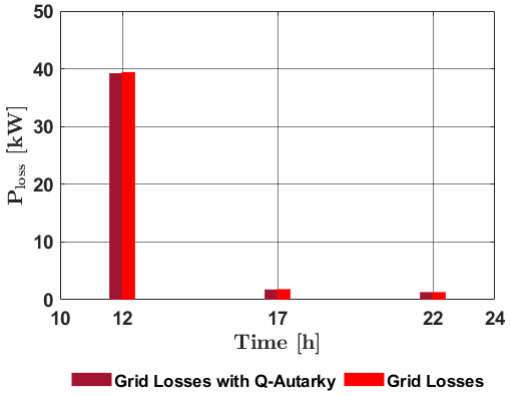

(d) $v = 1.01$ pu new ZIP coefficients

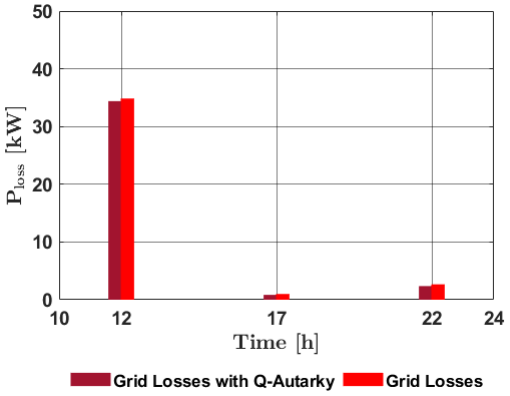

(e) $v = 1.06$ pu

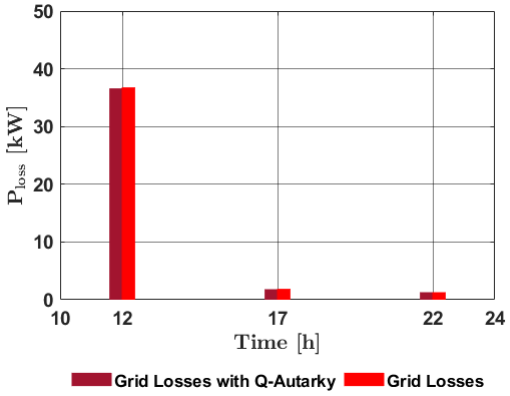

(f) $v = 1.06$ pu new ZIP coefficients

Figure B.30: Different losses with LVRs in the Large Urban Grid-Link.

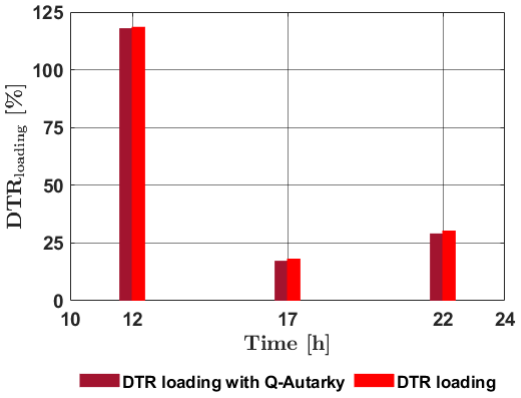

(a) $v = 0.96$ pu

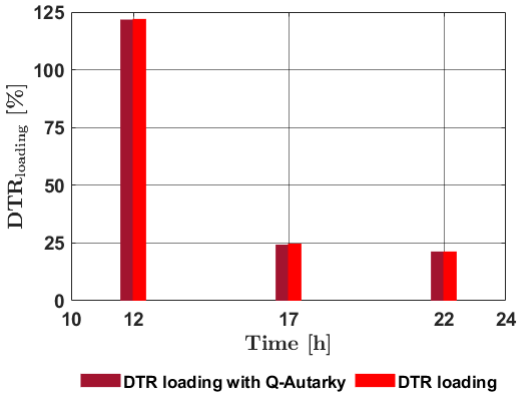

(b) $v = 0.96$ pu new ZIP coefficients

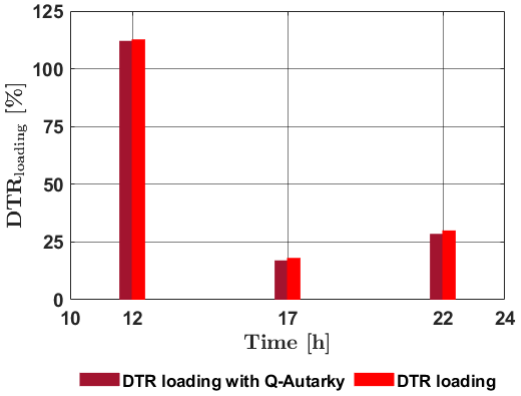

(c) $v = 1.01$ pu

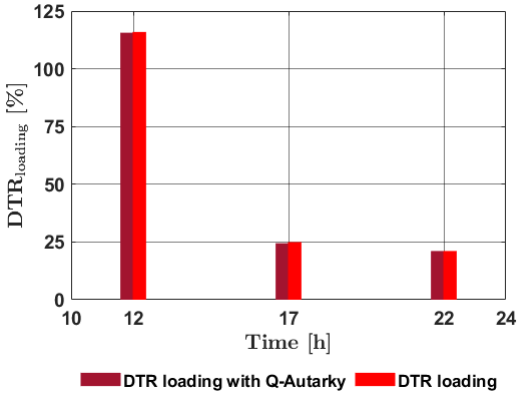

(d) $v = 1.01$ pu new ZIP coefficients

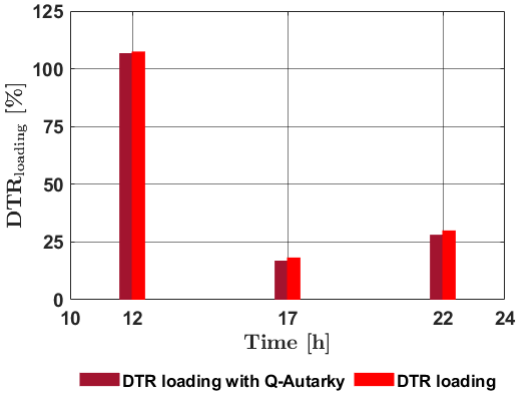

(e) $v = 1.06$ pu

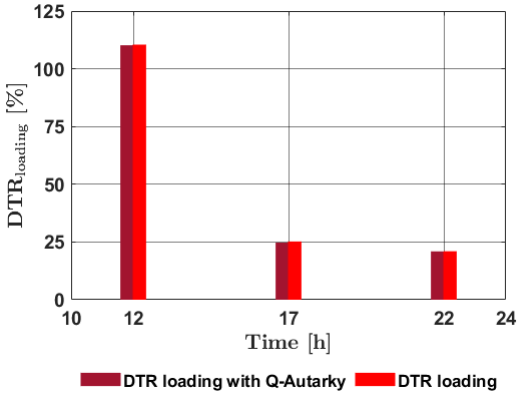

(f) $v = 1.06$ pu new ZIP coefficients

Figure B.31: Different loading of the DTR with LVRs in the Large Urban Grid-Link.

B.2.6 Large Urban Grid-Link OLTC-DTR

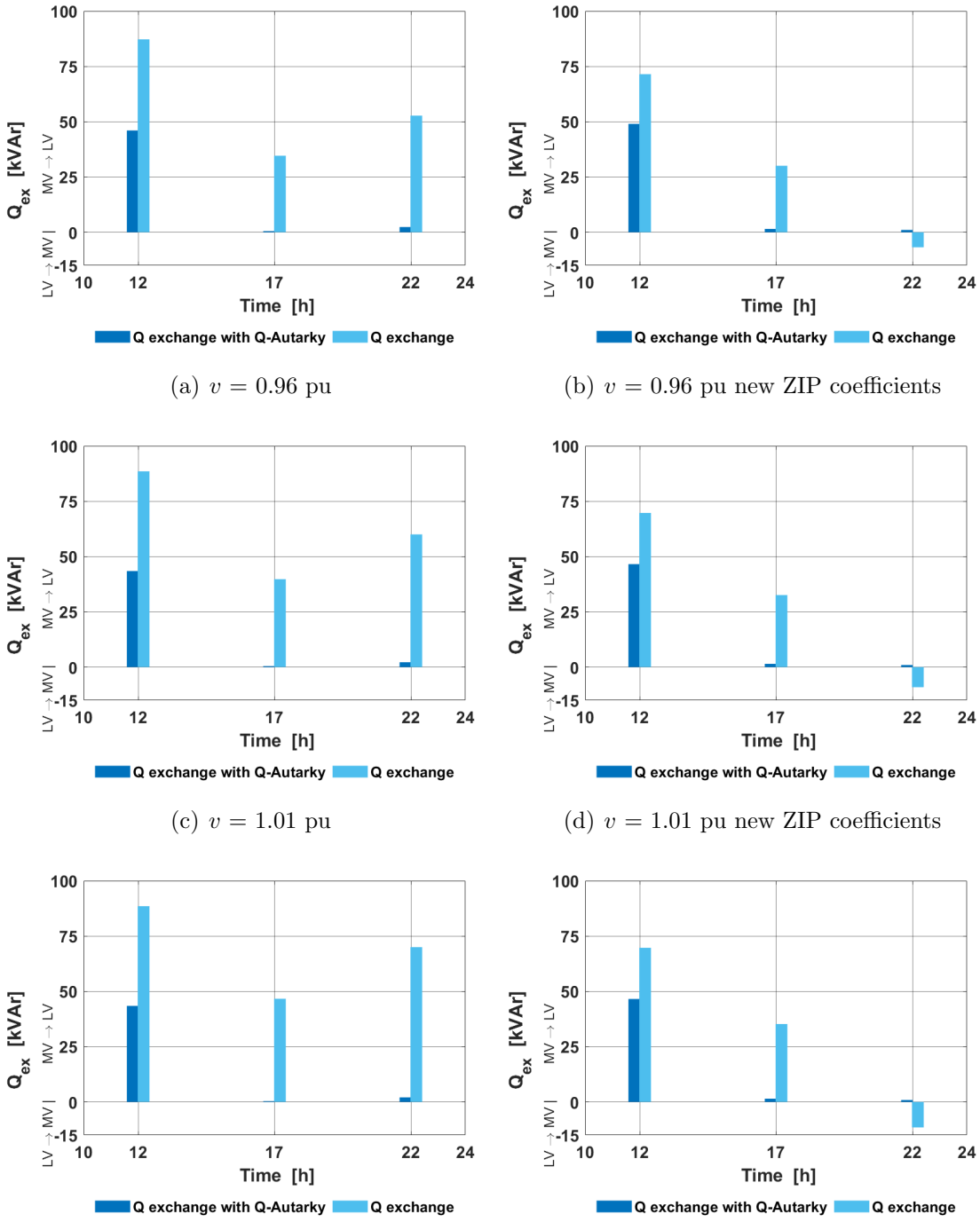

(a) $v = 0.96$ pu

(b) $v = 0.96$ pu new ZIP coefficients

(c) $v = 1.01$ pu

(d) $v = 1.01$ pu new ZIP coefficients

(e) $v = 1.06$ pu

(f) $v = 1.06$ pu new ZIP coefficients

Figure B.32: Different reactive power exchanges with OLTC-DTR in the Large Urban Grid-Link.

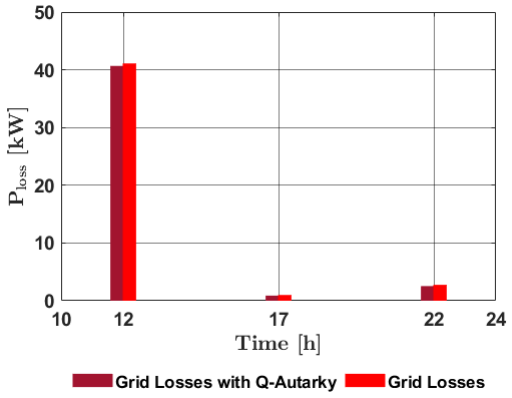

(a) $v = 0.96$ pu

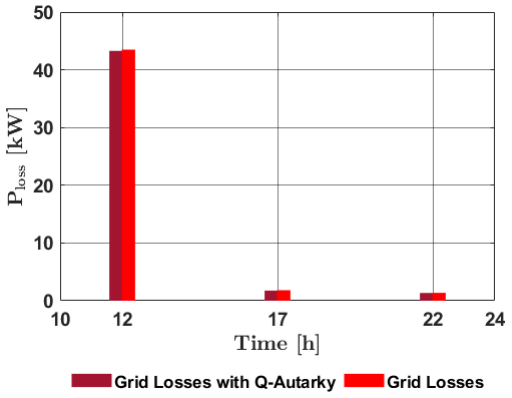

(b) $v = 0.96$ pu new ZIP coefficients

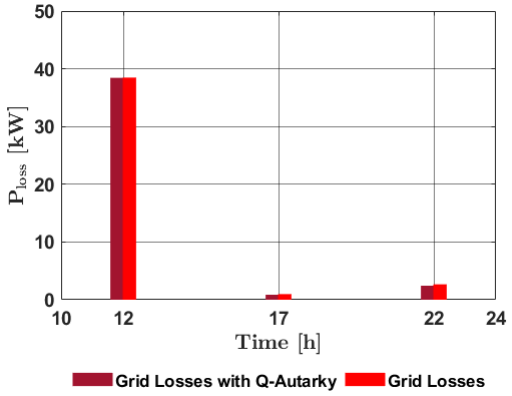

(c) $v = 1.01$ pu

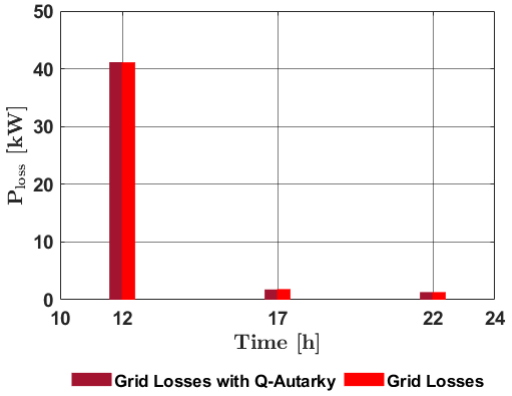

(d) $v = 1.01$ pu new ZIP coefficients

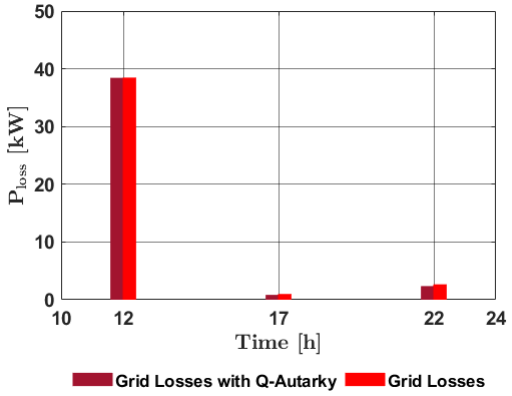

(e) $v = 1.06$ pu

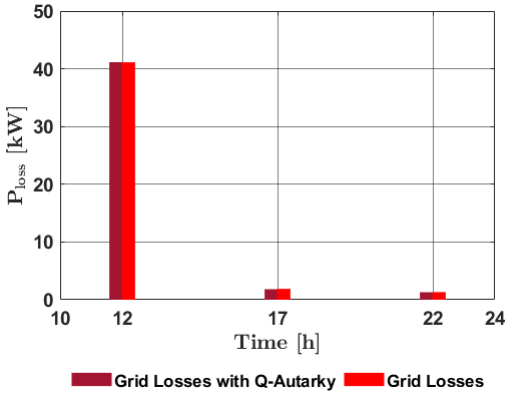

(f) $v = 1.06$ pu new ZIP coefficients

Figure B.33: Different losses with OLTC-DTR in the Large Urban Grid-Link.

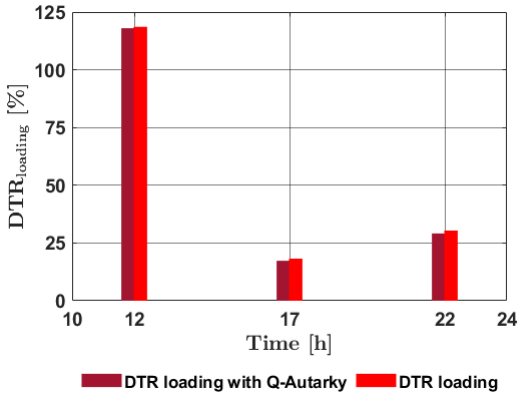

(a) $v = 0.96$ pu

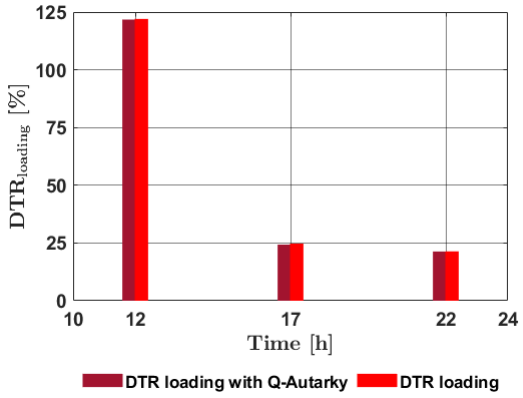

(b) $v = 0.96$ pu new ZIP coefficients

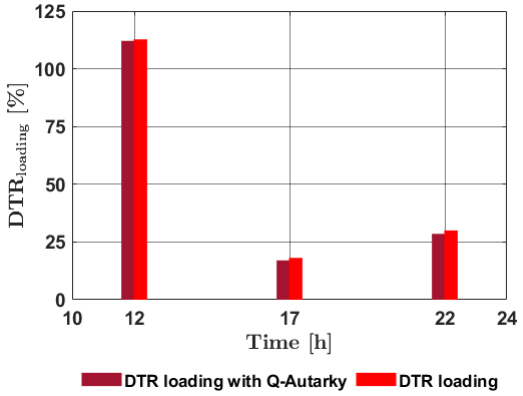

(c) $v = 1.01$ pu

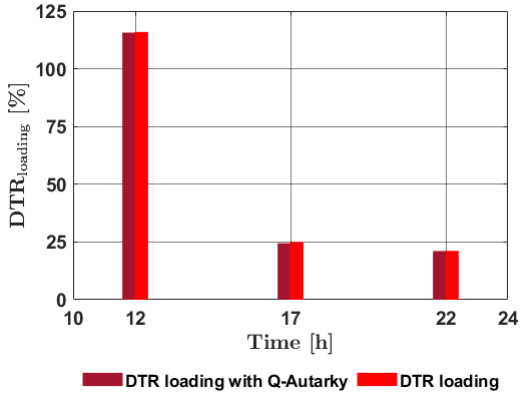

(d) $v = 1.01$ pu new ZIP coefficients

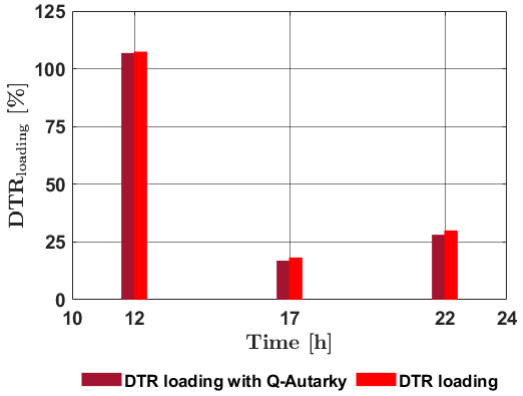

(e) $v = 1.06$ pu

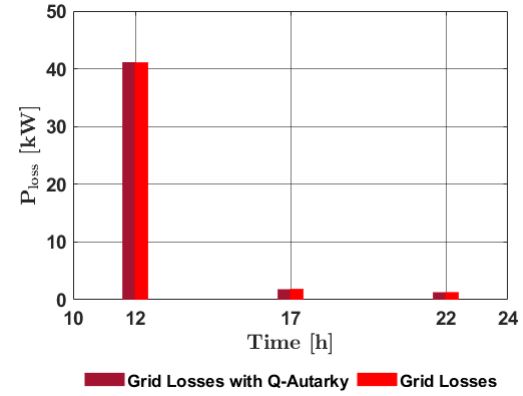

(f) $v = 1.06$ pu new ZIP coefficients

Figure B.34: Different loading of the DTR with OLTC-DTR in the Large Urban Grid-Link.

Erklärung

Hiermit erkläre ich, dass die vorliegende Arbeit gemäß dem Code of Conduct – Regeln zur Sicherung guter wissenschaftlicher Praxis (in der aktuellen Fassung des jeweiligen Mitteilungsblattes der TU Wien), insbesondere ohne unzulässige Hilfe Dritter und ohne Benutzung anderer als der angegebenen Hilfsmittel, angefertigt wurde. Die aus anderen Quellen direkt oder indirekt übernommenen Daten und Konzepte sind unter Angabe der Quelle gekennzeichnet.
Die Arbeit wurde bisher weder im In– noch im Ausland in gleicher oder in ähnlicher Form in anderen Prüfungsverfahren vorgelegt.

Wien, im November 2019

Andreas Potucek